

# Supporting Information

for the article

## Preventing Pd-NHC bond cleavage and switching from nano-scale to molecular catalytic systems: amines and bases as catalyst activators

Oleg V. Khazipov,<sup>a,c</sup> Maxim A. Shevchenko,<sup>a,c</sup> Dmitry V. Pasyukov,<sup>a</sup> Andrey Yu. Chernenko,<sup>a</sup> Alexander V. Astakhov,<sup>a,c</sup> Victor A. Tafeenko,<sup>b</sup> Victor M. Chernyshev,<sup>a,c\*</sup> Valentine P. Ananikov<sup>a,b,c\*</sup>

<sup>a</sup> Platov South-Russian State Polytechnic University (NPI), Prosveschenya 132, Novocherkassk, 346428, Russia

<sup>b</sup> Lomonosov Moscow State University, Leninskie Gory 1, 119991 Moscow, Russia

<sup>c</sup> Zelinsky Institute of Organic Chemistry, Russian Academy of Sciences, Leninsky Prospect 47, Moscow, 119991, Russia

## Contents

S1. Additional experimental data on the reactions of Pd-PEPSSI complexes with amines and transformations of corresponding amino complexes .....	2
S2. Additional experimental data on the Pd/NHC catalysis of C-S cross-coupling reactions .....	7
S3. NMR spectra .....	13
S4. Single Crystal X-Ray Diffraction Data .....	99
S5. Data of the QTAIM (quantum theory of atoms in molecules) analysis of molecular structures of compounds 2a, 2g, 2k, 2y.....	108
S6. TEM, FE-SEM/EDS data.....	110

---

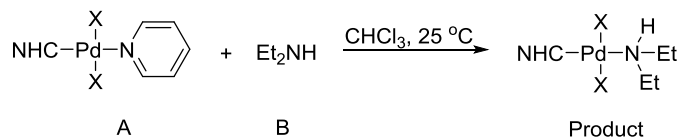
\* Corresponding author.

Email address: chern13@yandex.ru (Victor M. Chernyshev), val@ioc.ac.ru (Valentine P. Ananikov)

# S1. Additional experimental data on the reactions of Pd-PEPSSI complexes with amines and transformations of corresponding amino complexes

Each point on the kinetic curves are determined experimentally three times (confidence limits are shown on the kinetic curves). The rate constant errors were calculated from the weighted linear regression.

A second order kinetics was assumed for the reaction of Pd-PEPSSI complexes with N,N-diethylamine.



The rate law can be expressed by the following equation:<sup>1</sup>

$$-\frac{d[A]}{dt} = -\frac{d[B]}{dt} = k[A][B]$$

If  $[A] = [B]$  the mathematical equation is simplified as:

$$-\frac{d[A]}{dt} = k[A]^2$$

Performing the integration gives the integrated rate law:

$$\frac{1}{[A]} - \frac{1}{[A]_0} = kt$$

This is the equation of a straight line in a plot of  $(1/[A] - 1/[A]_0)$  versus time ( $t$ ) should be linear with the slope equal to  $k$  if the reaction follows the second-order kinetics.

In the reactions of Pd-PEPSSI complexes **1a,d,e,f,g,j** with Et<sub>2</sub>NH, the initial concentrations of starting complex and Et<sub>2</sub>NH were equal (0.01 M). Corresponding plots of  $(1/[A] - 1/[A]_0)$  versus ( $t$ ) obtained from the kinetic data (Figures 2 and S2) are straight lines presented on the Figure S1 which indicate the second order kinetics for the substitution reaction between complexes **1a,d,e,f,g,j** and Et<sub>2</sub>NH (first order with respect to each reactant).

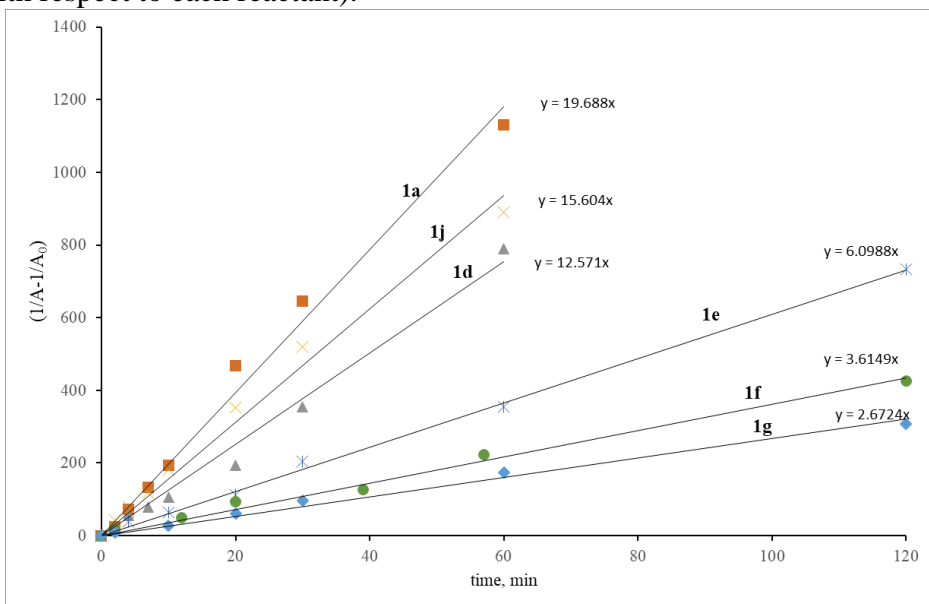
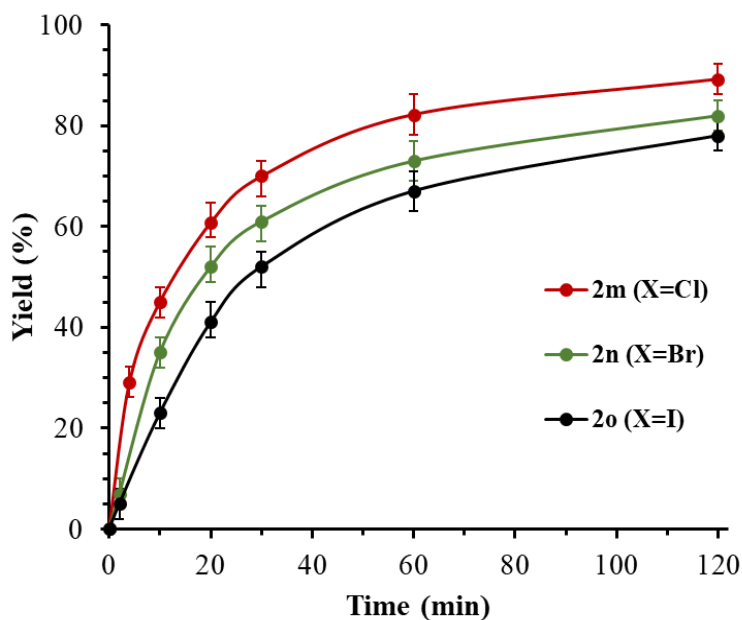


**Figure S1.** Graphic representation of second order reactions **1a,d-g,j** with NHEt<sub>2</sub> (reaction conditions: **1** (0.05 mmol), Et<sub>2</sub>NH (0.05 mmol), CHCl<sub>3</sub> (5 mL), 25±0.5 °C)

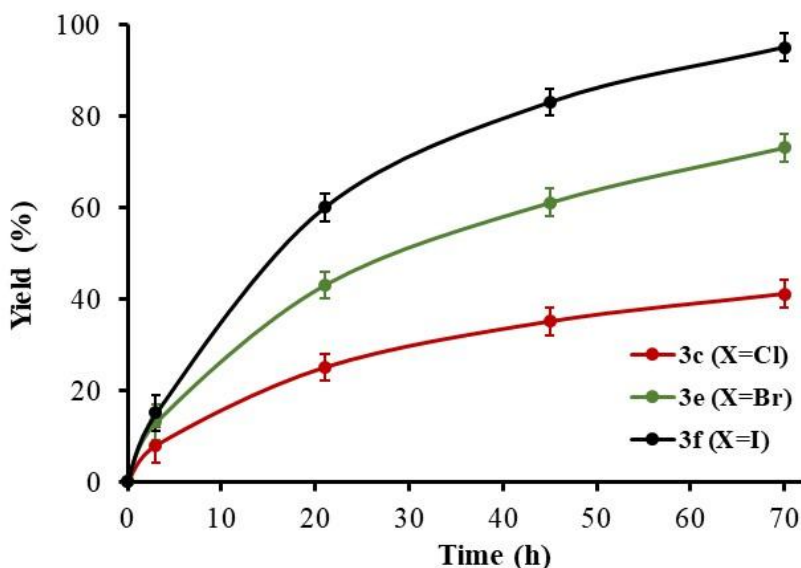
Values of the rates constants are calculated for different complexes Pd-NHC **1a,d-g,j** as the slope of the plot of  $(1/[A] - 1/[A]_0)$  versus (time) with units of  $\text{M}^{-1}\cdot\text{min}^{-1}$  and displayed in Table S1.

Table S1. The rate constants  $k$  measured for the reaction of complexes **1a,d-g,j** with  $\text{Et}_2\text{NH}$

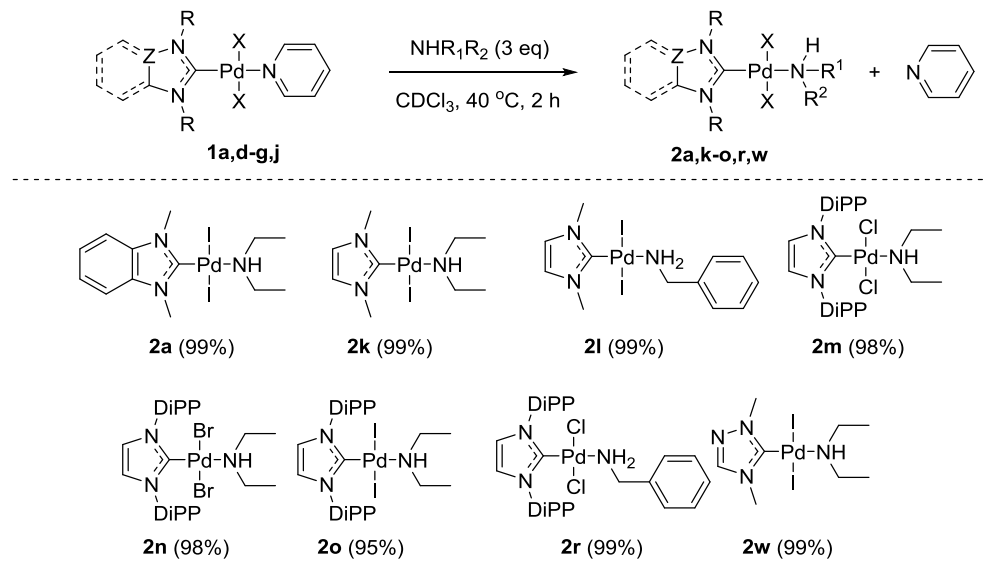
Pd-NHC-PEPPSI	The second-order rate constant $k$ , $\text{M}^{-1}\cdot\text{min}^{-1}$	Experimental error
<b>1a</b>	19.7	2.1
<b>1d</b>	12.6	1.5
<b>1e</b>	6.1	0.4
<b>1f</b>	3.6	0.5
<b>1g</b>	2.7	0.3
<b>1j</b>	15.6	2.1



**Figure S2.** Kinetic plots for the formation of complexes **2m**, **2n**, and **2o** in the reaction of complexes **1e**, **1f**, **1g** with  $\text{Et}_2\text{NH}$ . Reaction conditions: **1e**, **1f**, **1g** (0.05 mmol),  $\text{Et}_2\text{NH}$  (0.05 mmol),  $\text{CHCl}_3$  (5 mL), 25 °C. The yields of compounds **2m**, **2n**, and **2o** were determined by HPLC.



**Figure S3.** Kinetic plots for the formation of compounds **3c,e,f** by thermal decomposition of complexes **2m-o**. Reaction conditions: **2m-o** (0.1 mmol), DMF (2 mL), 140 °C.



**Scheme S1.** NMR yields of amino-complexes **2a,k-o,r,w** in the reaction of complexes **1a,d-g,j** with aliphatic amines.

Table S2. Optimization of the reaction between **1g** and Et<sub>2</sub>NH to give **2o**.<sup>a</sup>

Nº	Solvent	[ <b>1g</b> ]:[NHEt <sub>2</sub> ] <sup>b</sup>	Temperature, (°C)	Time (min)	Yield <b>2o</b> (%)
1	CHCl <sub>3</sub>	1:1.1	25	2	9 <sup>c</sup>
2	CHCl <sub>3</sub>	1:1.1	25	30	61 <sup>c</sup>
3	MeCN	1:1.1	25	2	48 <sup>c</sup>
4	MeCN	1:1.1	25	30	93 <sup>c</sup>
5	1,4-dioxane	1:1.0	25	2	36 <sup>c</sup>
6	1,4-dioxane	1:1.1	25	2	41 <sup>c</sup>
7	1,4-dioxane	1:1.1	25	30	86 <sup>c</sup>
8	1,4-dioxane	1:2	25	2	62 <sup>c</sup>
9	1,4-dioxane	1:2	25	30	96 <sup>c</sup>
10	1,4-dioxane	1:1.1	50	2	79 <sup>c</sup>
11	1,4-dioxane	1:1.1	50	30	99 <sup>c</sup> /94 <sup>d</sup>
12	1,4-dioxane	1:1.1	80	30	97 <sup>c,e</sup>

<sup>a</sup>Reaction conditions: Pd-NHC PEPPSI **1g** (0.05 mmol), Et<sub>2</sub>NH, solvent (5 mL).

<sup>b</sup>In molar ratio.

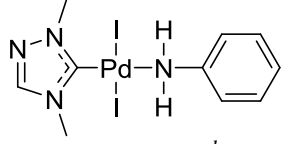
<sup>c</sup>HPLC yield.

<sup>d</sup>Isolated yields.

<sup>e</sup>Pd black observed.

Table S3. Yields of complexes **2** in the reactions of Pd-PEPSSI complexes **1** with arylamines.<sup>a</sup>

Entry	Starting complex	[1]/[ArNH <sub>2</sub> ], mol/mol	Solvent/t	Time	Product (yield)
1	<b>1a</b>	1:1.3	1,4-dioxane (50 °C)	0.5 h	 <b>2y</b> (19%) <sup>c</sup>
2	<b>1a</b>	1:1.3	1,4-dioxane (50 °C)	10 h	 <b>2y</b> (56%) <sup>c</sup>
3	<b>1a</b>	1:1.3	1,4-dioxane (100 °C)	2 h	 <b>2y</b> (48%) <sup>c</sup>
4	<b>1a</b>	1:1.3	DMF (120 °C)	2 h	 <b>2y</b> (48%) <sup>d</sup>
5	<b>1a</b>	1:10	DMF (120 °C)	20 min	 <b>2y</b> (83%) <sup>d</sup>
6	<b>1a</b>	1:10	DMF (120 °C)	1 h	 <b>2y</b> (72%) <sup>d,e</sup>
7	<b>1a</b>	1:10	DMF (140 °C)	20 min	 <b>2y</b> (75%) <sup>d,e</sup>
8	<b>1a</b>	1:10	DMF (120 °C)	20 min	 <b>2z</b> (85%) <sup>d</sup>
9	<b>1a</b>	1:10	DMF (120 °C)	20 min	 <b>2aa</b> (81%) <sup>d</sup>
10	<b>1a</b>	1:10	DMF (120 °C)	20 min	 <b>2ab</b> (63%) <sup>d</sup>
11	<b>1d</b>	1:3	CDCl <sub>3</sub> (40 °C)	8 h	 <b>2ac</b> (13%) <sup>c</sup>
12	<b>1d</b>	1:10	DMF (120 °C)	20 min	 <b>2ac</b> (82%) <sup>d</sup>
13	<b>1e</b>	1:3	CDCl <sub>3</sub> (40 °C)	8 h	 <b>2ad</b> (20%) <sup>c</sup>
14	<b>1e</b>	1:10	DMF (120 °C)	20 min	 <b>2ad</b> (72%)

15	<b>1j</b>	1:10	DMF (120 °C)	20 min	 <b>2ae</b> (78%) <sup>d</sup>
----	-----------	------	--------------	--------	--

<sup>a</sup> Reaction conditions: Pd-NHC PEPPSI **1** (0.034 mmol), PhNH<sub>2</sub>, solvent (0.5 mL).

<sup>b</sup> In molar ratio.

<sup>c</sup> Yield determined by <sup>1</sup>H NMR.

<sup>d</sup> Isolated yields.

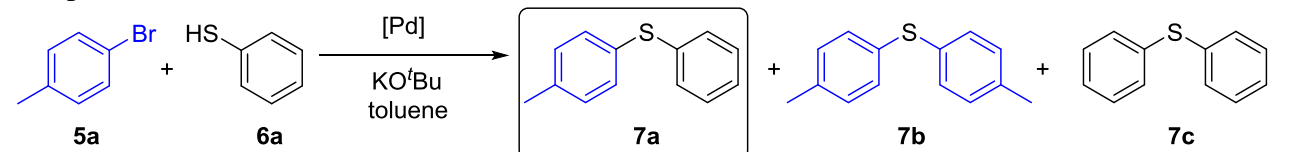
<sup>e</sup> Pd black observed.

## References

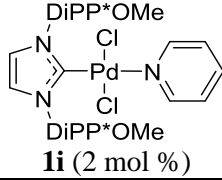
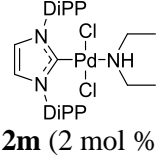
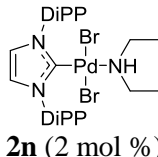
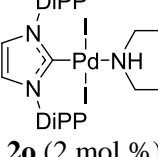
- (1) The Kinetic Analysis of Experimental Data In *An Introduction to Chemical Kinetics*; Robson, W. M., Ed. 2005.

## S2. Additional experimental data on the Pd/NHC catalysis of C-S cross-coupling reactions

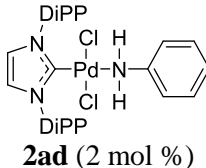
Table S4. Catalytic activity of Pd/NHC complexes in the C-S cross-coupling reaction between compounds **5a** and **6a**.<sup>a</sup>



Entry	[Pd] precatalyst	Pre-activation conditions <sup>b</sup>	React. temp.	React. time	Conv. of <b>5a</b>	Product (GC-MS yield)
1.		25 °C, 5 min	25 °C	1 h	2%	<b>7a</b> (0%) <b>7b</b> (0%) <b>7c</b> (trace)
2.	<b>1e</b> (2 mol %)	25 °C, 5 min	60 °C	1 h	5%	<b>7a</b> (3%) <b>7b</b> (trace) <b>7c</b> (trace)
3.	<b>1e</b> (2 mol %)	Without pre-activation	110 °C	1 h	100%	<b>7a</b> (71%) <b>7b</b> (14%) <b>7c</b> (15%)
4.	<b>1e</b> (2 mol %) + Et <sub>2</sub> NH (4 mol %)	25 °C, 5 min	25 °C	1 h	82%	<b>7a</b> (79%) <b>7b</b> (0%) <b>7c</b> (0%)
5.	<b>1e</b> (2 mol %) + Et <sub>2</sub> NH (4 mol %)	25 °C, 5 min	25 °C	8 h	92%	<b>7a</b> (87%) <b>7b</b> (trace%) <b>7c</b> (trace%)
6.	<b>1e</b> (2 mol %) + Et <sub>2</sub> NH (4 mol %)	25 °C, 5 min	25 °C	12 h	98%	<b>7a</b> (92%) <b>7b</b> (trace%) <b>7c</b> (trace%)
7.	<b>1e</b> (2 mol %) + morph. (4 mol %)	25 °C, 5 min	25 °C	12 h	99%	<b>7a</b> (91%) <b>7b</b> (trace%) <b>7c</b> (trace%)
8.	<b>1e</b> (2 mol %) + Et <sub>2</sub> NH (4 mol %)	25 °C, 5 min	25 °C	16 h	100%	<b>7a</b> (92%) <b>7b</b> (trace%) <b>7c</b> (1%)
9.	<b>1e</b> (2 mol %) + Et <sub>2</sub> NH (8 mol %)	25 °C, 5 min	25 °C	12 h	100%	<b>7a</b> (90%) <b>7b</b> (trace%) <b>7c</b> (trace%)
10.	<b>1e</b> (1 mol %) <sup>b</sup> + Et <sub>2</sub> NH (4 mol %)	25 °C, 5 min	25 °C	12 h	76%	<b>7a</b> (74%) <b>7b</b> (trace%) <b>7c</b> (trace%)
11.	<b>1e</b> (2 mol %) + Et <sub>3</sub> N (8 mol %)	140 °C, 1h, without $KO^tBu$ , <sup>c</sup> then 25 °C, 5 min	25 °C	1 h	39%	<b>7a</b> (36%) <b>7b</b> (trace) <b>7c</b> (trace)
12.		25 °C, 5 min	25 °C	1 h	2%	0

13.	<b>1h</b> (2 mol %)	Without pre-activation	110 °C	1 h	63%	<b>7a</b> (55%) <b>7b</b> (trace) <b>7c</b> (3%)
14.	<b>1h</b> (2 mol %)	Without pre-activation	110 °C	16 h	100%	<b>7a</b> (89%) <b>7b</b> (3%) <b>7c</b> (6%)
15.	 <b>1i</b> (2 mol %)	25 °C, 5 min	25 °C	1 h	2%	0
16.	<b>1i</b> (2 mol %) + Et <sub>2</sub> NH(4 mol %)	25 °C, 5 min	25 °C	1 h	13%	<b>7a</b> (13%) <b>7b</b> (0%) <b>7c</b> (0%)
17.	<b>1i</b> (2 mol %)	Without pre-activation	60 °C	1 h	0	0
18.	<b>1i</b> (2 mol %)	Without pre-activation	110 °C	1 h	65%	<b>7a</b> (58%) <b>7b</b> (trace) <b>7c</b> (2%)
19.	<b>1i</b> (2 mol %)	Without pre-activation	110 °C	16 h	100%	<b>7a</b> (90%) <b>7b</b> (3%) <b>7c</b> (4%)
20.	 <b>2m</b> (2 mol %)	25 °C, 5 min	25 °C	1 h	85%	<b>7a</b> (83%) <b>7b</b> (trace) <b>7c</b> (trace)
21.	<b>2m</b> (2 mol %)	25 °C, 5 min	25 °C	10 h	98%	<b>7a</b> (96%) <b>7b</b> (trace) <b>7c</b> (trace)
22.	<b>2m</b> (2 mol %)	140 °C, 1h, without KO'Bu, <sup>c</sup> then 25 °C, 5 min	25 °C	1 h	62%	<b>7a</b> (53%) <b>7b</b> (trace) <b>7c</b> (trace)
23.	<b>2m</b> (2 mol %)	25 °C, 5 min	60 °C	1 h	94%	<b>7a</b> (89%) <b>7b</b> (4%) <b>7c</b> (1%)
24.	<b>2m</b> (2 mol %)	25 °C, 5 min	80 °C	1 h	100%	<b>7a</b> (71%) <b>7b</b> (11%) <b>7c</b> (16%)
25.	<b>2m</b> (2 mol %)	25 °C, 5 min	80 °C	10 h	100%	<b>7a</b> (53%) <b>7b</b> (16%) <b>7c</b> (19%)
26.	<b>2m</b> (2 mol %)	25 °C, 5 min	110 °C	1 h	100%	<b>7a</b> (51%) <b>7b</b> (20%) <b>7c</b> (25%)
27.	 <b>2n</b> (2 mol %)	25 °C, 5 min	25 °C	1 h	83%	<b>7a</b> (80%) <b>7b</b> (trace) <b>7c</b> (trace)
28.	 <b>2o</b> (2 mol %)	25 °C, 5 min	25 °C	1 h	79%	<b>7a</b> (77%) <b>7b</b> (trace) <b>7c</b> (trace)

29.		25 °C, 5 min	25 °C	1 h	83%	<b>7a</b> (81%) <b>7b</b> (trace) <b>7c</b> (trace)
30.		25 °C, 5 min	25 °C	1 h	62%	<b>7a</b> (51%) <b>7b</b> (trace) <b>7c</b> (trace)
31.		25 °C, 5 min	25 °C	1 h	80%	<b>7a</b> (77%) <b>7b</b> (trace) <b>7c</b> (trace)
32.		25 °C, 5 min	25 °C	1 h	3%	<b>7a</b> (trace) <b>7b</b> (0%) <b>7c</b> (trace)
33.		25 °C, 5 min	25 °C	1 h	14%	<b>7a</b> (12%) <b>7b</b> (0%) <b>7c</b> (0%)
34.	<b>2u</b> (2 mol %)	60 °C, 5 min	25 °C	1 h	24%	<b>7a</b> (23%) <b>7b</b> (0%) <b>7c</b> (0%)
35.		25 °C, 5 min	25 °C	1 h	17%	<b>7a</b> (15%) <b>7b</b> (0%) <b>7c</b> (0%)
36.	<b>2v</b> (2 mol %)	60 °C, 5 min	25 °C	1 h	27%	<b>7a</b> (24%) <b>7b</b> (trace) <b>7c</b> (trace)
37.	<b>2v</b> (2 mol %)	25 °C, 5 min	60 °C	1 h	53%	<b>7a</b> (48%) <b>7b</b> (trace) <b>7c</b> (1%)
38.	<b>2v</b> (2 mol %)	25 °C, 5 min	60 °C	16 h	100%	<b>7a</b> (95%) <b>7b</b> (trace) <b>7c</b> (1%)
39.	<b>2v</b> (2 mol %)	25 °C, 5 min	80 °C	1 h	100%	<b>7a</b> (94%) <b>7b</b> (trace) <b>7c</b> (3%)
40.	<b>2v</b> (2 mol %)	25 °C, 5 min	110 °C	1 h	100%	<b>7a</b> (86%) <b>7b</b> (4%) <b>7c</b> (2%)
41.	<b>2v</b> (2 mol %)	Without preactivation	110 °C	1 h	100%	<b>7a</b> (87%) <b>7b</b> (4%) <b>7c</b> (3%)
42.		25 °C, 5 min	25 °C	1 h	5%	<b>7a</b> (trace) <b>7b</b> (0%) <b>7c</b> (trace)

43.	<b>2x</b> (2 mol %)	Without pre-activation	60 °C	1 h	8%	<b>7a</b> (6%) <b>7b</b> (trace) <b>7c</b> (trace)
44.	<b>2x</b> (2 mol %)	140 °C, 1h, without KO'Bu, <sup>c</sup> then 25 °C, 5 min	25 °C	1 h	47%	<b>7a</b> (42%) <b>7b</b> (trace) <b>7c</b> (trace)
45.	<b>2x</b> (2 mol %)	Without pre-activation	110 °C	1 h	100%	<b>7a</b> (73%) <b>7b</b> (10%) <b>7c</b> (14%)
46.	<b>2x</b> (2 mol %) + Et <sub>2</sub> NH (4 mol %)	25 °C, 5 min	25 °C	1 h	78%	<b>7a</b> (76%) <b>7b</b> (trace) <b>7c</b> (trace)
47.	 <b>2ad</b> (2 mol %)	25 °C, 5 min	25 °C	1 h	2%	0
48.	<b>2ad</b> (2 mol %)	Without pre-activation	110 °C	1 h	100%	<b>7a</b> (69%) <b>7b</b> (13%) <b>7c</b> (15%)
49.	<b>2ad</b> (2 mol %) <sup>b</sup> + Et <sub>2</sub> NH (4 mol %)	25 °C, 5 min	25 °C	1 h	74%	<b>7a</b> (71%) <b>7b</b> (0%) <b>7c</b> (trace)

<sup>a</sup> Conditions: Pd-precatalyst (1-2 mol. % of [Pd] relative to **5a**), Bu'OK (0.4 mmol), **5a** (0.25 mmol), PhSH (0.26 mmol), toluene (2 mL).

<sup>b</sup> Stirring the reaction mixture of a precatalyst (Pd/NHC or Pd/NHC with amine), aryl bromide (**5a**) and KO'Bu (unless otherwise specified) in toluene at the defined temperature within the specified time before the addition of PhSH.

<sup>c</sup> A mixture of a Pd/NHC or Pd/NHC with amine and DMF (1 mL) was heated at stirring at 140 °C for 1 h in argon atmosphere. Then DMF was evaporated in argon flow and the residue of a formed precatalyst was dissolved in toluene (2 mL). Then aryl bromide (**5a**) and KO'Bu were added in argon atmosphere to the toluene solution of the precatalyst and the resulted mixture was stirred at 25 °C for 5 min before the addition of PhSH.

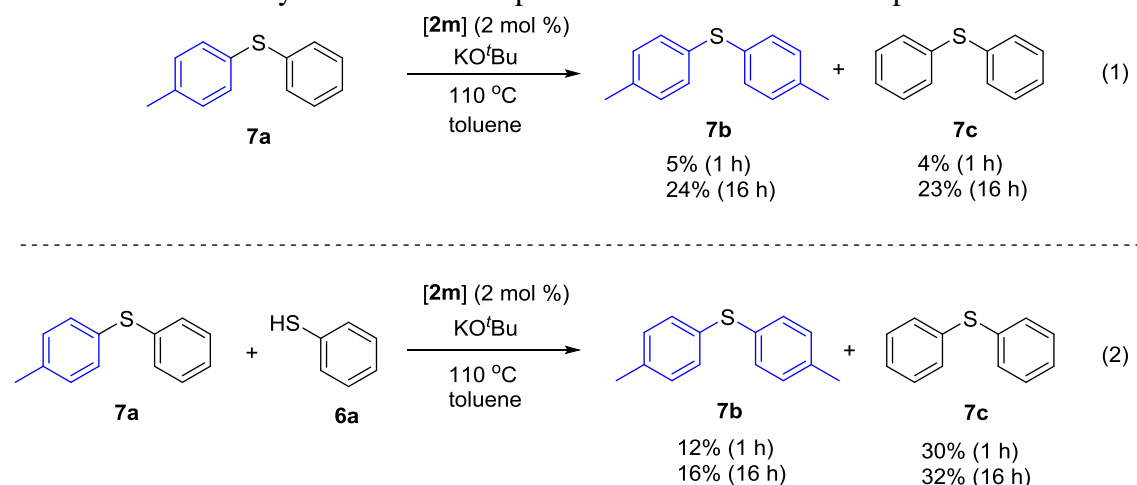
Table S5. Optimization of conditions for the reaction between 1-chloro-2-methylbenzene and PhSH.<sup>a</sup>

Entry	[Pd] precatalyst	Pre-activation conditions <sup>b</sup>	React. temp.	React. time	Conv. of <b>5d</b>	Product (GC-MS yield)
1.		25 °C, 5 min	25 °C	16 h	2%	<b>7e</b> (trace%)
2.	<b>1e</b> (2 mol %)	Without preactivation	110 °C	1 h	100 %	<b>7e</b> (45%) <b>7q</b> (20%) <b>7c</b> (27%)
3.	<b>1e</b> (2 mol %) + Et <sub>2</sub> NH (2 mol %)	25 °C, 5 min	25 °C	16 h	11%	<b>7e</b> (7%) <b>7q</b> (trace%) <b>7c</b> (trace%)
4.	<b>1e</b> (2 mol %) + Et <sub>2</sub> NH (4 mol %)	25 °C, 5 min	25 °C	16 h	25%	<b>7e</b> (23%) <b>7q</b> (trace%) <b>7c</b> (trace%)
5.	<b>1e</b> (2 mol %) + Et <sub>2</sub> NH (2 mol %)	25 °C, 5 min	60 °C	16 h	51%	<b>7e</b> (37%) <b>7q</b> (6%) <b>7c</b> (9%)
6.	<b>1e</b> (2 mol %) + Et <sub>2</sub> NH (4 mol %)	25 °C, 5 min	60 °C	16 h	68%	<b>7e</b> (42%) <b>7q</b> (8%) <b>7c</b> (12%)
7.	<b>1e</b> (2 mol %) + Et <sub>2</sub> NH (2 mol %)	25 °C, 5 min	80 °C	16 h	81%	<b>7e</b> (49%) <b>7q</b> (16%) <b>7c</b> (19%)
8.	<b>1e</b> (2 mol %) + Et <sub>2</sub> NH (4 mol %)	25 °C, 5 min	80 °C	24 h	100%	<b>7e</b> (55%) <b>7q</b> (24%) <b>7c</b> (21%)
9.	<b>1i</b> (1.5 mol %) + morph. (4 mol %)	60 °C, 5 min	60 °C	16 h	100%	<b>7e</b> (96%) <b>7q</b> (trace%) <b>7c</b> (trace %)
10.		60 °C, 5 min	60 °C	16 h	68%	<b>7e</b> (63%) <b>7q</b> (trace%) <b>7c</b> (trace%)
11.		60 °C, 5 min	60 °C	16 h	100%	<b>7e</b> (96%) <b>7q</b> (0%) <b>7c</b> (1%)

<sup>a</sup> Conditions: Pd-precatalyst (1-2 mol. % of [Pd] relative to **5a**), Bu'OK (0.4 mmol), **5a** (0.25 mmol), PhSH (0.26 mmol), toluene (2 mL).

<sup>b</sup> Stirring the reaction mixture of a precatalyst (Pd/NHC or Pd/NHC with amine), ArBr (**5**) and KO'Bu (unless otherwise specified) in toluene at the defined temperature within the specified time before addition of PhSH. In some specified cases, KO'Bu was added after preactivation, together with PhSH.

**Scheme S2.** Pd-catalyzed formation of products **7b** and **7c** from compounds **7a** and **6a**.<sup>a,b,c</sup>



<sup>a</sup> Conditions of the reaction (1): a mixture of complex **2m** (0.005 mmol), Bu'OK (0.4 mmol), and compound **7a** (0.25 mmol) was stirred in toluene (2 mL) at 110 °C in argon atmosphere for specified time then analyzed by GC-MS.  
 Conditions of the reaction (2): a mixture of complex **2m** (0.005 mmol), Bu'OK (0.4 mmol), compound **7a** (0.125 mmol) and compound **6a** (0.125 mmol) was stirred in toluene (2 mL) at 110 °C in argon atmosphere for specified time then analyzed by GC-MS. <sup>b</sup> GC-MS yields of compounds **7b** and **7c** averaged from two runs are presented. <sup>c</sup> No any products were detected in the absence of complex **2m**.

**Scheme S3.** The plausible mechanism of Pd/NHC catalyzed C-S cross-coupling reaction.<sup>1</sup>

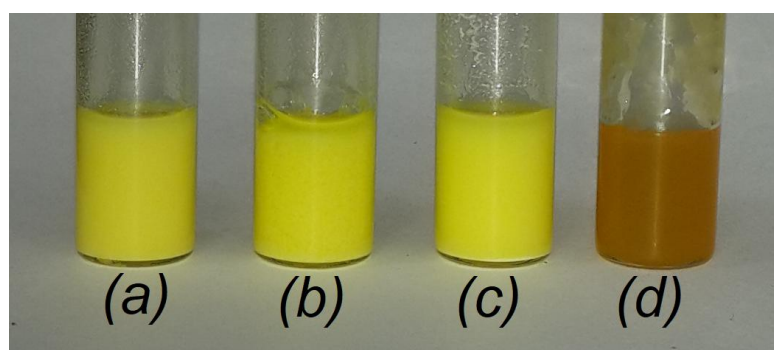
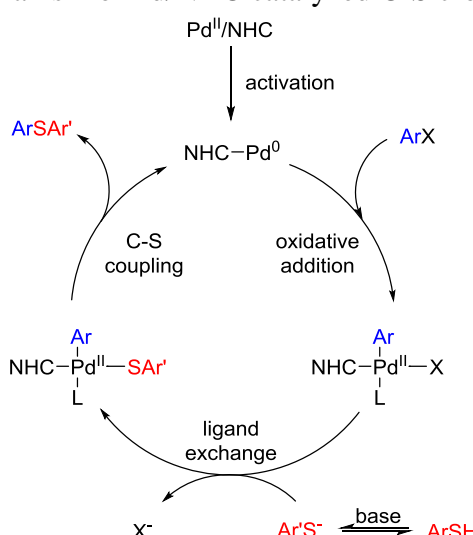


**Figure S4.** Photos of reaction mixtures 1 h after the preactivation of various Pd/NHC precatalysts and addition of PhSH: *a* – precatalyst **1e**, *b* - precatalyst **2x**, *c* - precatalyst **2ad**, *d* – precatalyst **2m**.

### References

- (1) Bastug, G.; Nolan, S. P. Carbon–Sulfur Bond Formation Catalyzed by [Pd(IPr\*OMe)(cin)Cl] (cin = cinnamyl). *The Journal of Organic Chemistry* **2013**, *78*, 9303-9308.

### **S3. NMR spectra**

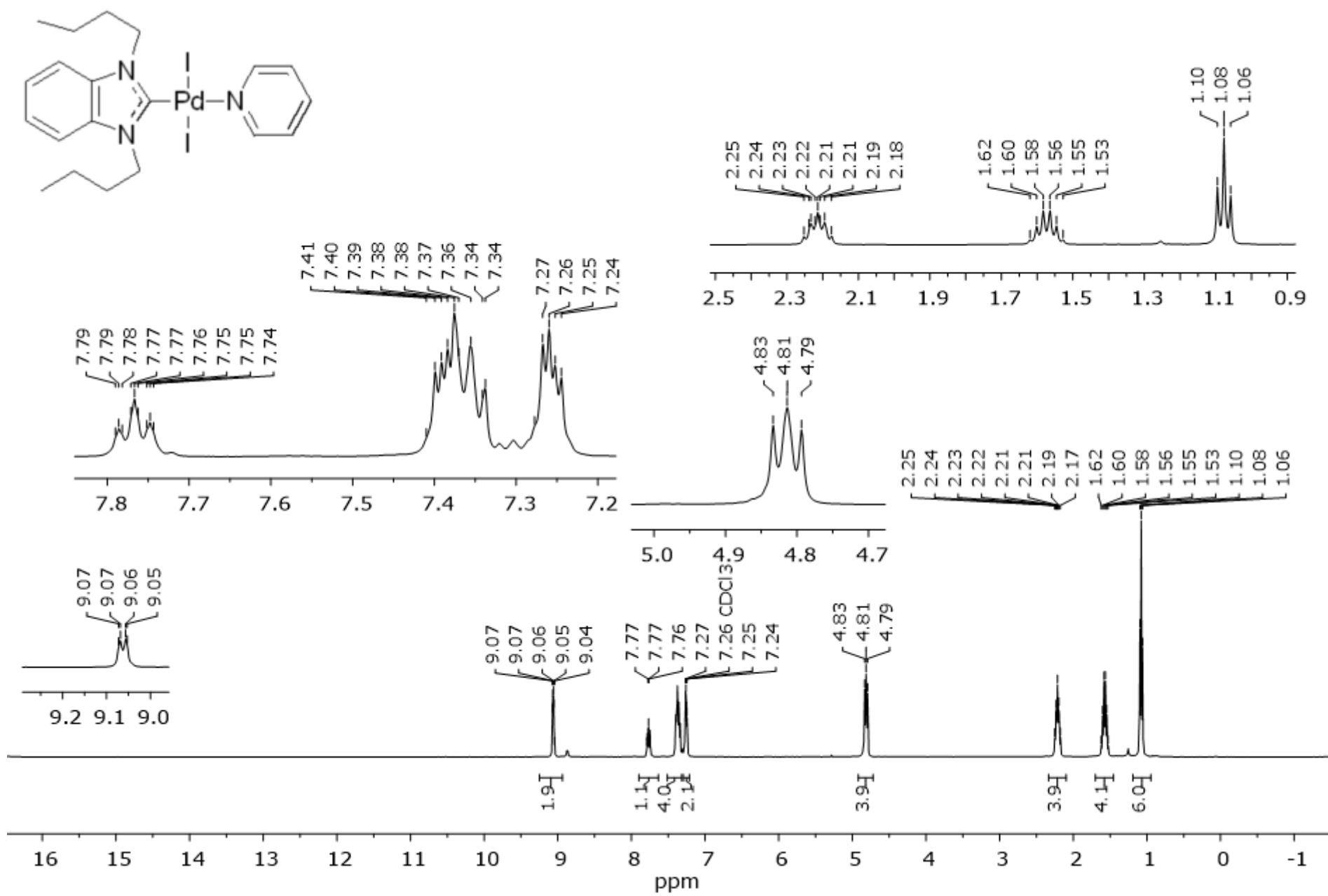


**Figure S5.** <sup>1</sup>H NMR spectrum of compound **1c** ( $\text{CDCl}_3$ , 500 MHz)

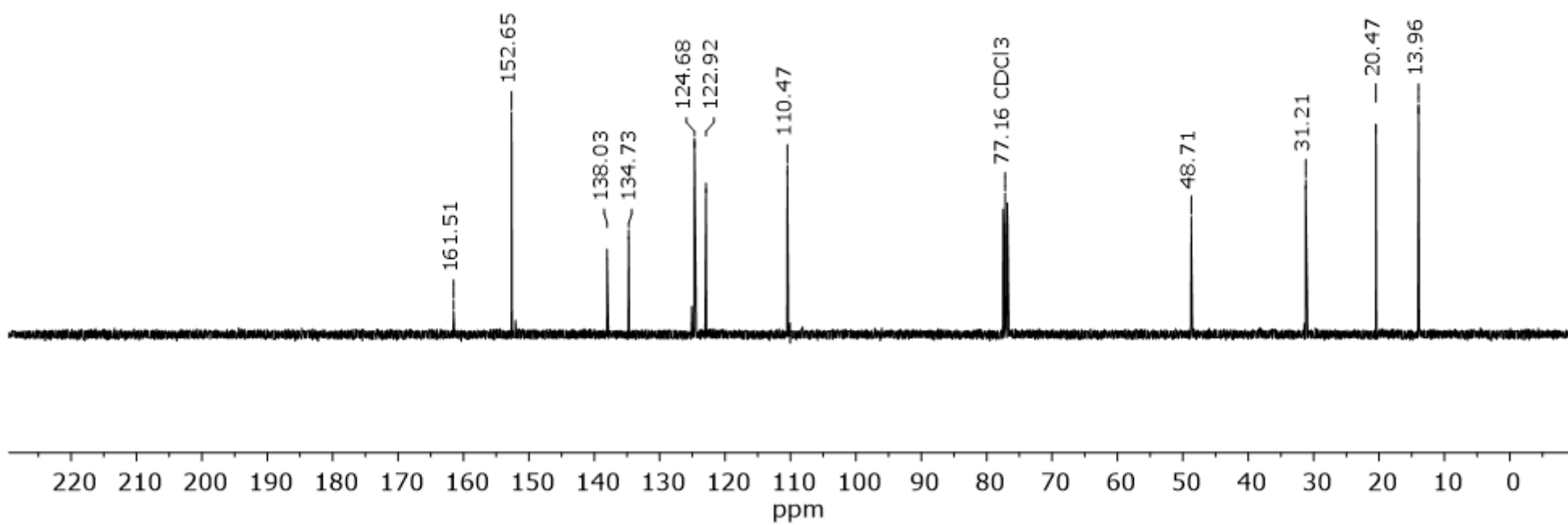
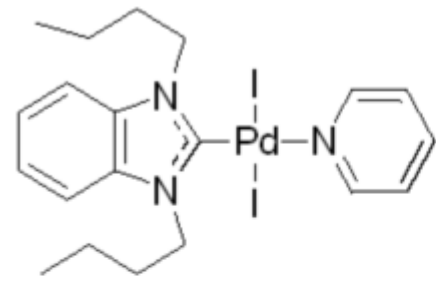


**Figure S6.**  $^{13}\text{C}$  NMR spectrum of compound **1c** (CDCl<sub>3</sub>, 125 MHz)

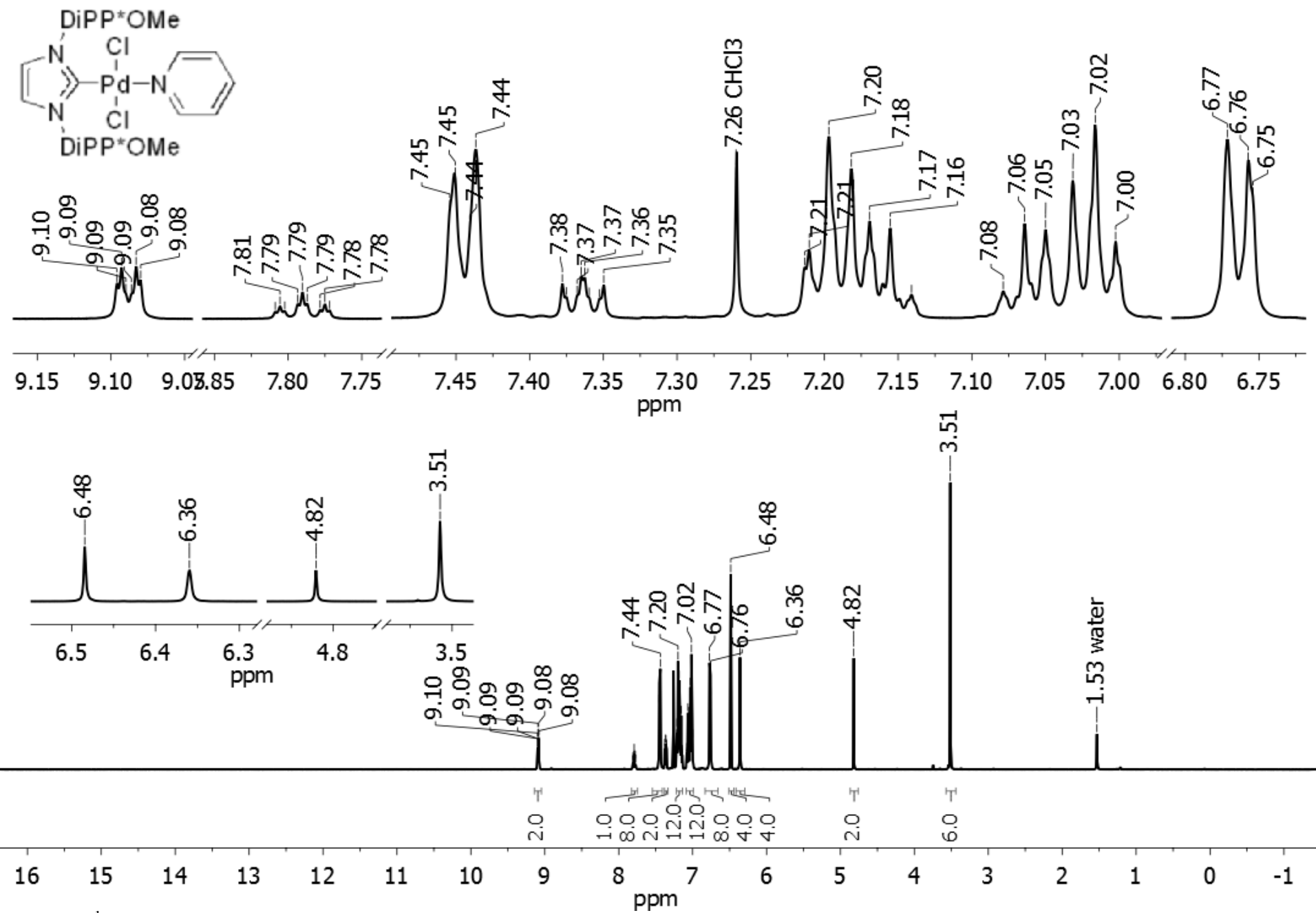


**Figure S7.**  $^1\text{H}$  NMR spectrum of compound **1i** ( $\text{CDCl}_3$ , 500 MHz)

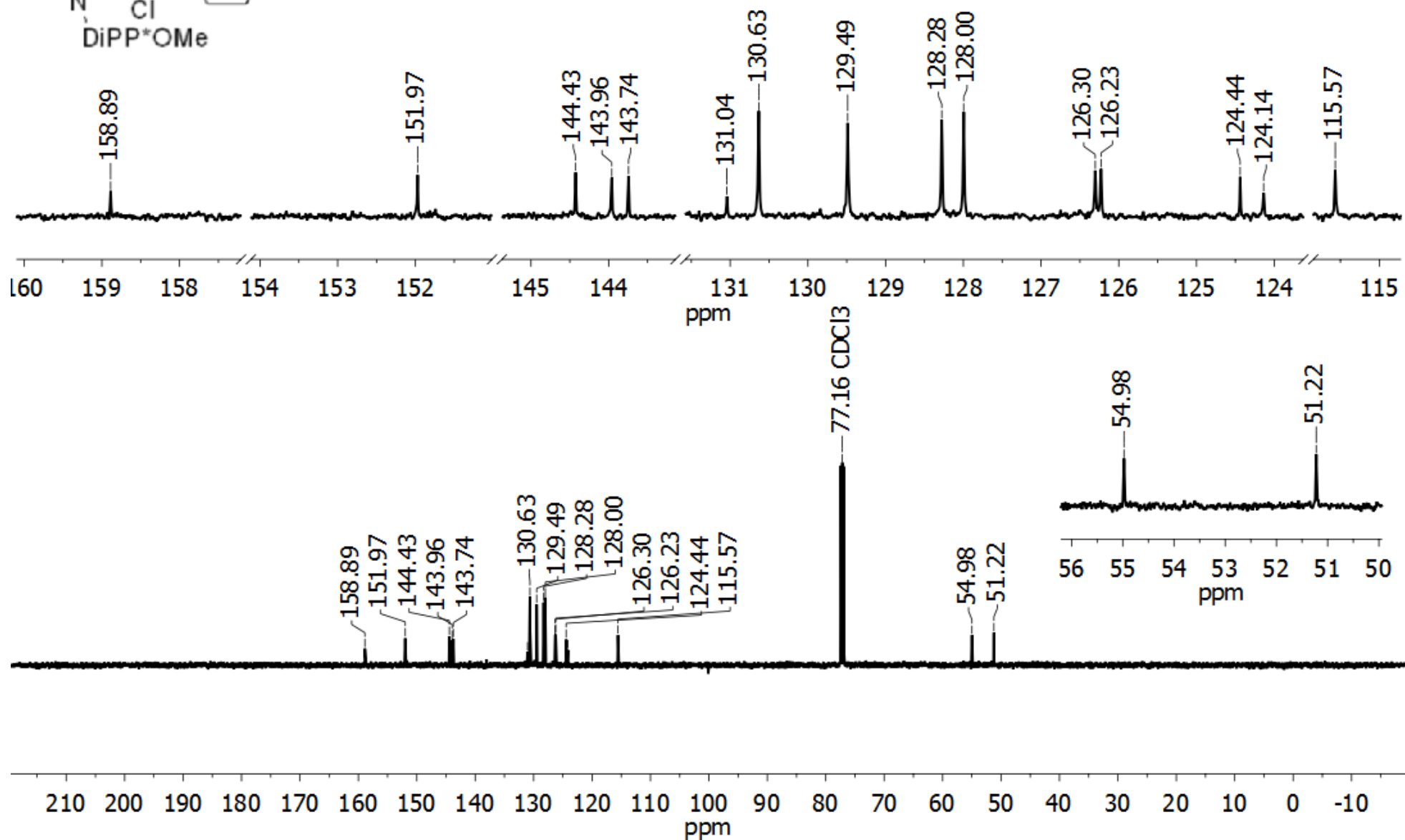
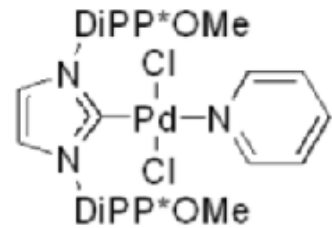
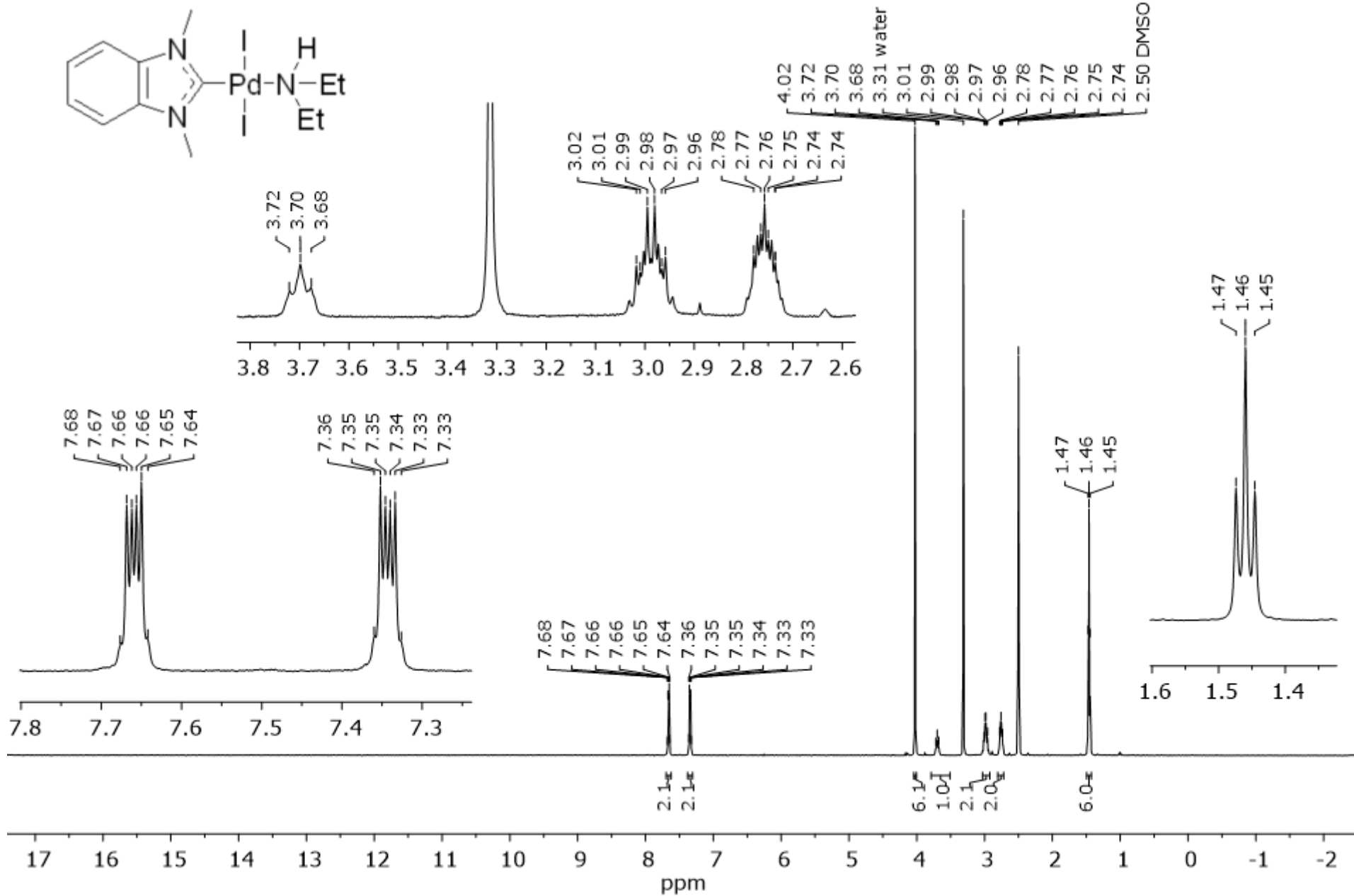
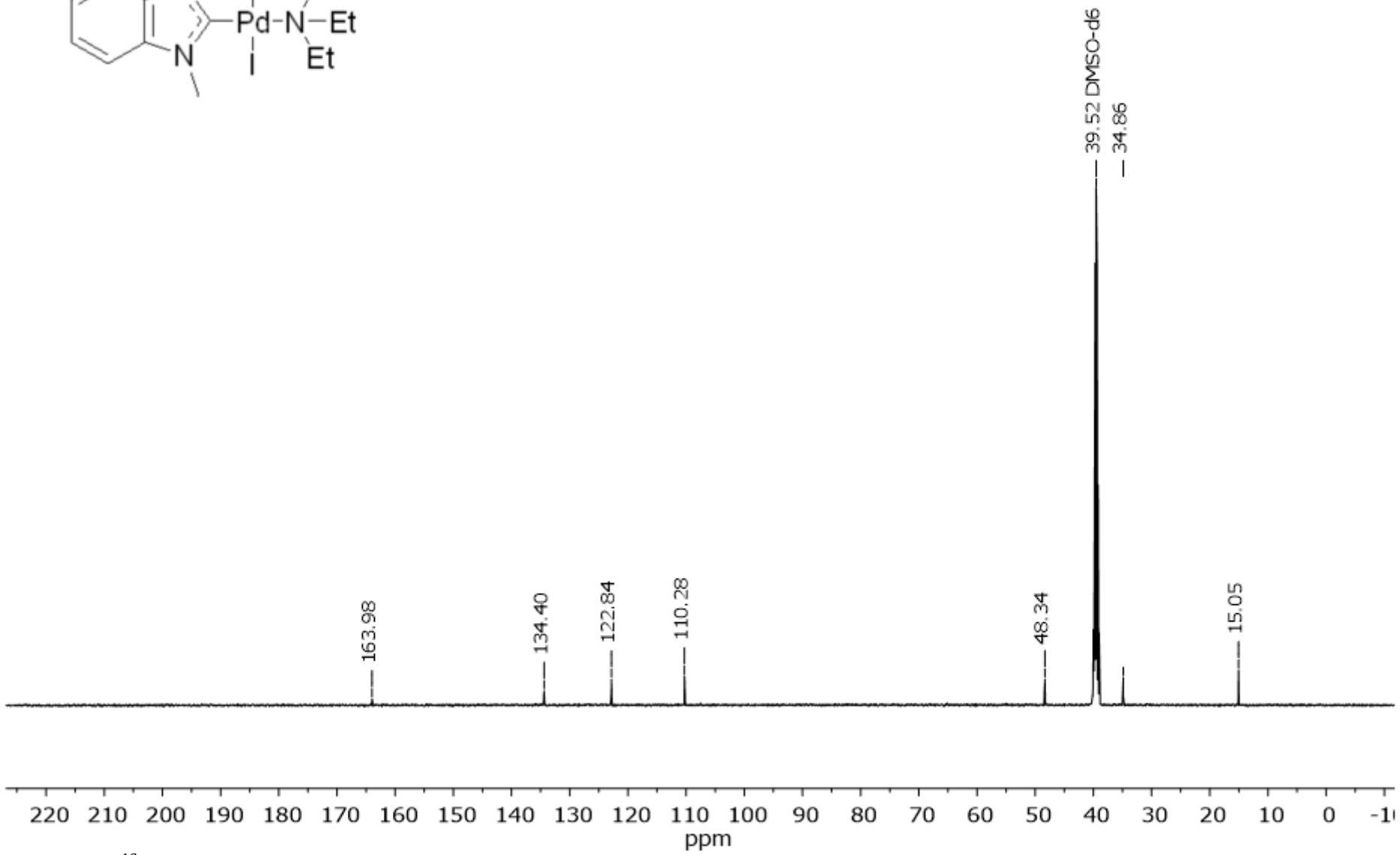
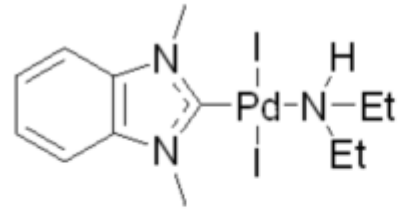


Figure S8. <sup>13</sup>C NMR spectrum of compound **1i** ( $\text{CDCl}_3$ , 125 MHz)



**Figure S9.**  $^1\text{H}$  NMR spectrum of compound **2a** (DMSO- $d_6$ , 500 MHz)



**Figure S10.**  $^{13}\text{C}$  NMR spectrum of compound **2a** (DMSO- $d_6$ , 125 MHz)

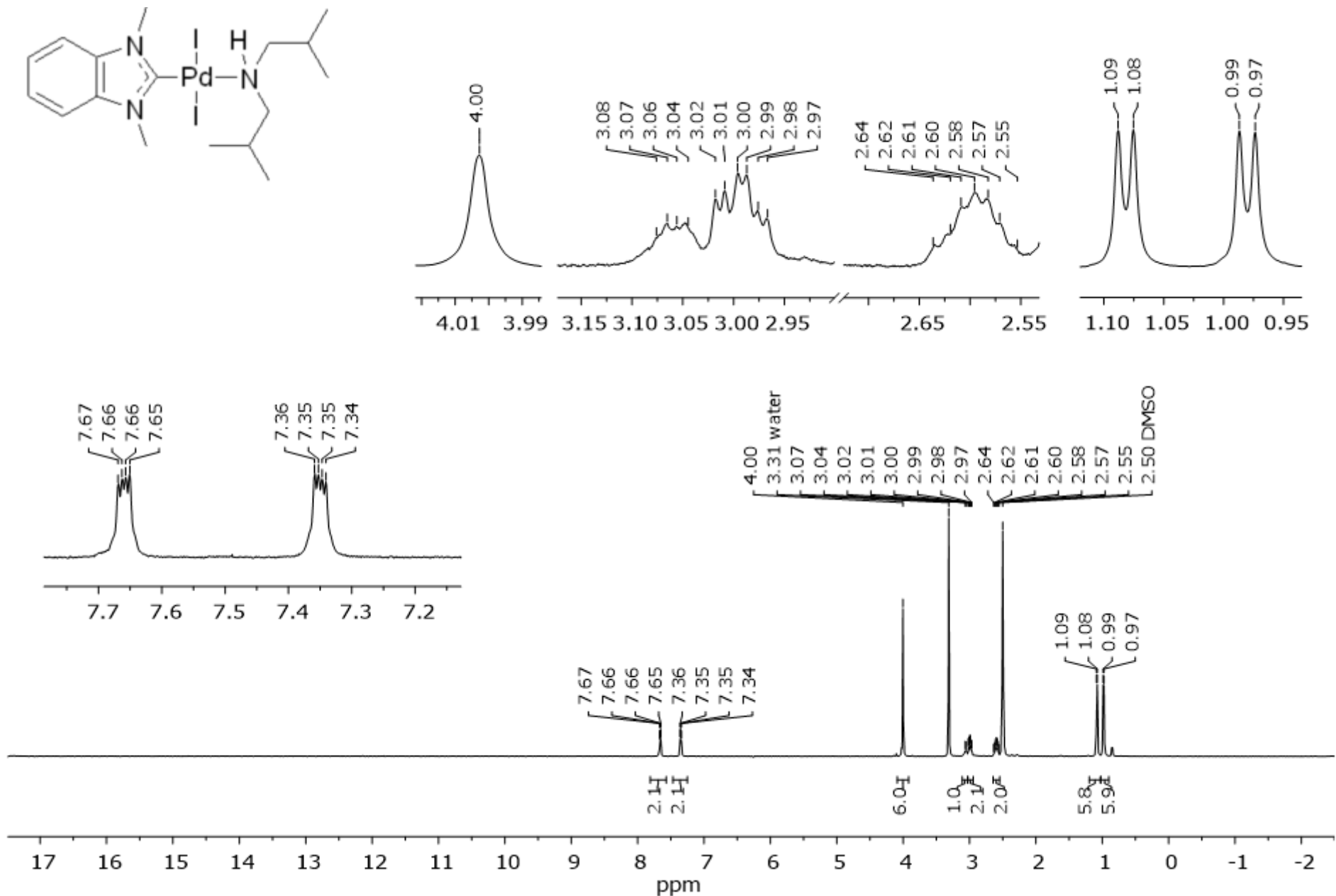
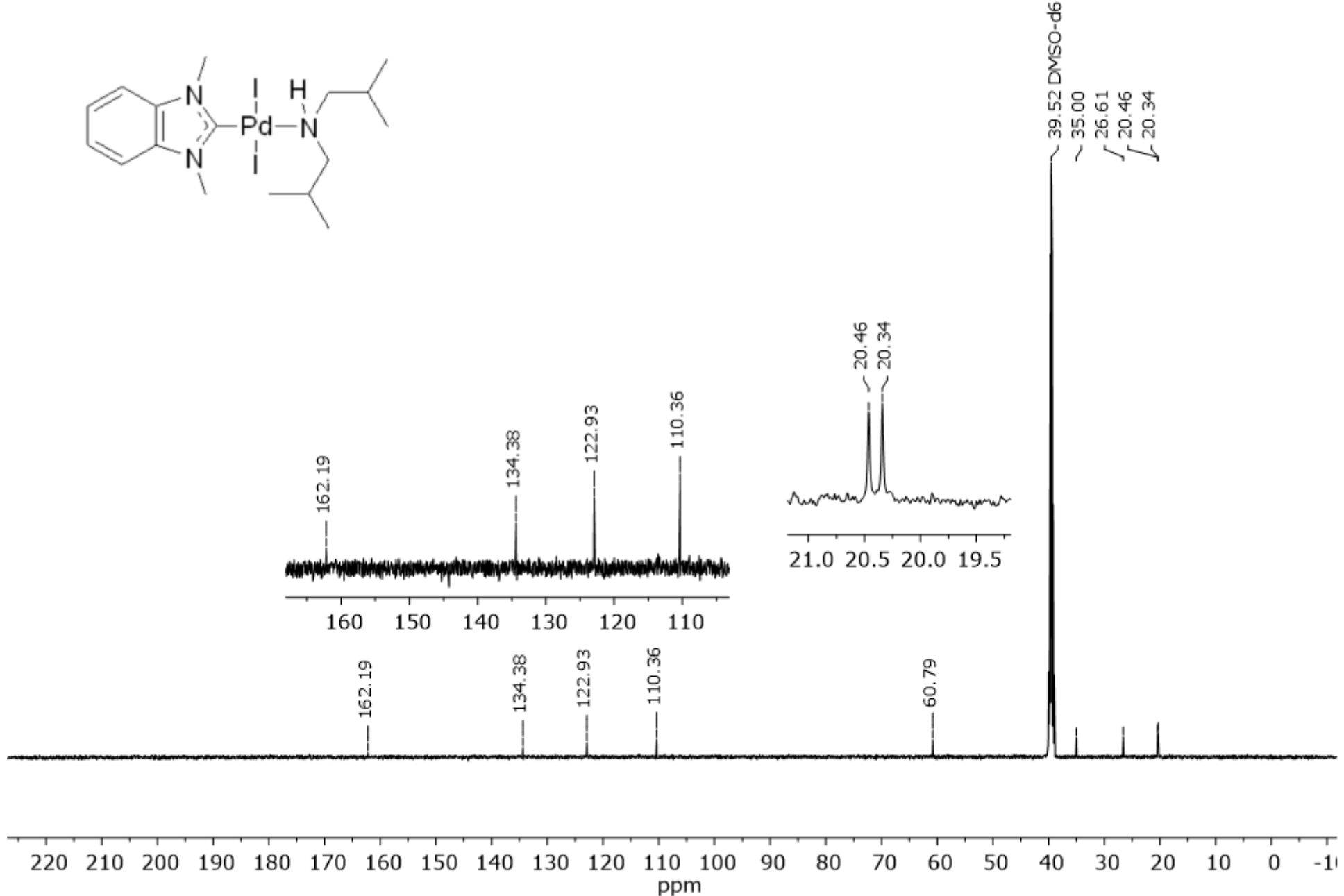
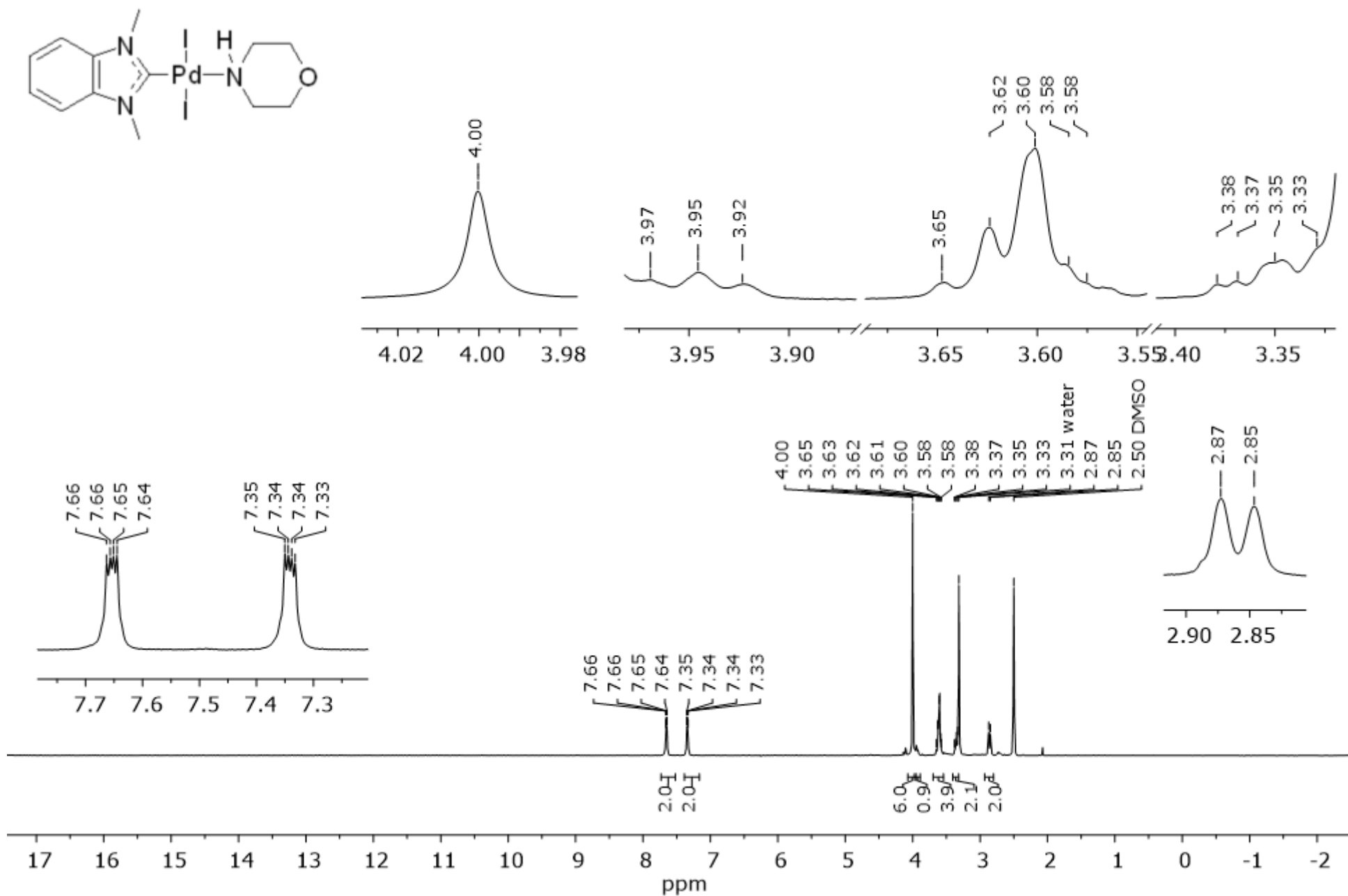


Figure S11.  $^1\text{H}$  NMR spectrum of compound **2b** ( $\text{DMSO}-d_6$ , 500 MHz)



**Figure S12.**  $^{13}\text{C}$  NMR spectrum of compound **2b** (DMSO- $d_6$ , 125 MHz)



**Figure S13.**  $^1\text{H}$  NMR spectrum of compound **2c** (DMSO- $d_6$ , 500 MHz)

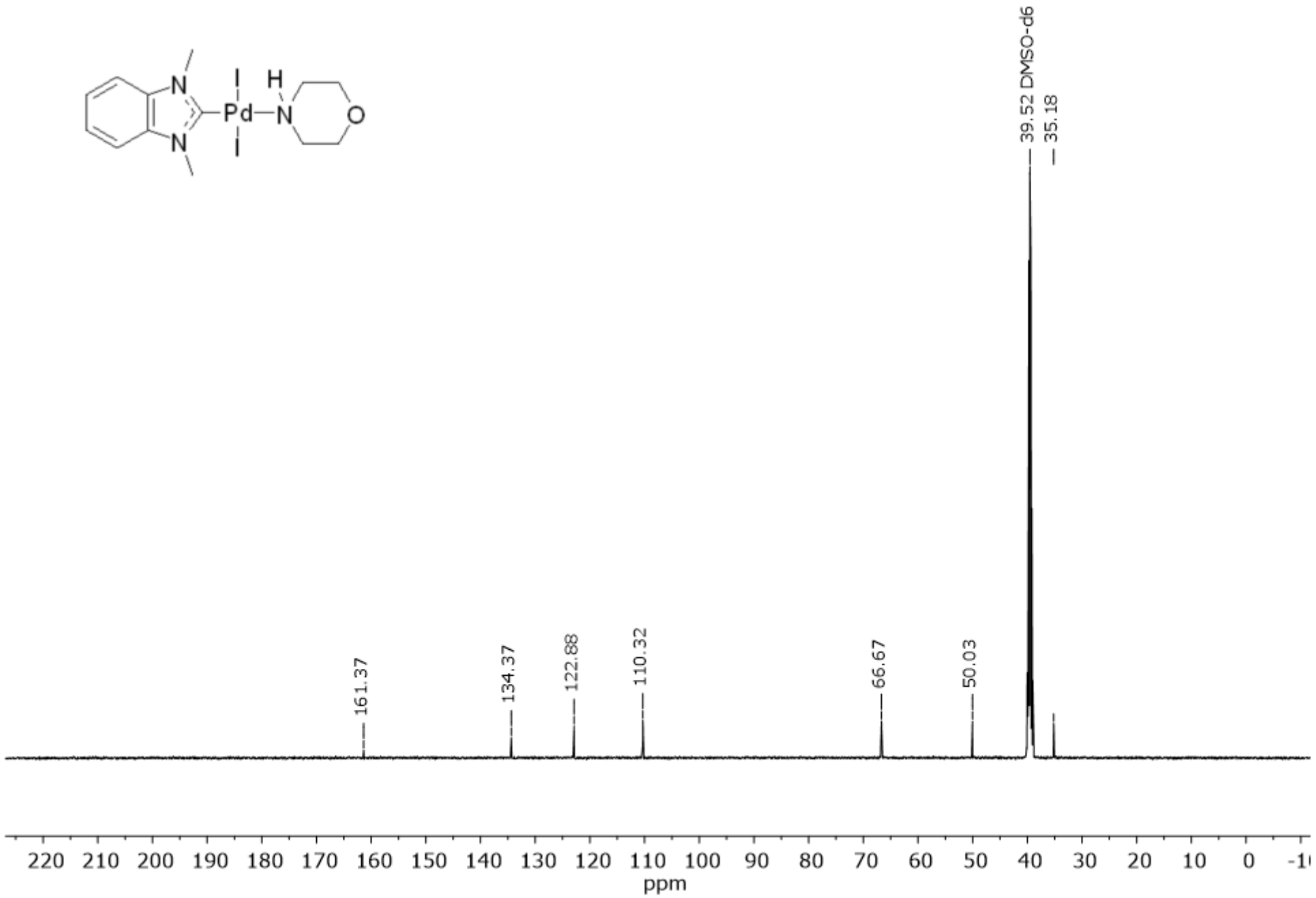


**Figure S14.**  $^{13}\text{C}$  NMR spectrum of compound **2c** (DMSO-*d*<sub>6</sub>, 125 MHz)

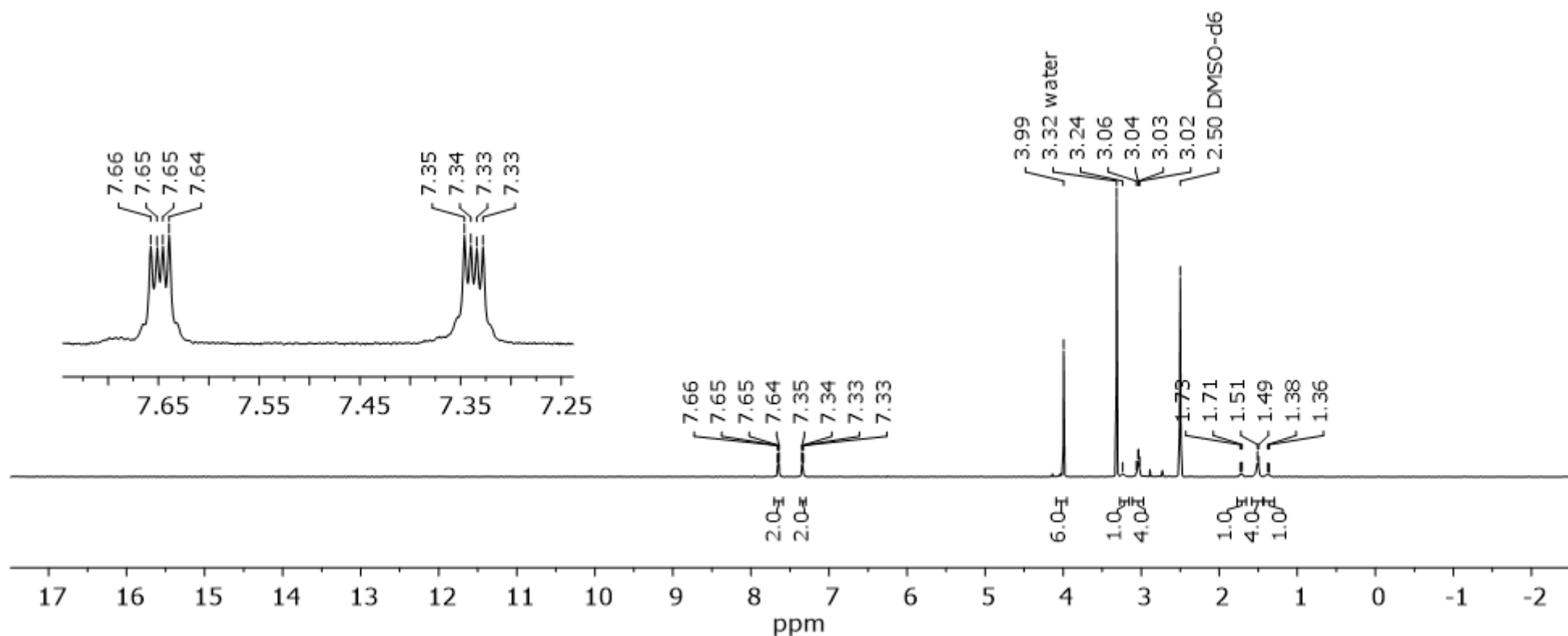
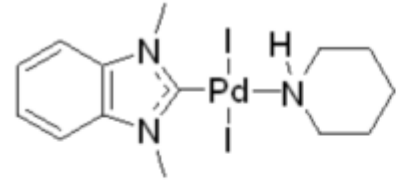


**Figure S15.** <sup>1</sup>H NMR spectrum of compound **2d** (DMSO-*d*<sub>6</sub>, 500 MHz)

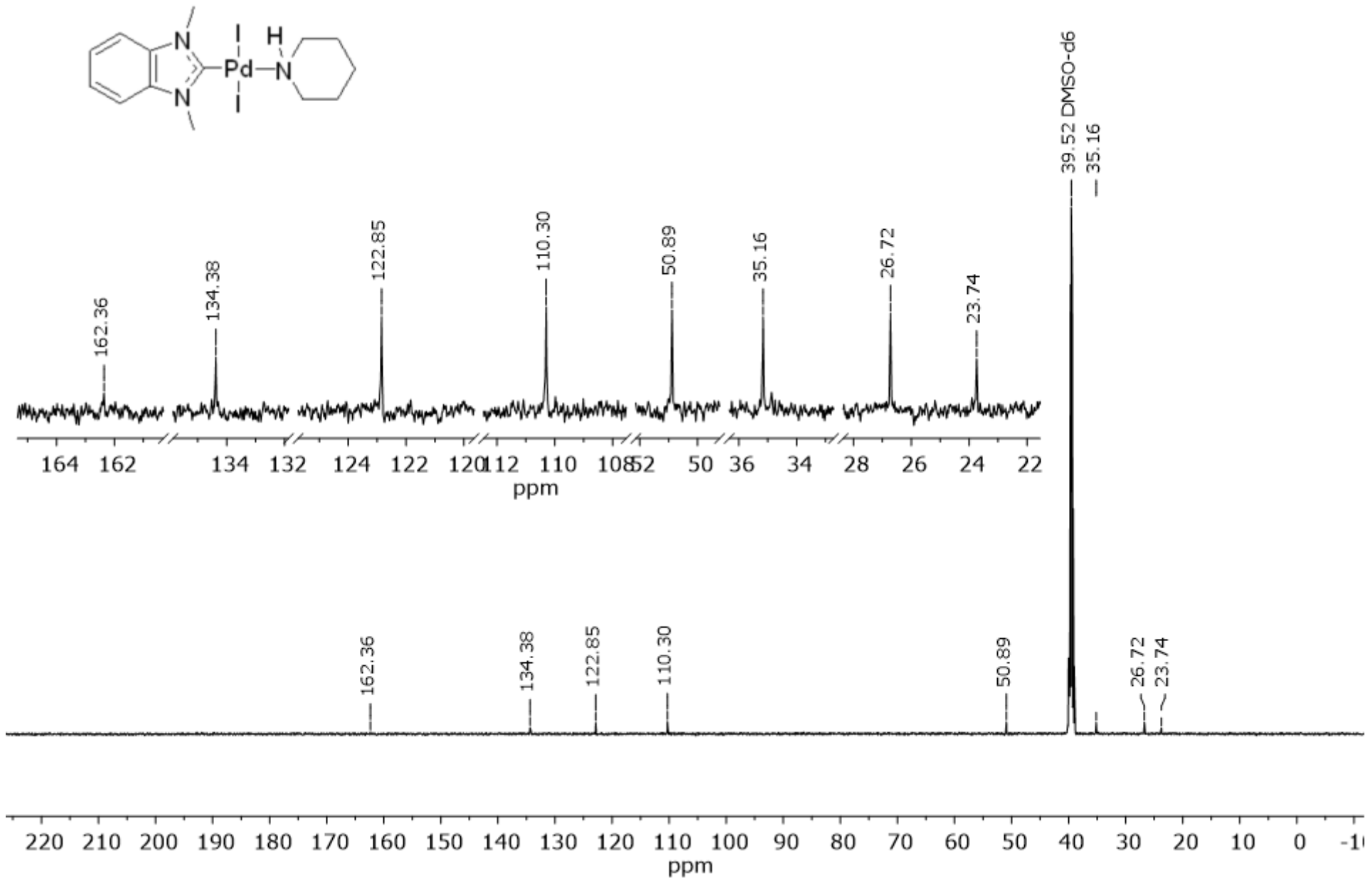


**Figure S16.**  $^{13}\text{C}$  NMR spectrum of compound **2d** (DMSO- $d_6$ , 125 MHz)

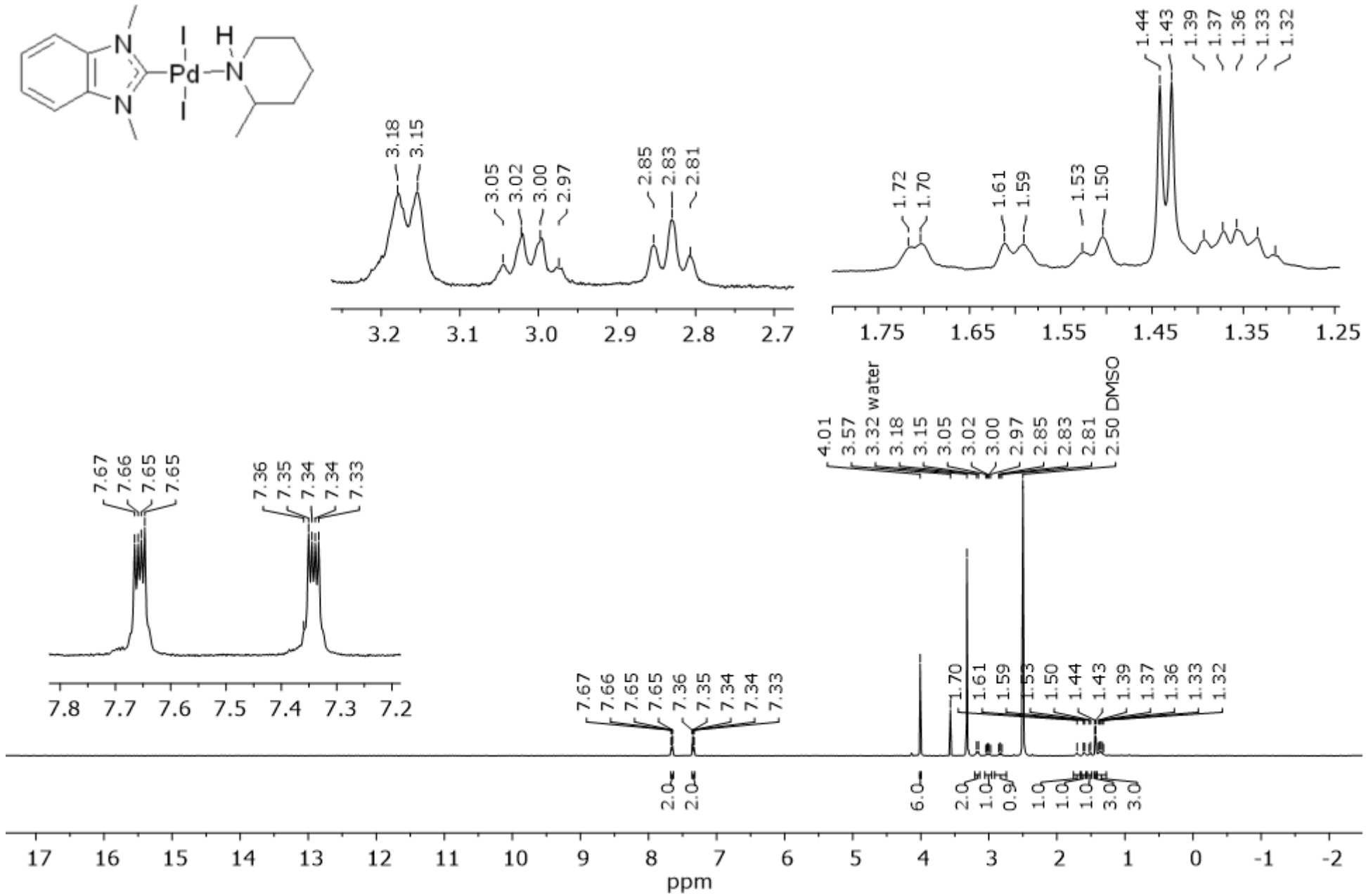


**Figure S17.**  $^1\text{H}$  NMR spectrum of compound **2e** ( $\text{DMSO}-d_6$ , 500 MHz)

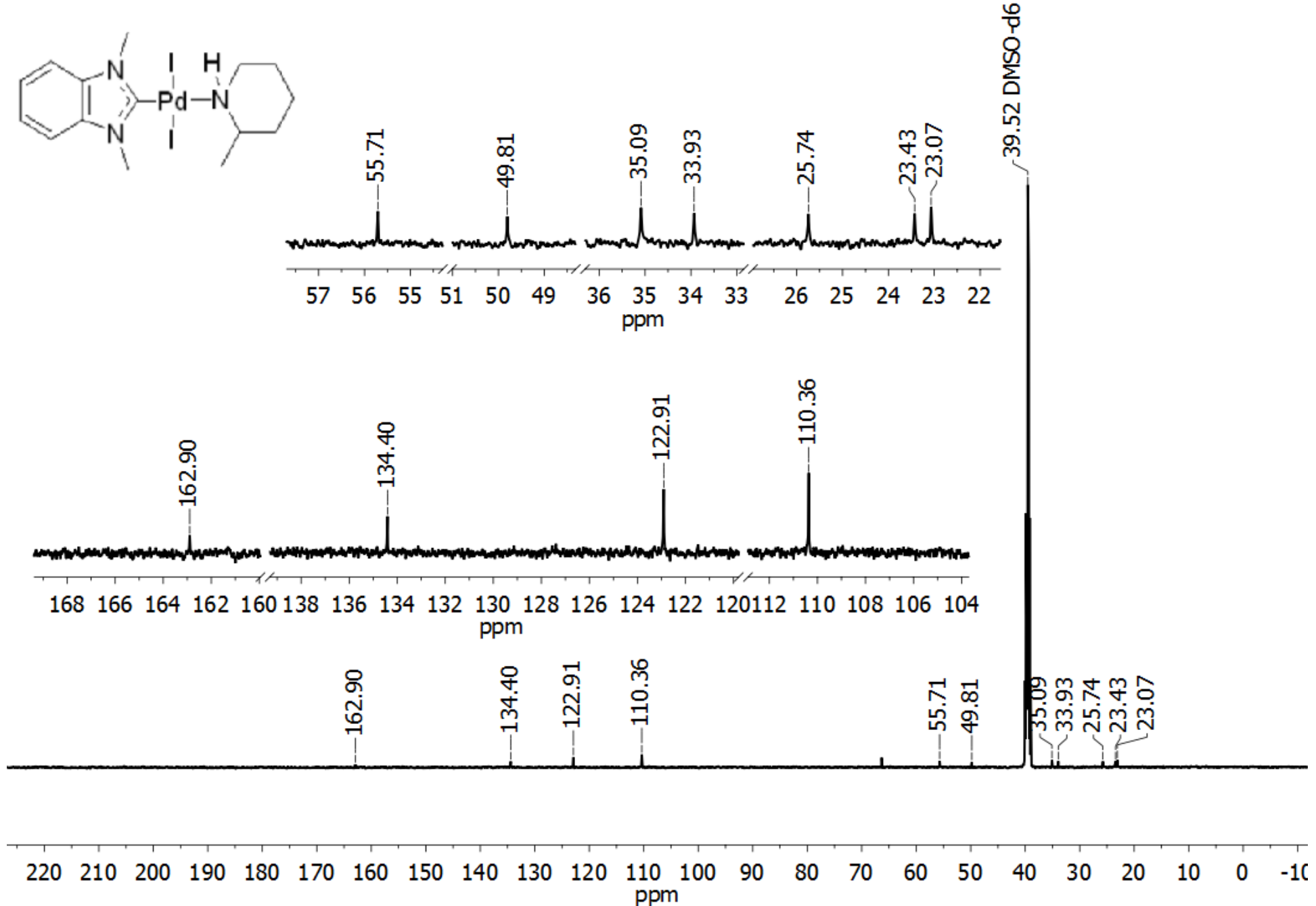
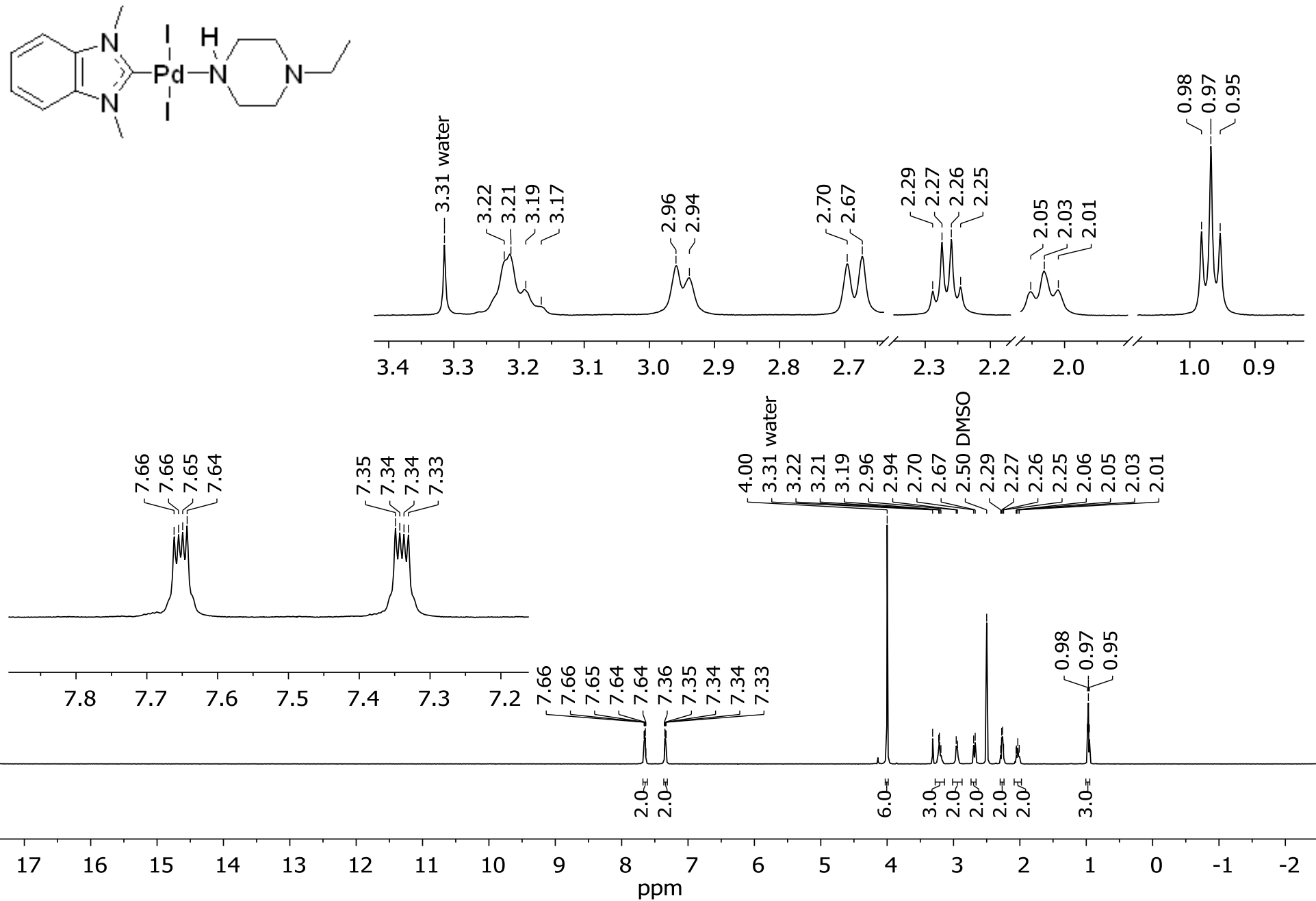
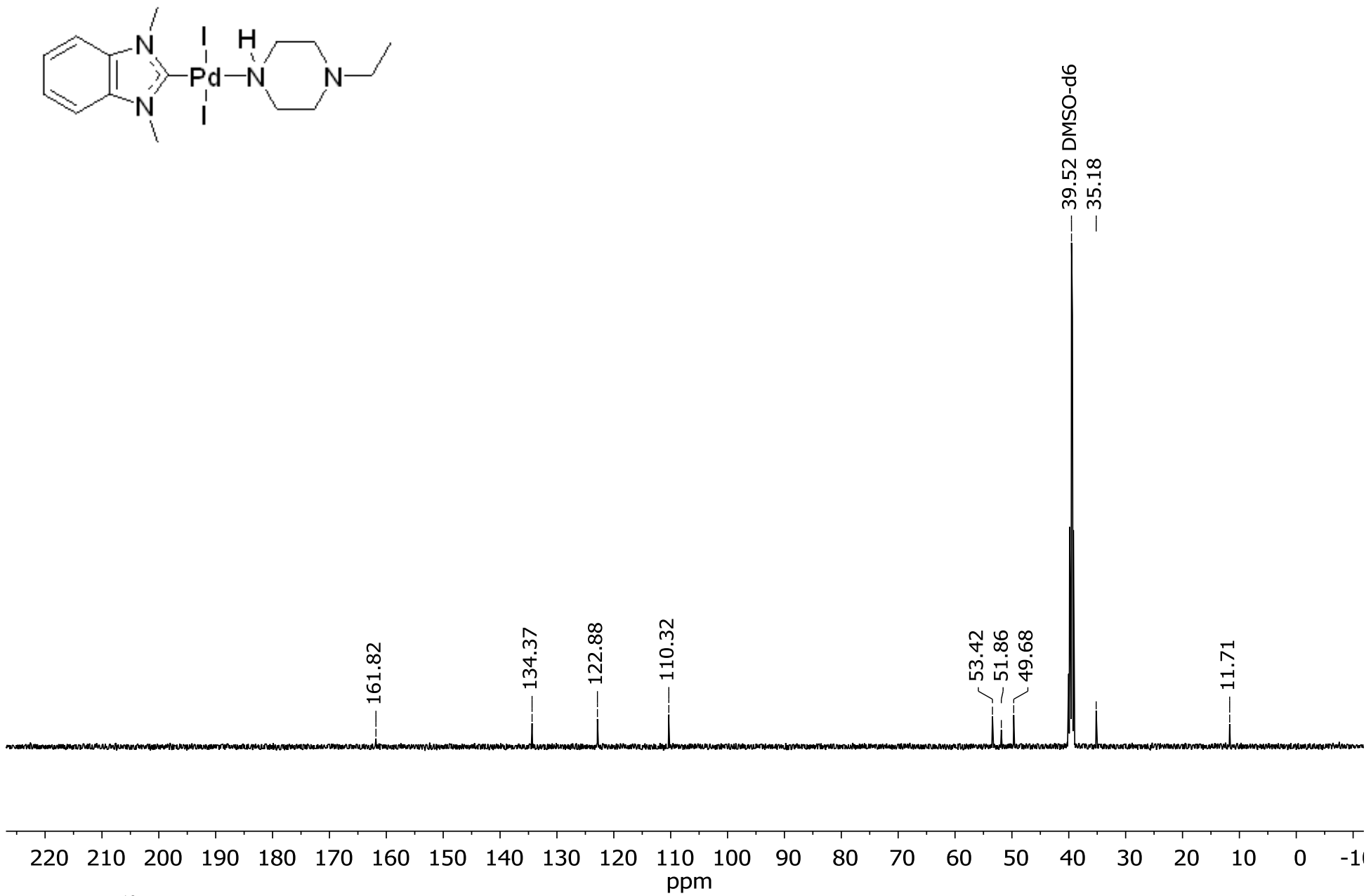


Figure S18.  $^{13}\text{C}$  NMR spectrum of compound **2e** (DMSO-*d*<sub>6</sub>, 125 MHz)



**Figure S19.**  $^1\text{H}$  NMR spectrum of compound **2f** ( $\text{DMSO}-d_6$ , 500 MHz)



**Figure S20.**  $^{13}\text{C}$  NMR spectrum of compound **2f** (DMSO- $d_6$ , 125 MHz)

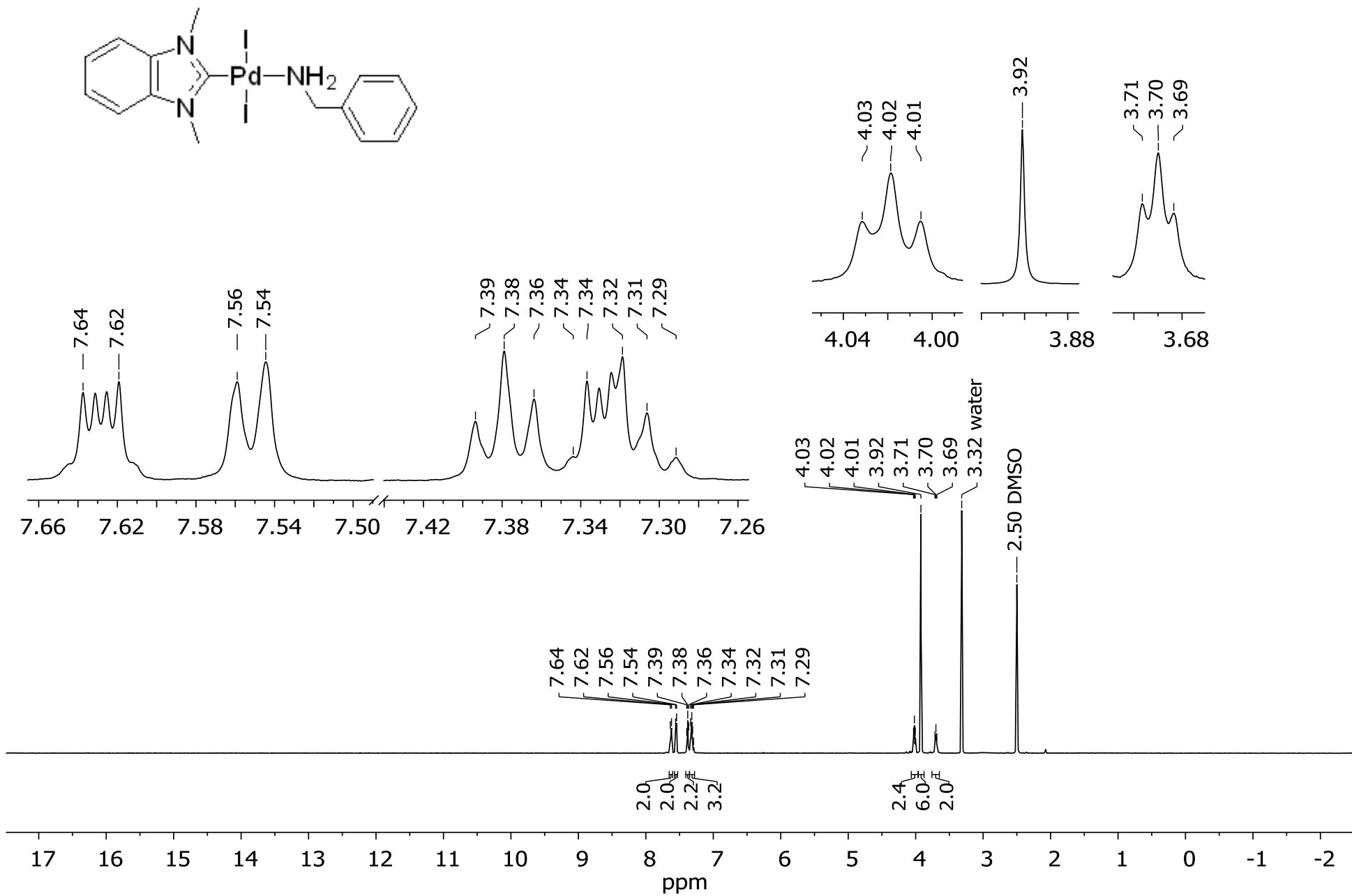


**Figure S21.** <sup>1</sup>H NMR spectrum of compound **2g** ( $\text{DMSO}-d_6$ , 500 MHz)

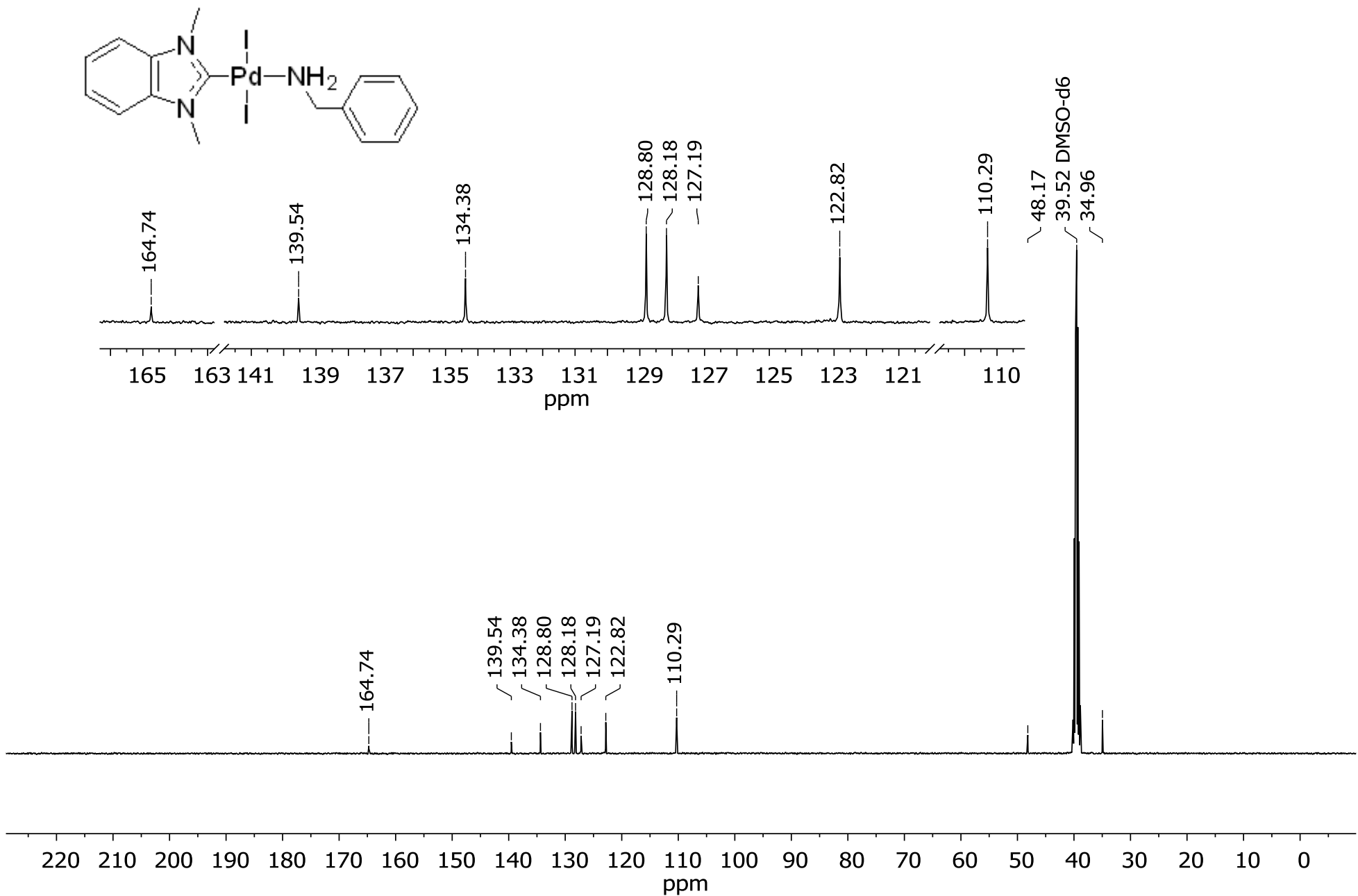


**Figure S22.**  $^{13}\text{C}$  NMR spectrum of compound **2g** (DMSO-*d*<sub>6</sub>, 125 MHz)

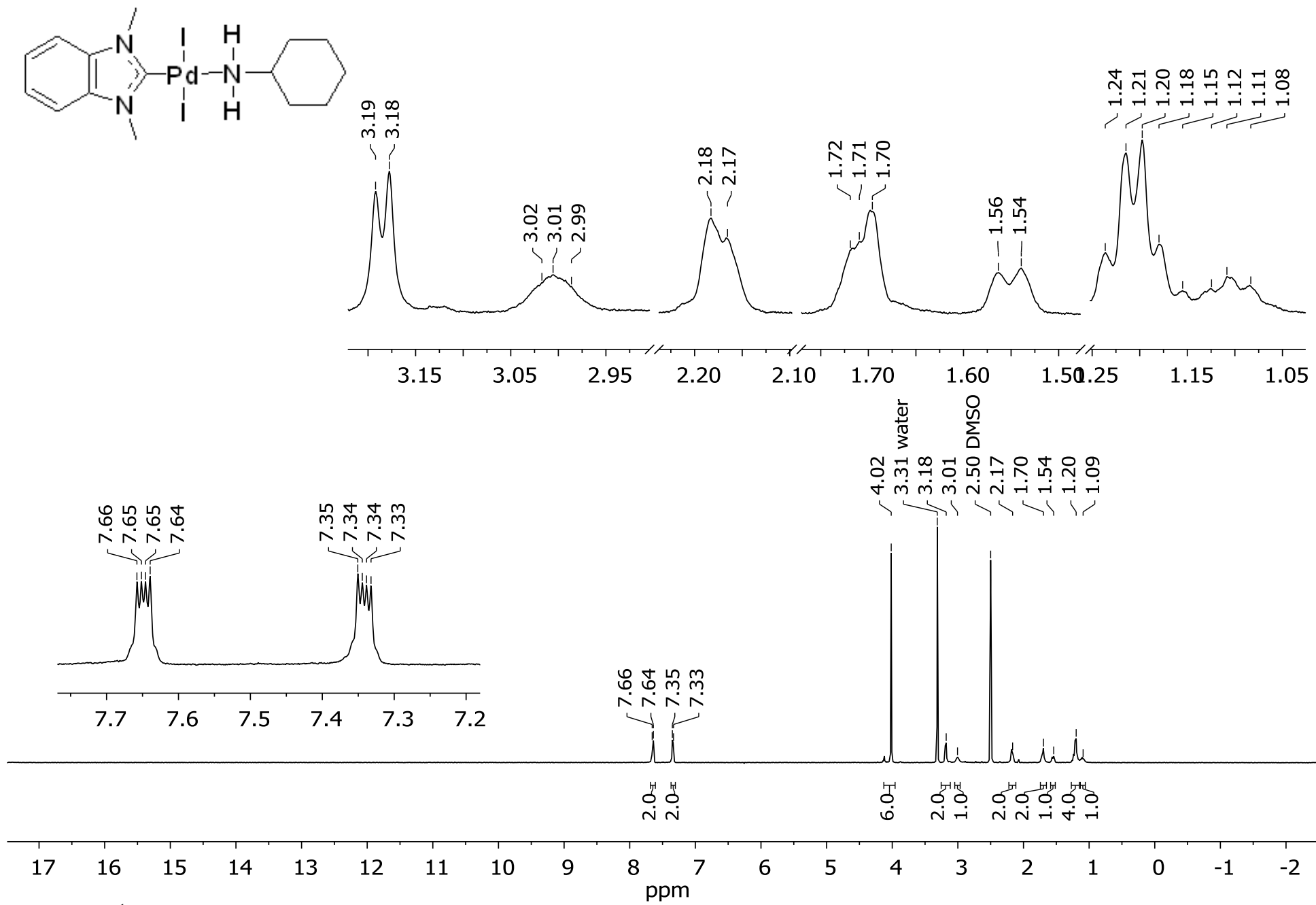


**Figure S23.**  $^1\text{H}$  NMR spectrum of compound **2h** ( $\text{DMSO}-d_6$ , 500 MHz)

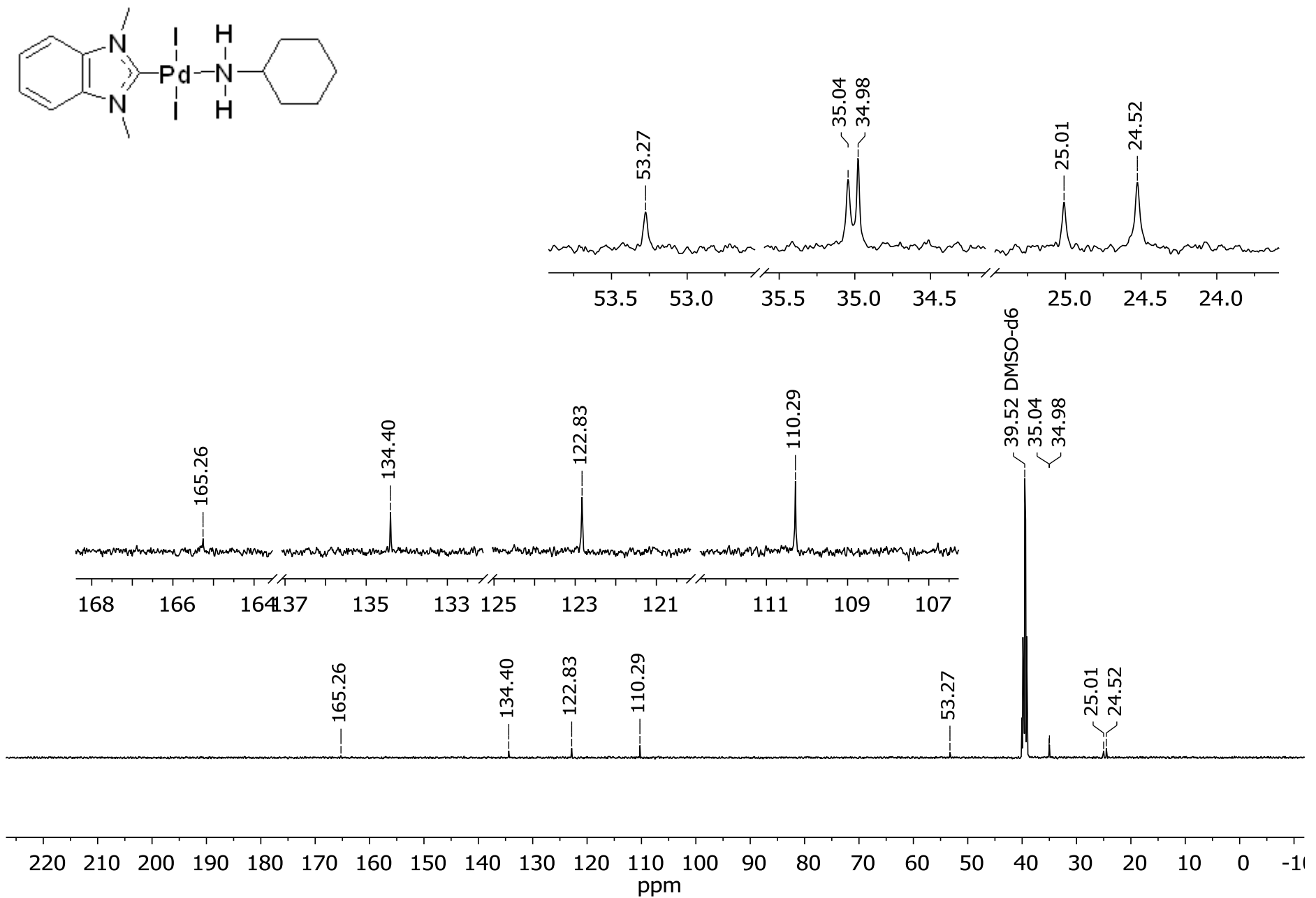


**Figure S24.**  $^{13}\text{C}$  NMR spectrum of compound **2h** (DMSO- $d_6$ , 125 MHz)

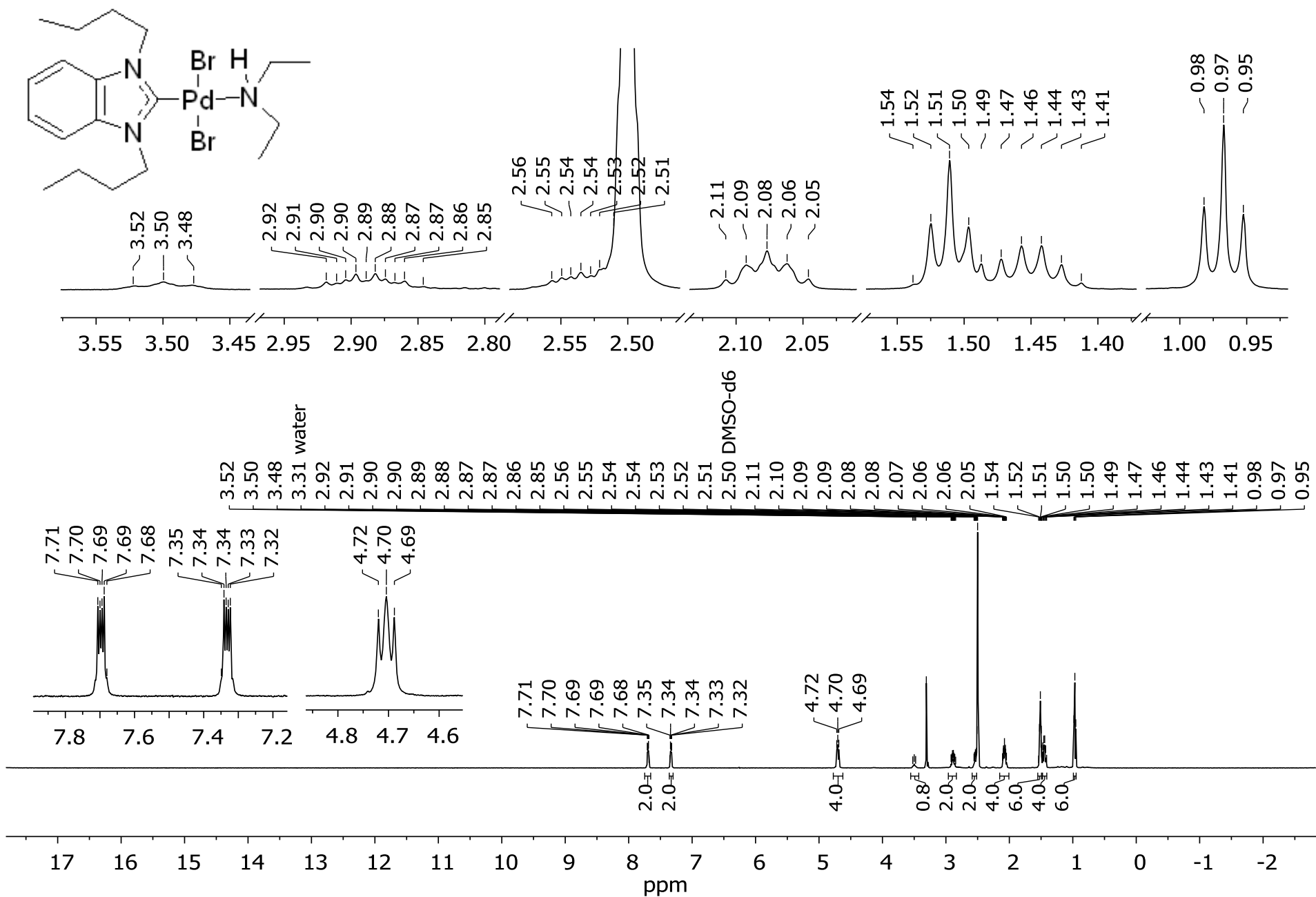


**Figure S25.**  $^1\text{H}$  NMR spectrum of compound **2i** ( $\text{DMSO}-d_6$ , 500 MHz)

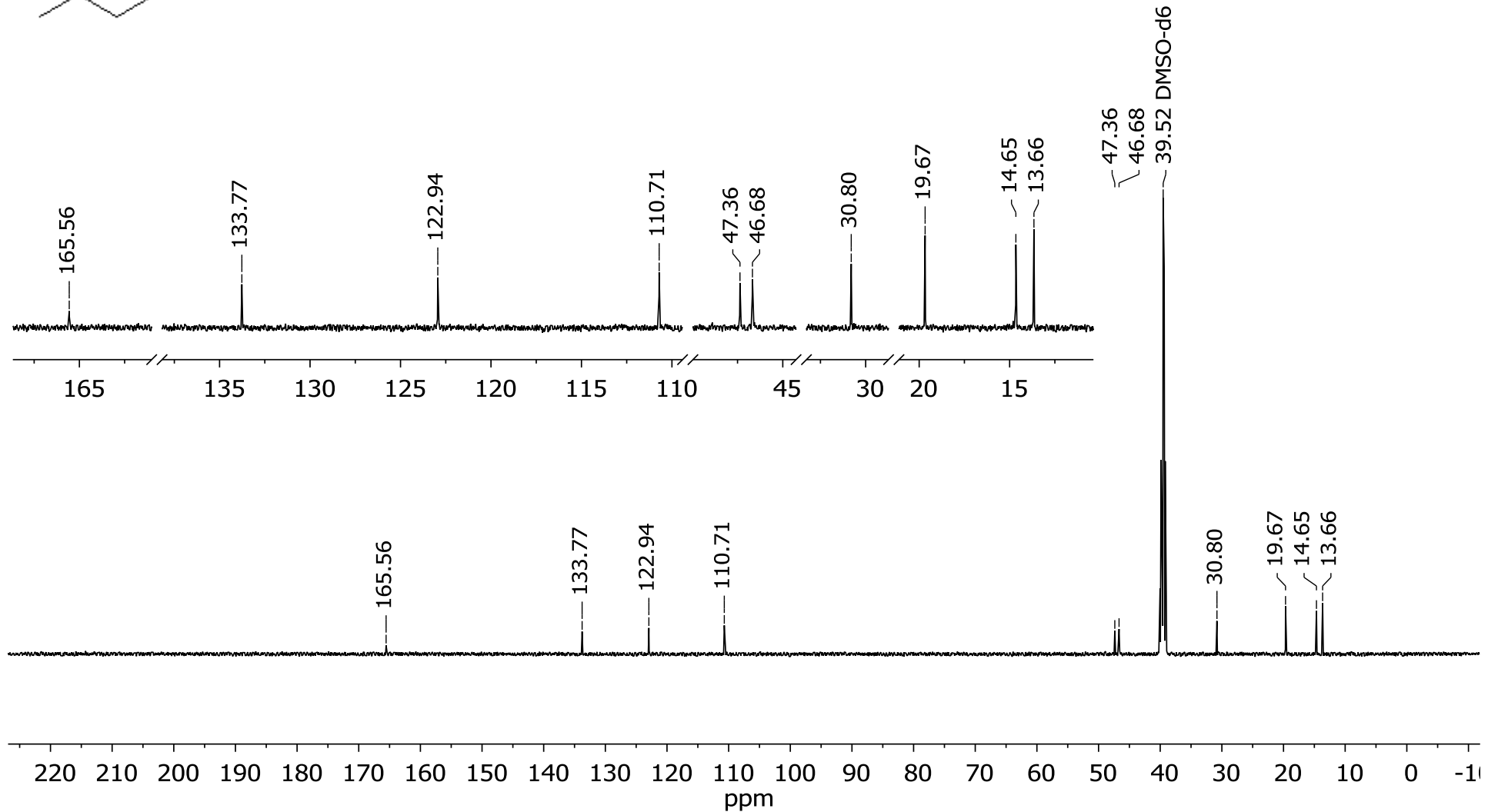
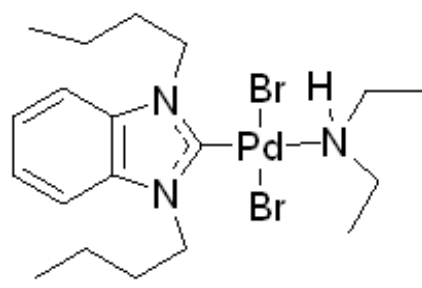
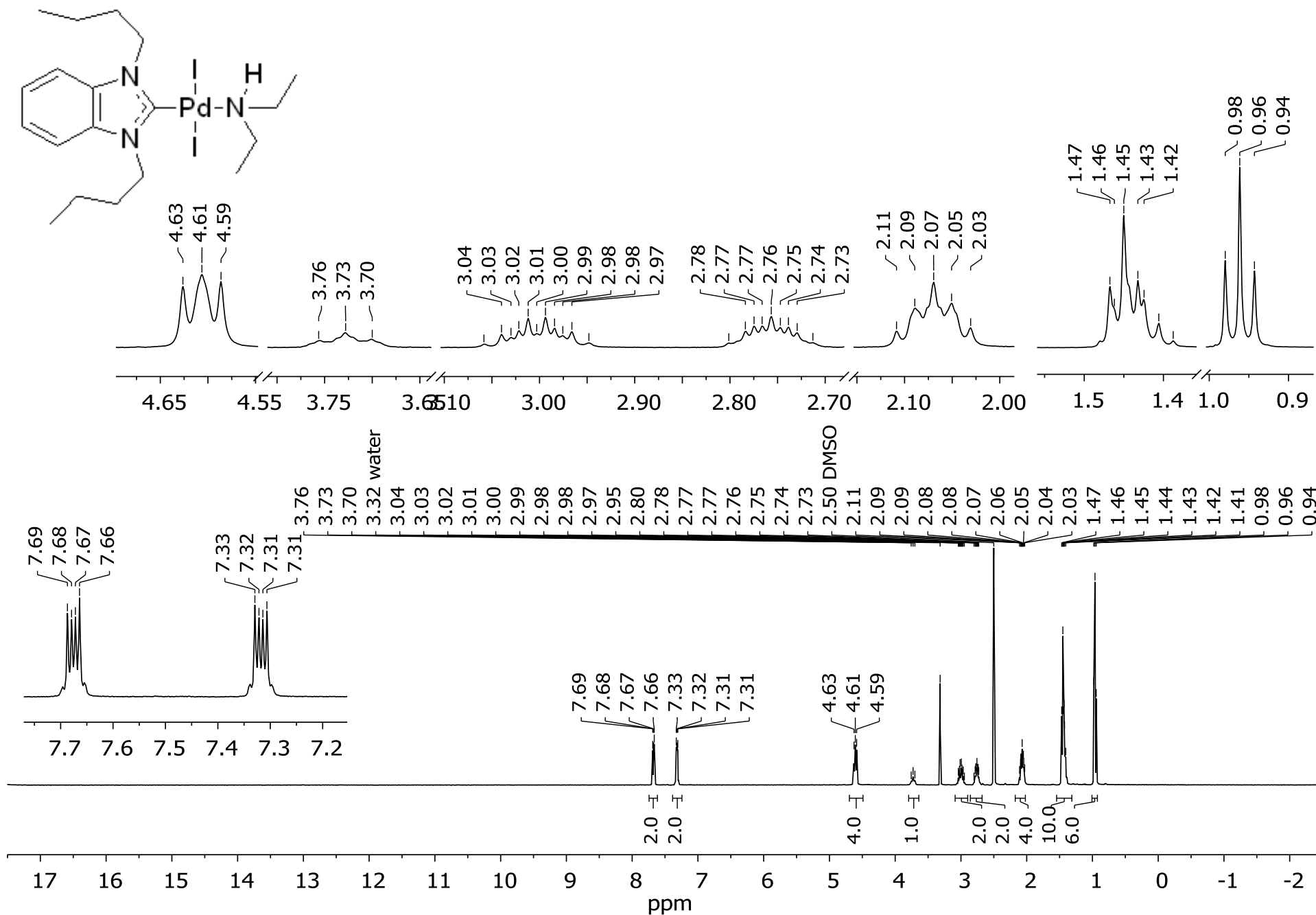


Figure S26.  $^{13}\text{C}$  NMR spectrum of compound **2i** (DMSO- $d_6$ , 125 MHz)



**Figure S27.**  $^1\text{H}$  NMR spectrum of compound **2j** (DMSO- $d_6$ , 500 MHz)

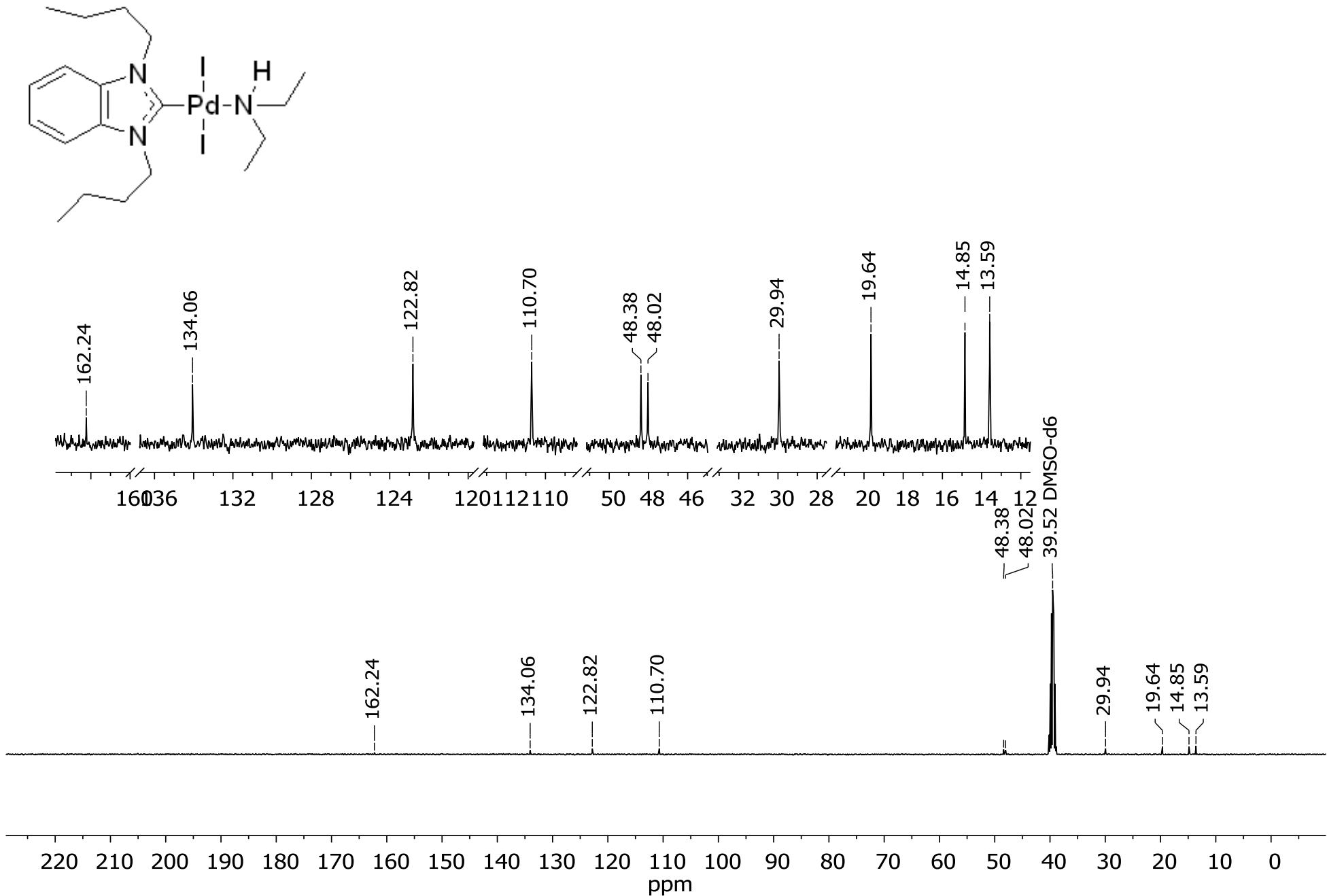
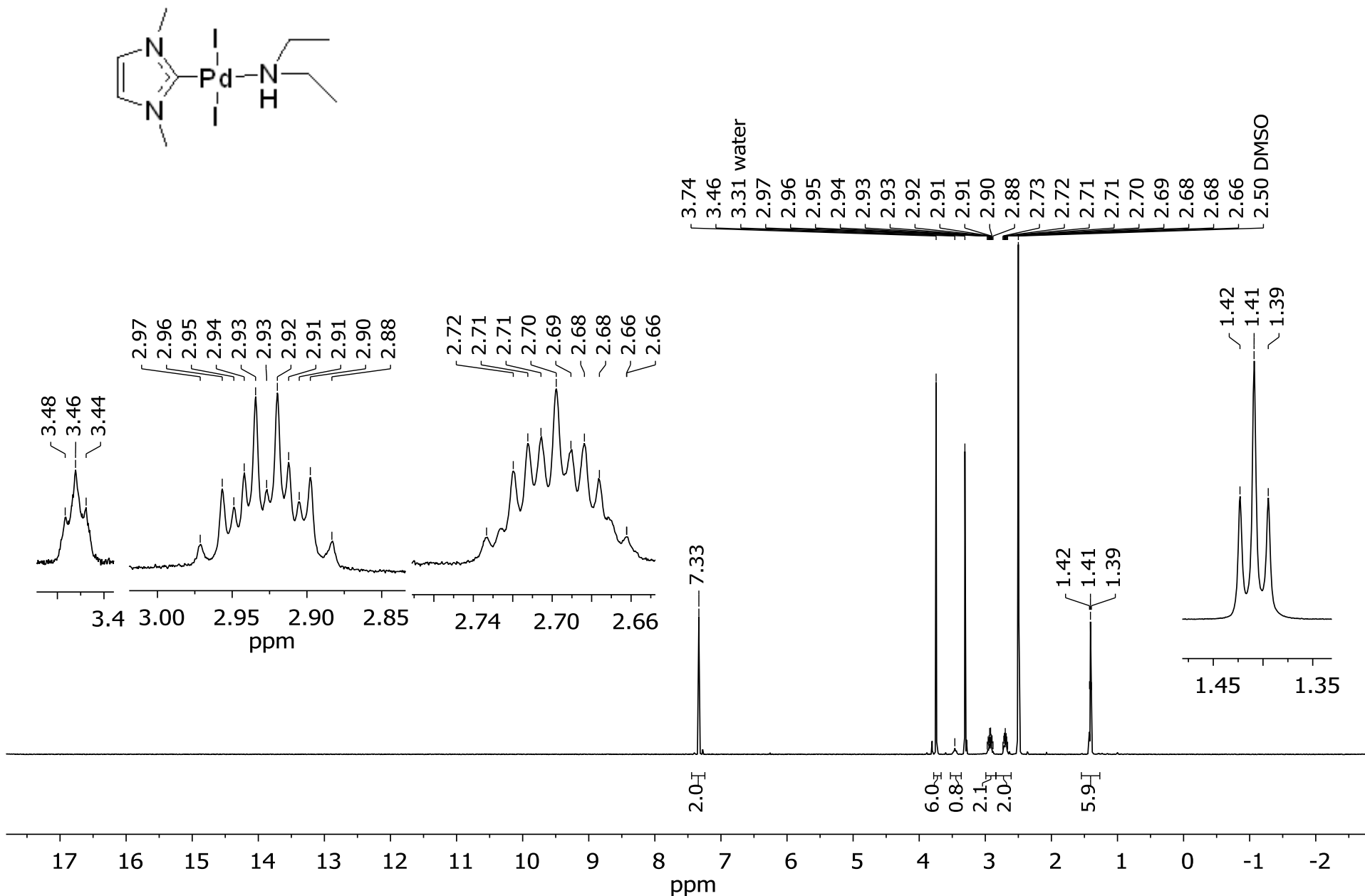
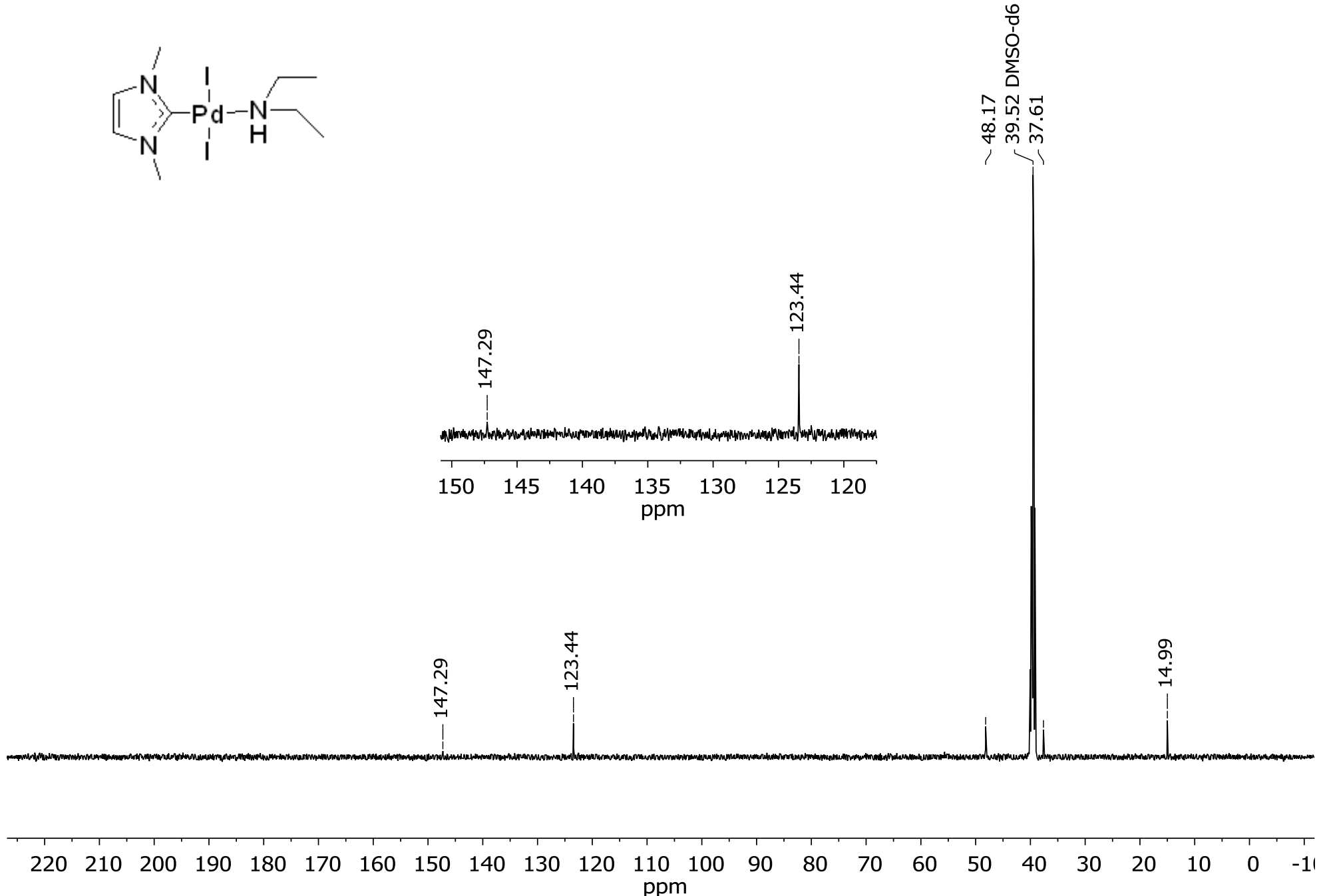


Figure S28.  $^{13}\text{C}$  NMR spectrum of compound **2j** (DMSO- $d_6$ , 125 MHz)



**Figure S29.**  $^1\text{H}$  NMR spectrum of compound **2k** ( $\text{DMSO}-d_6$ , 500 MHz)



**Figure S30.**  $^{13}\text{C}$  NMR spectrum of compound **2k** ( $\text{DMSO}-d_6$ , 125 MHz)

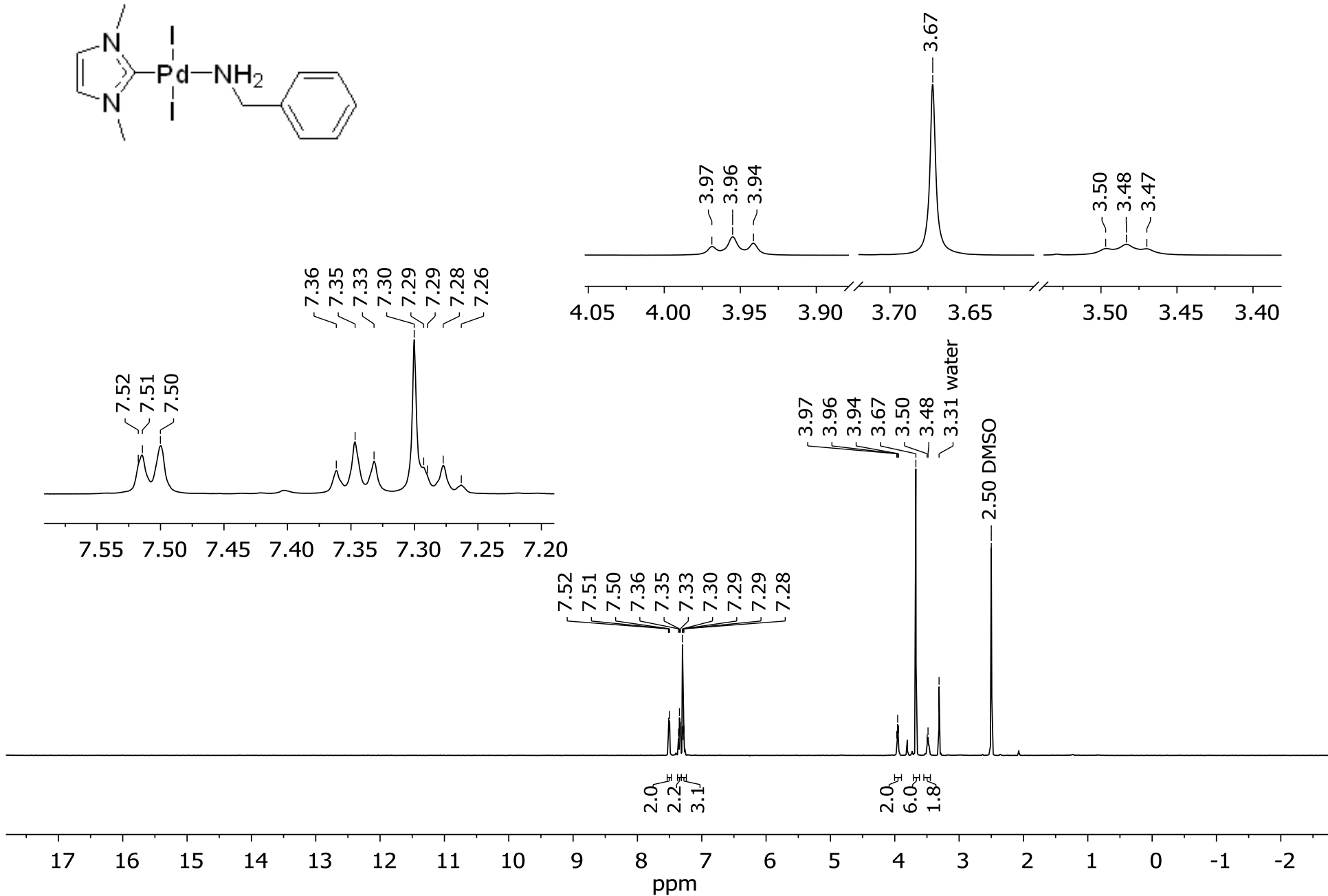


**Figure S31.**  $^1\text{H}$  NMR spectrum of compound **2l** ( $\text{DMSO}-d_6$ , 500 MHz)

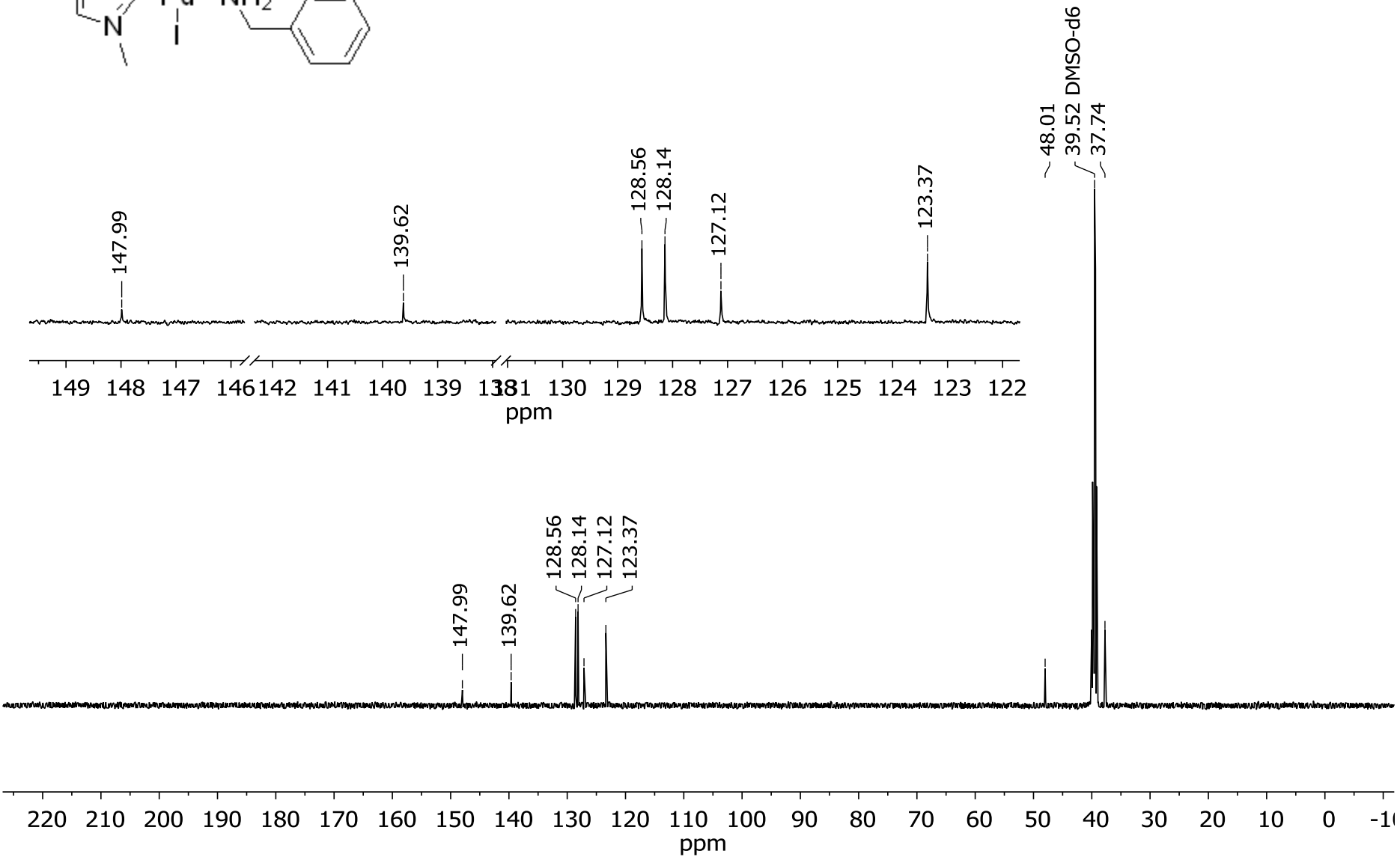
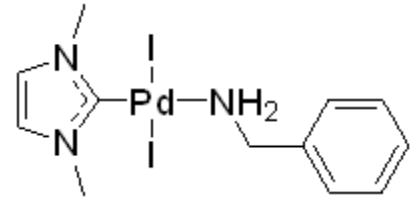


**Figure S32.**  $^{13}\text{C}$  NMR spectrum of compound **2l** (DMSO- $d_6$ , 125 MHz)

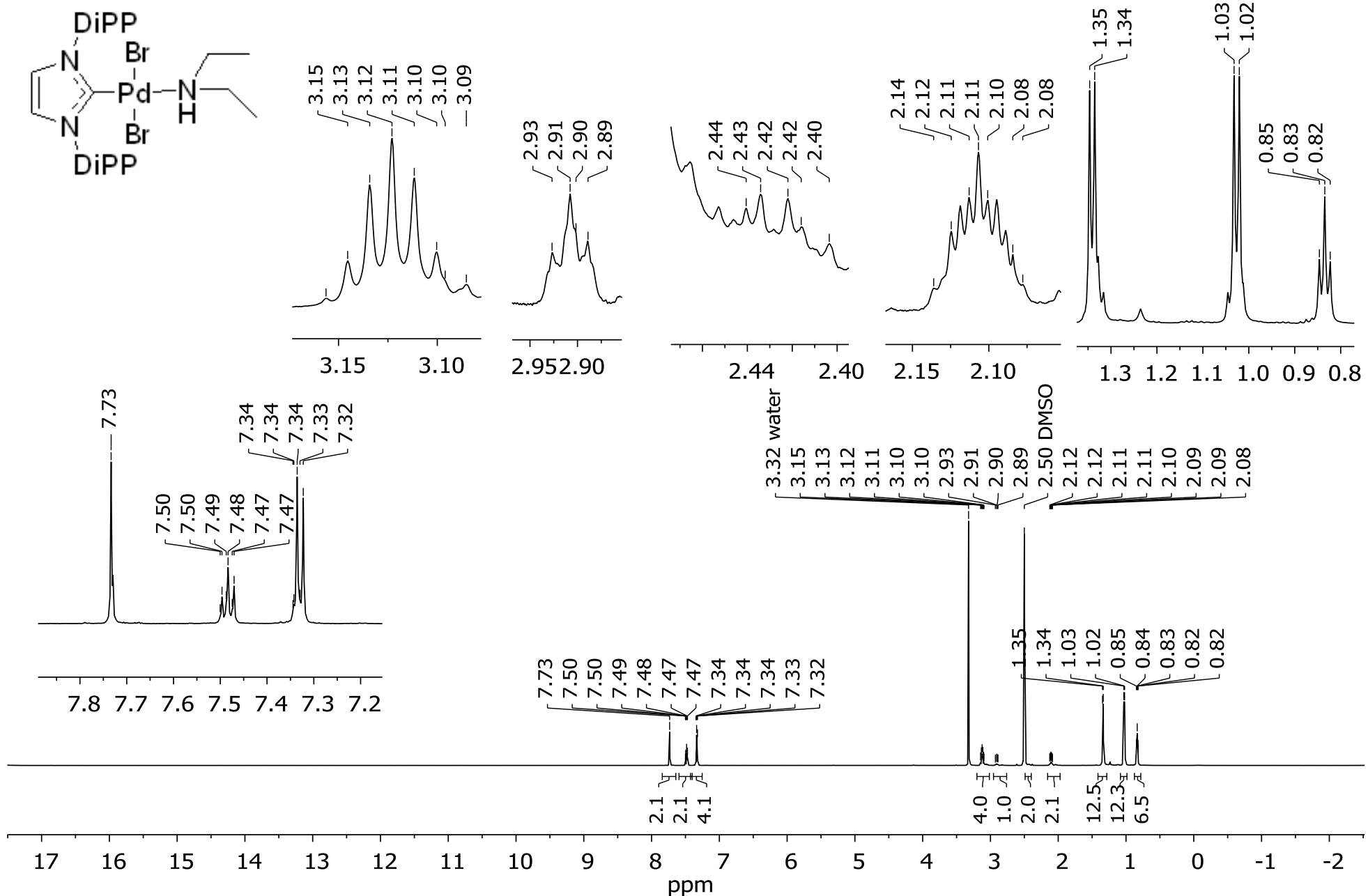


**Figure S33.** <sup>1</sup>H NMR spectrum of compound **2n** (DMSO-*d*<sub>6</sub>, 500 MHz)

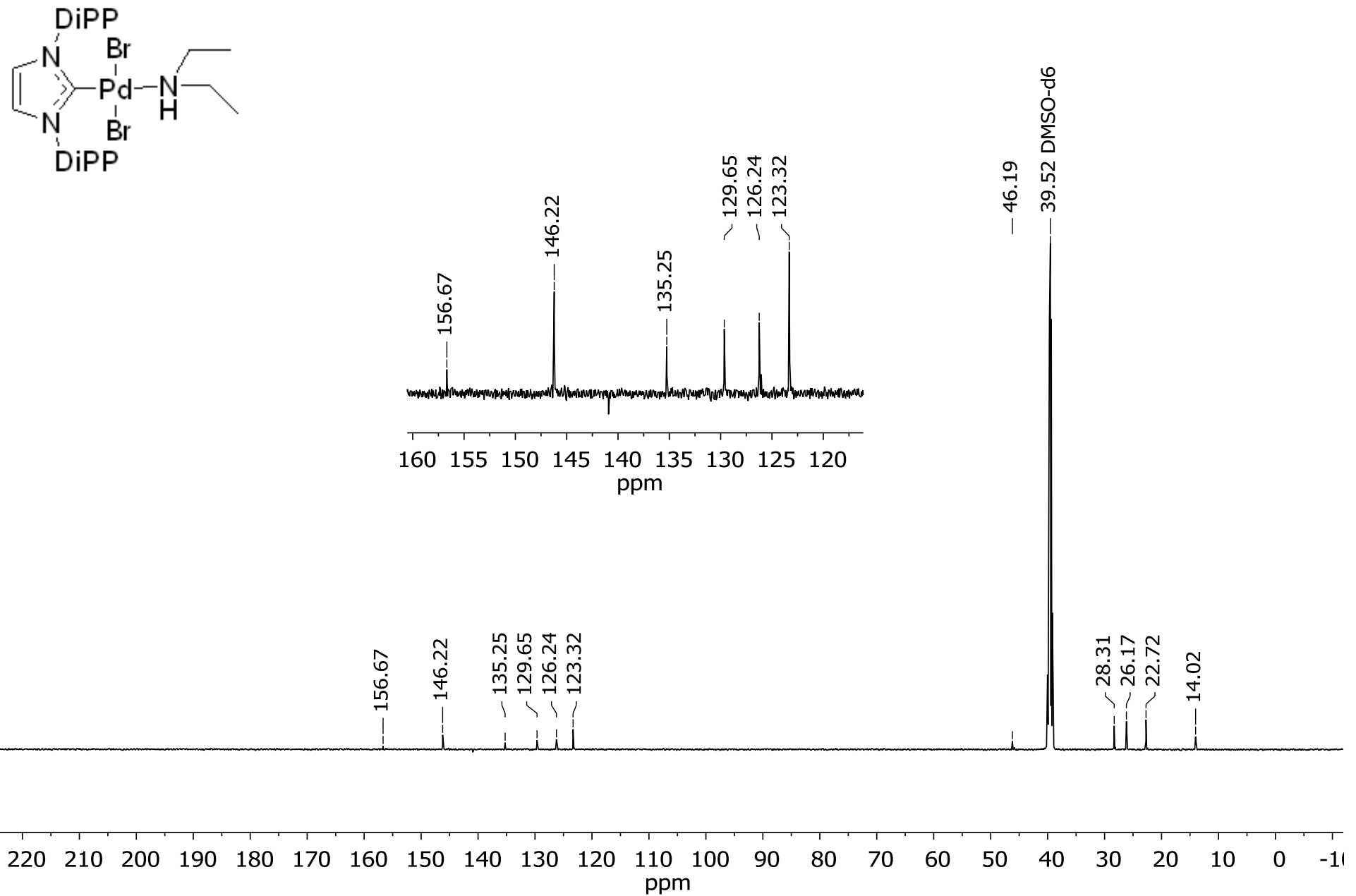


**Figure S34.**  $^{13}\text{C}$  NMR spectrum of compound **2n** (DMSO- $d_6$ , 125 MHz)

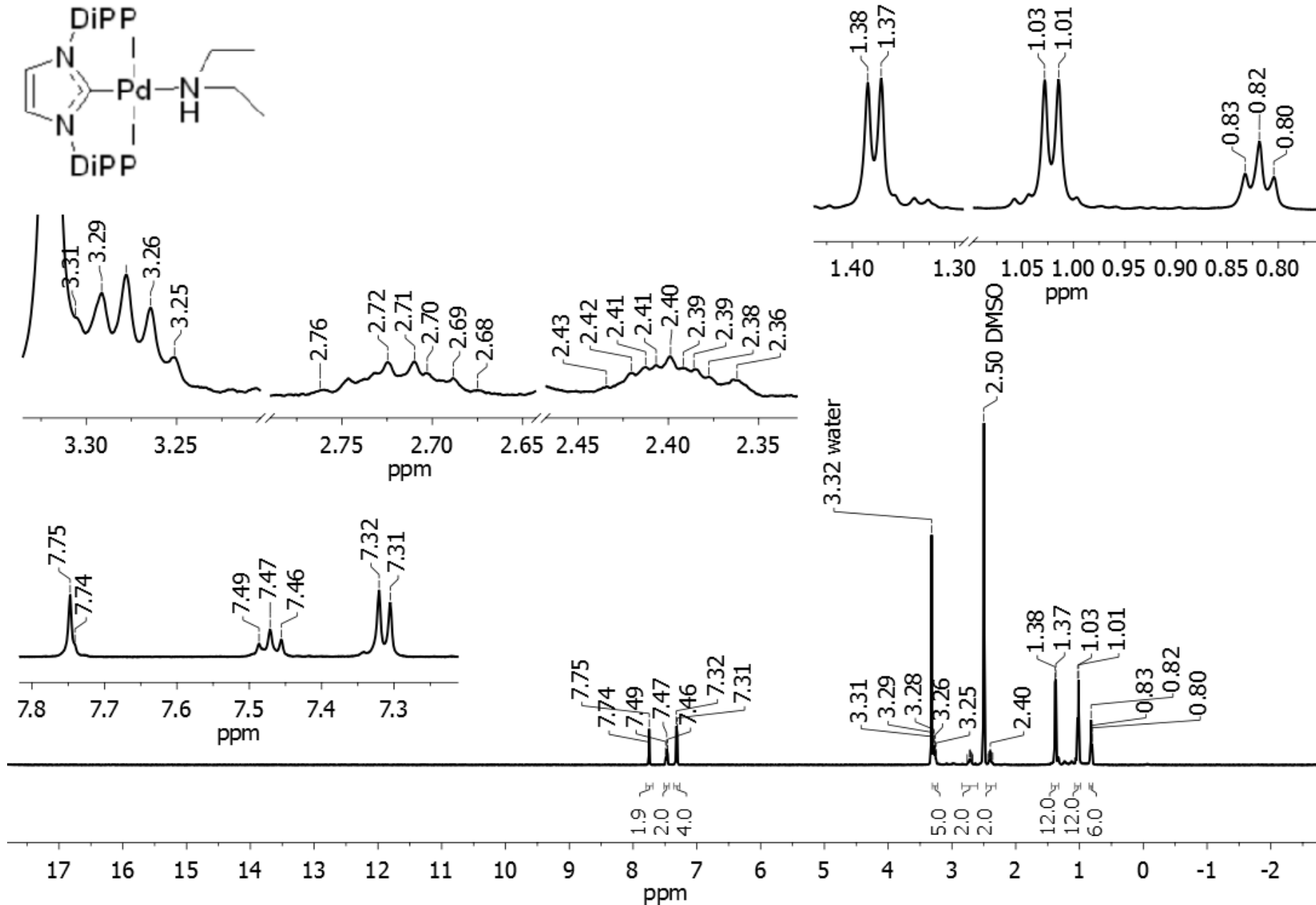
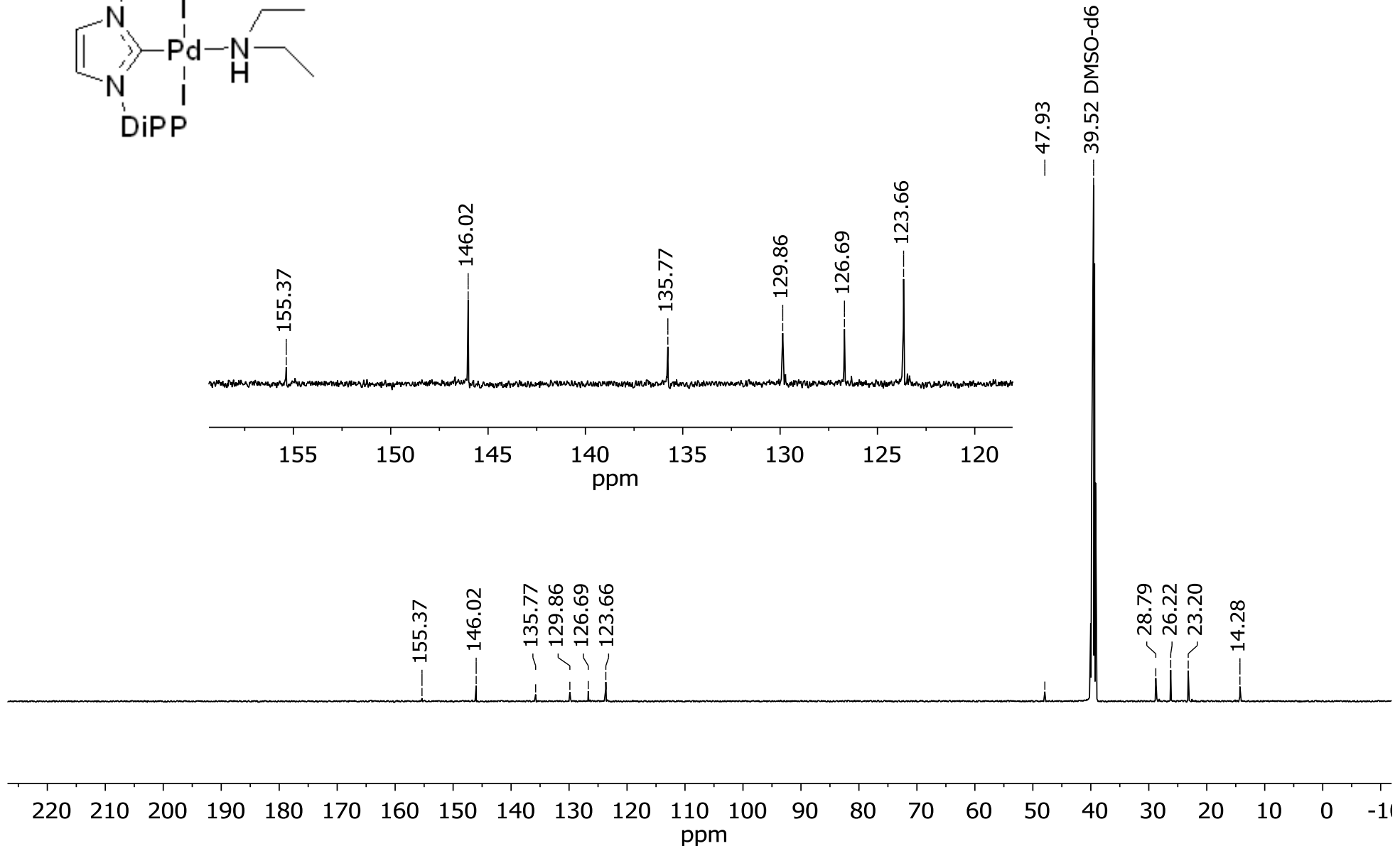
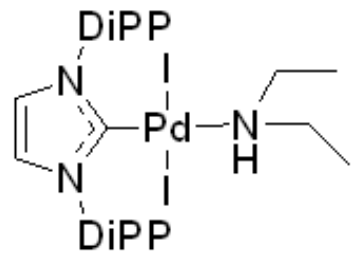
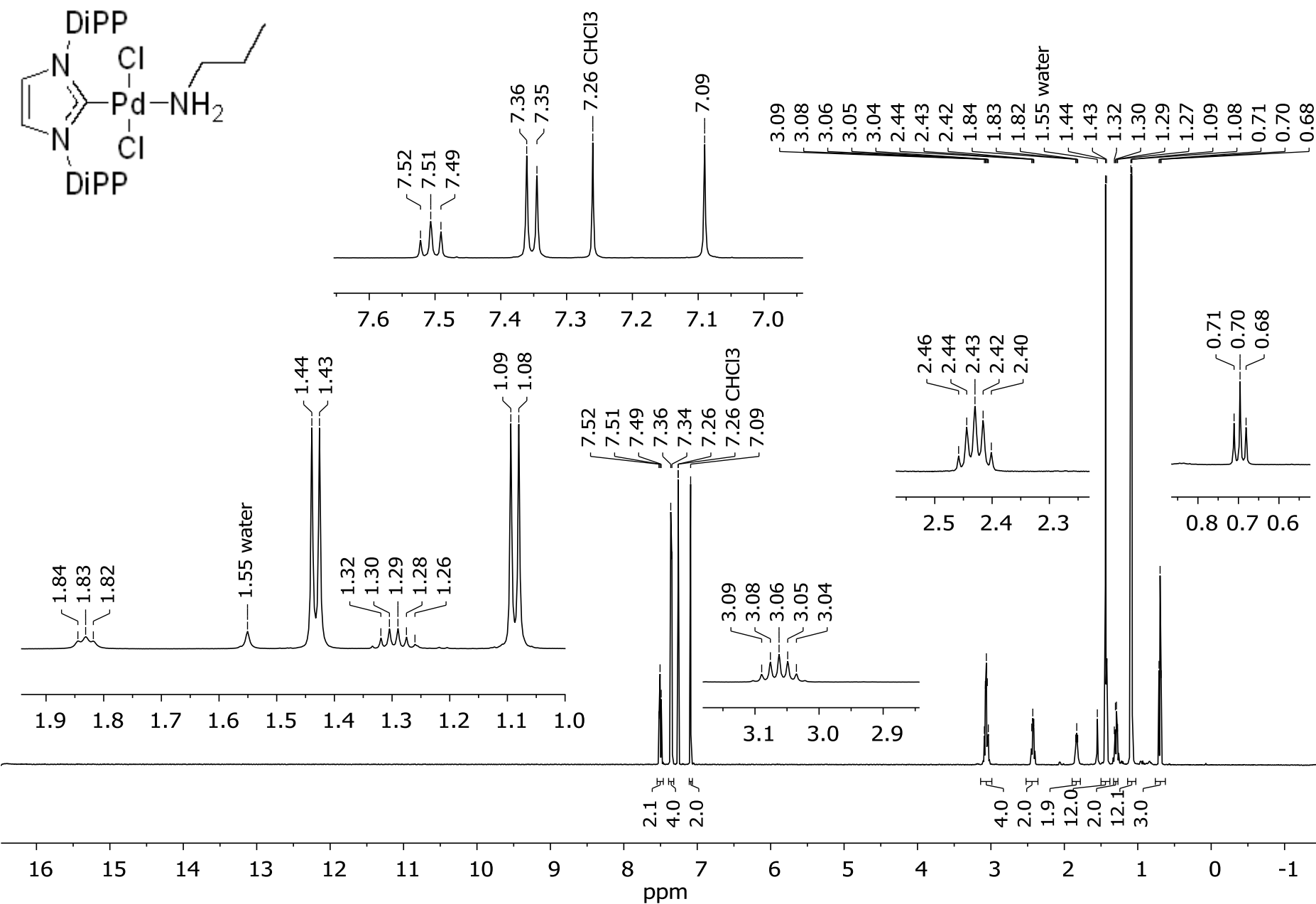


Figure S35. <sup>1</sup>H NMR spectrum of compound **2o** (DMSO-*d*<sub>6</sub>, 500 MHz)



**Figure S36.** <sup>13</sup>C NMR spectrum of compound **2o** (DMSO-*d*<sub>6</sub>, 125 MHz)



**Figure S37.** <sup>1</sup>H NMR spectrum of compound **2q** ( $\text{CDCl}_3$ , 500 MHz)

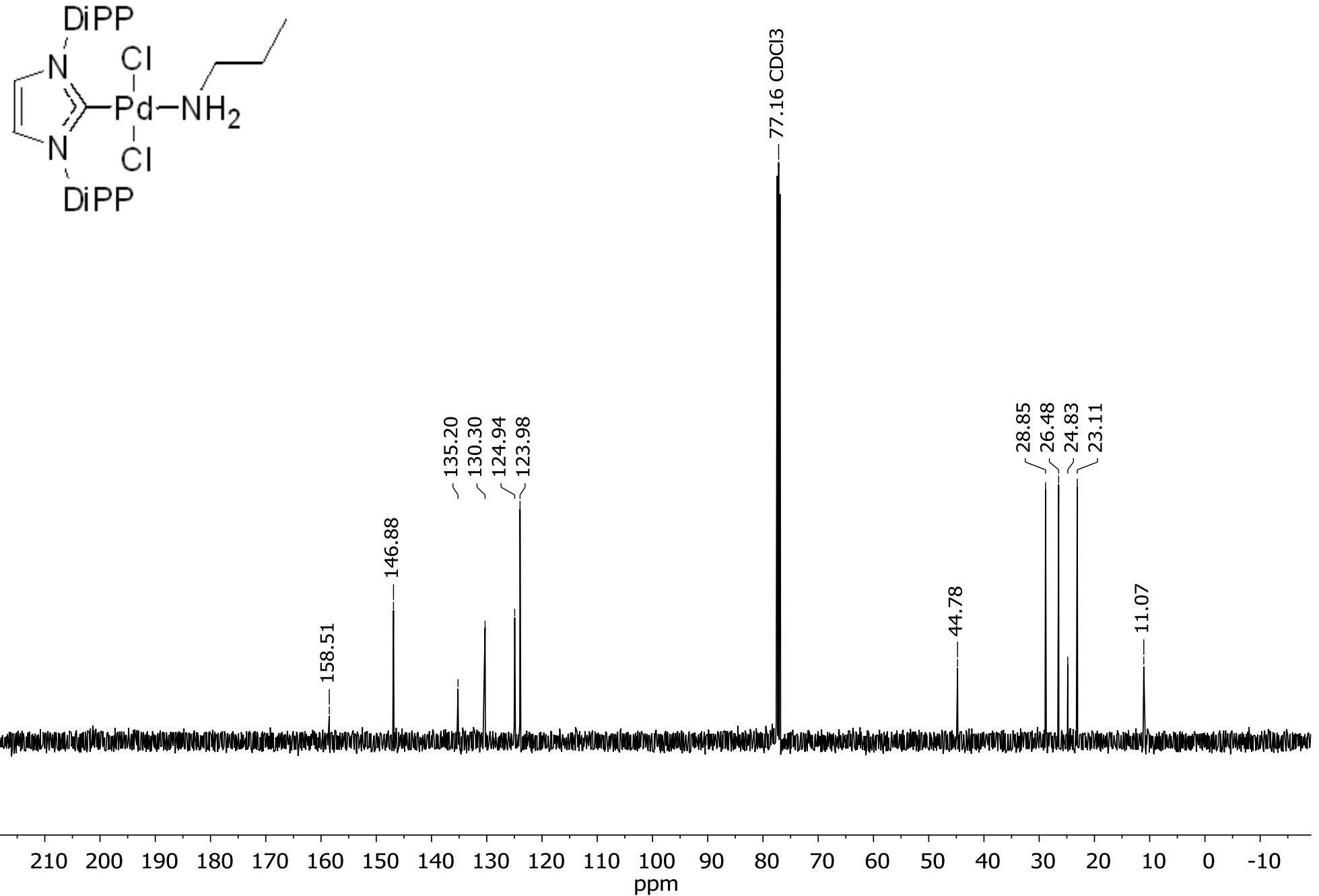
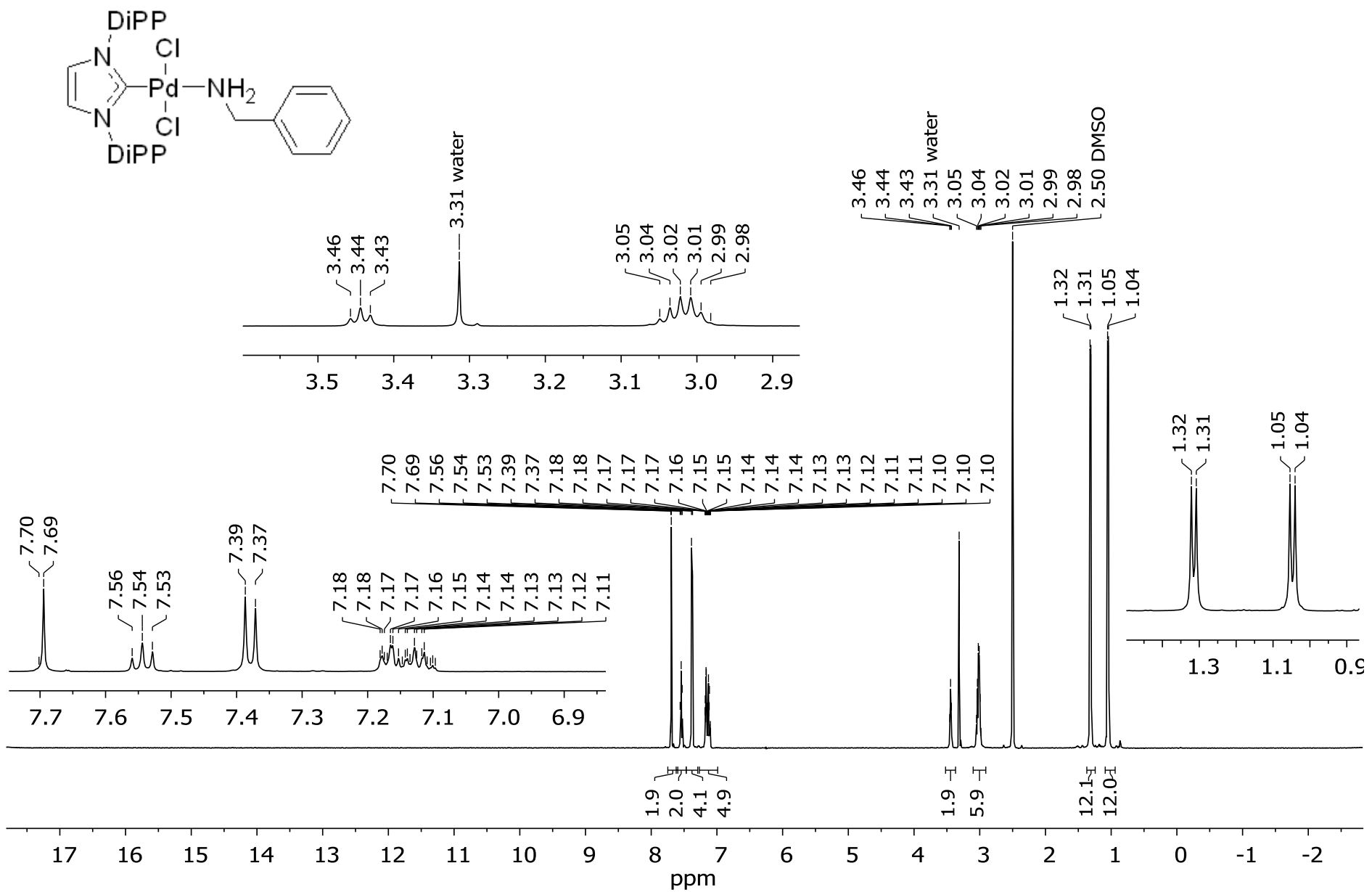
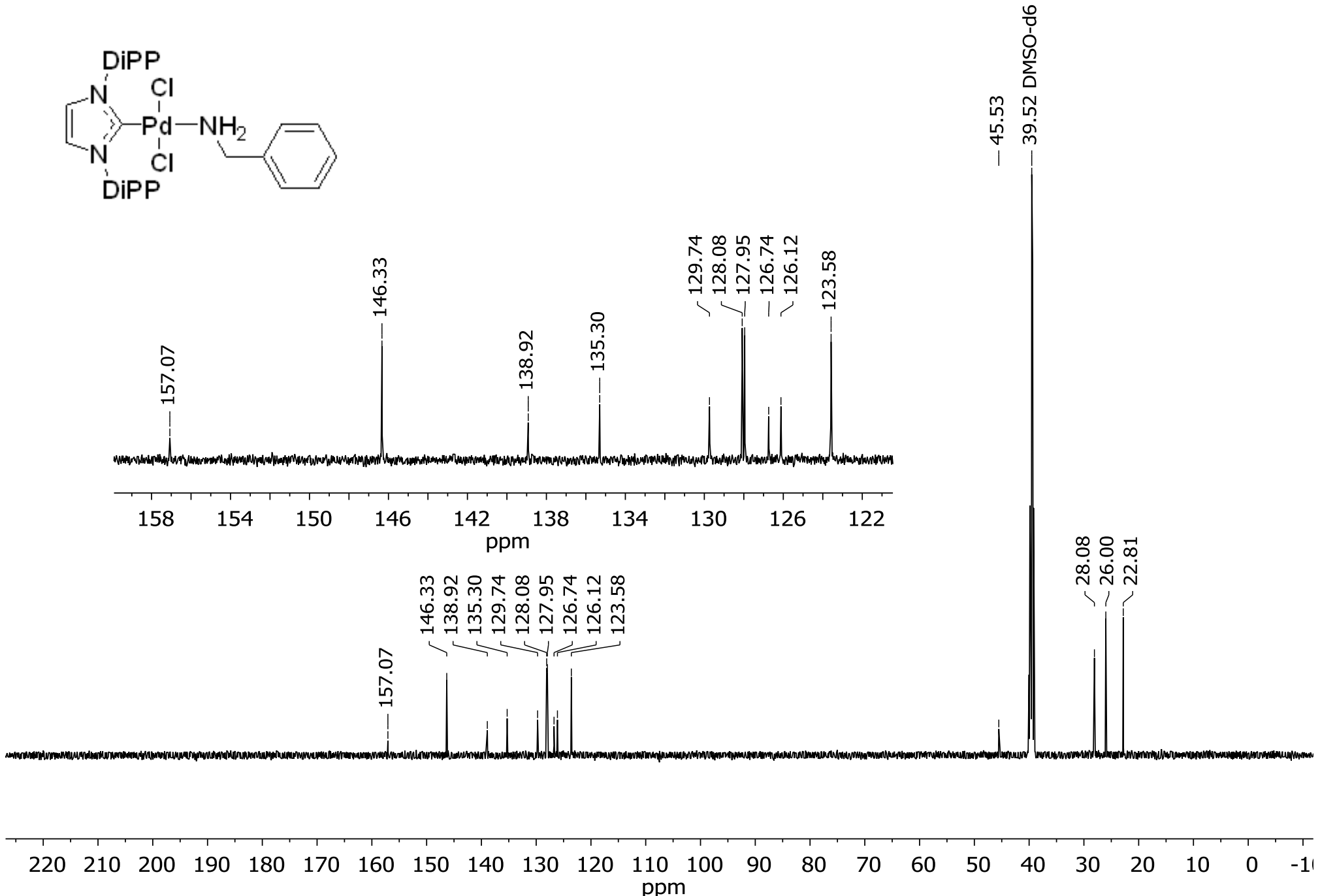
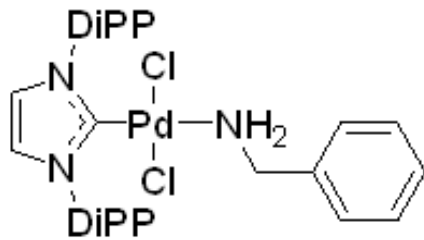


Figure S38.  $^{13}\text{C}$  NMR spectrum of compound **2q** ( $\text{CDCl}_3$ , 125 MHz)



**Figure S39.** <sup>1</sup>H NMR spectrum of compound **2r** (DMSO-*d*<sub>6</sub>, 500 MHz)



**Figure S40.** <sup>13</sup>C NMR spectrum of compound **2r** (DMSO-*d*<sub>6</sub>, 125 MHz)

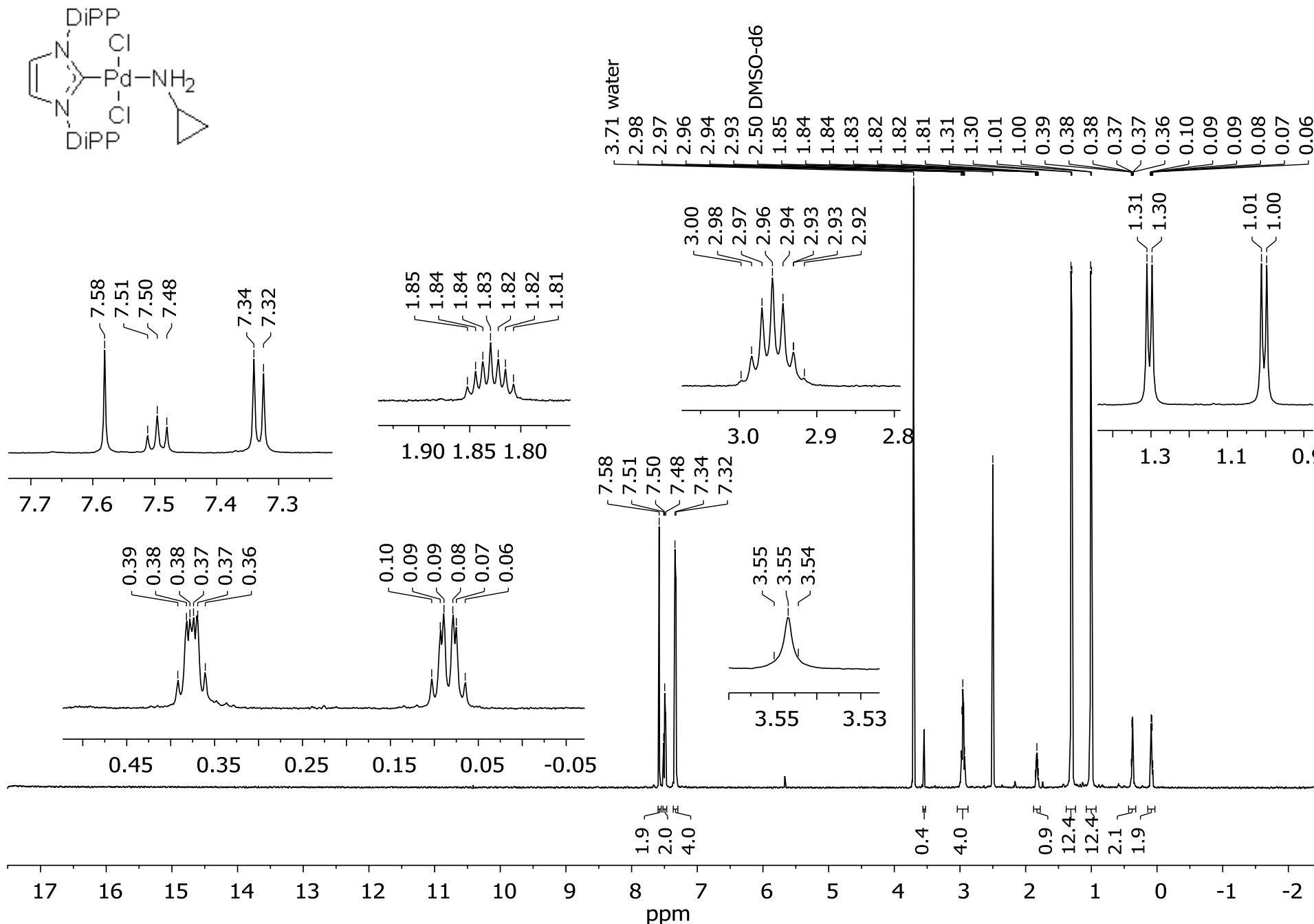


**Figure S41.** <sup>1</sup>H NMR spectrum of compound **2s** (DMSO-*d*<sub>6</sub>, 500 MHz)

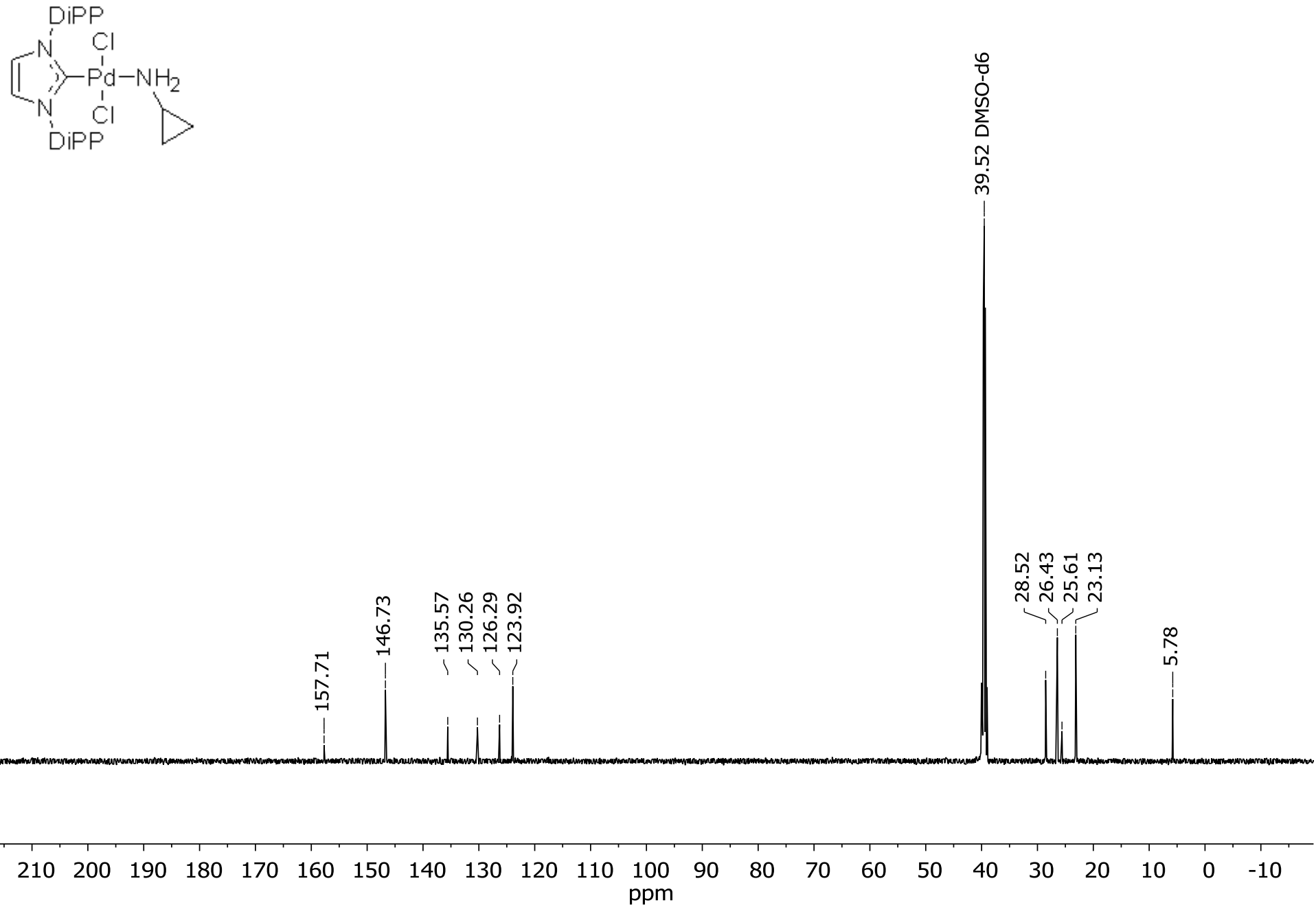


**Figure S42.**  $^{13}\text{C}$  NMR spectrum of compound **2s** (DMSO-*d*<sub>6</sub>, 125 MHz)

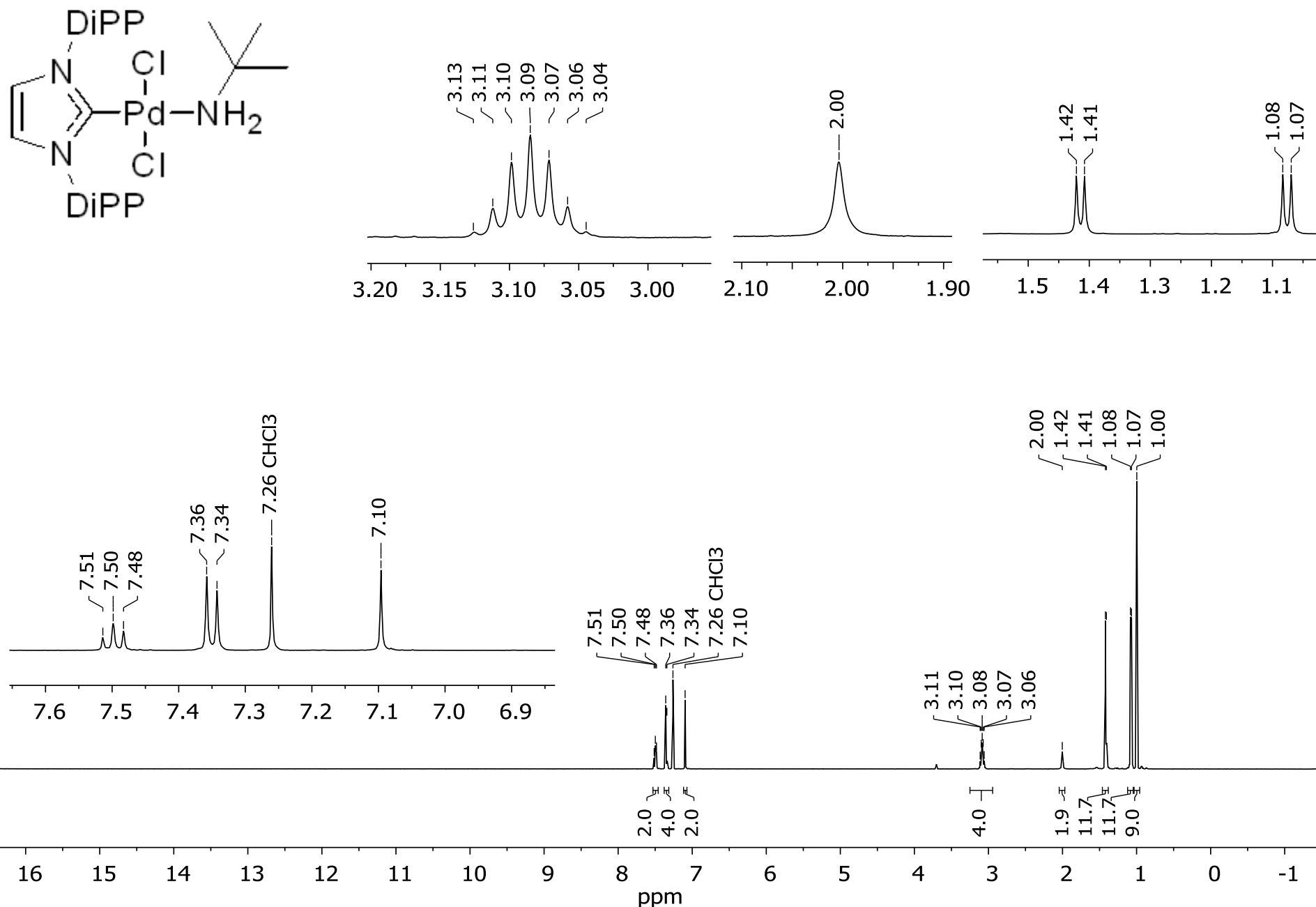
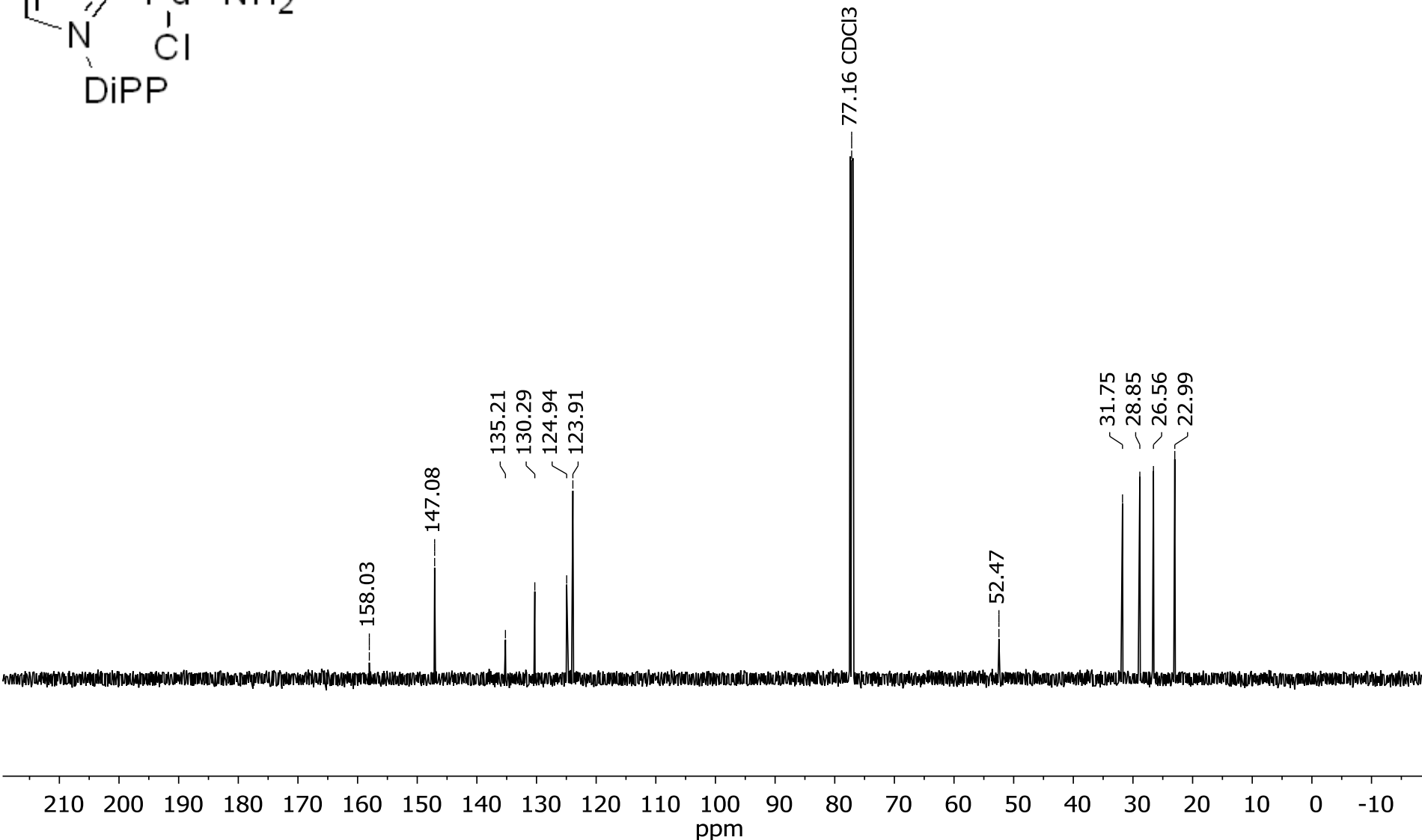
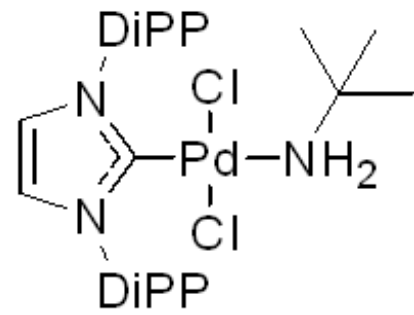
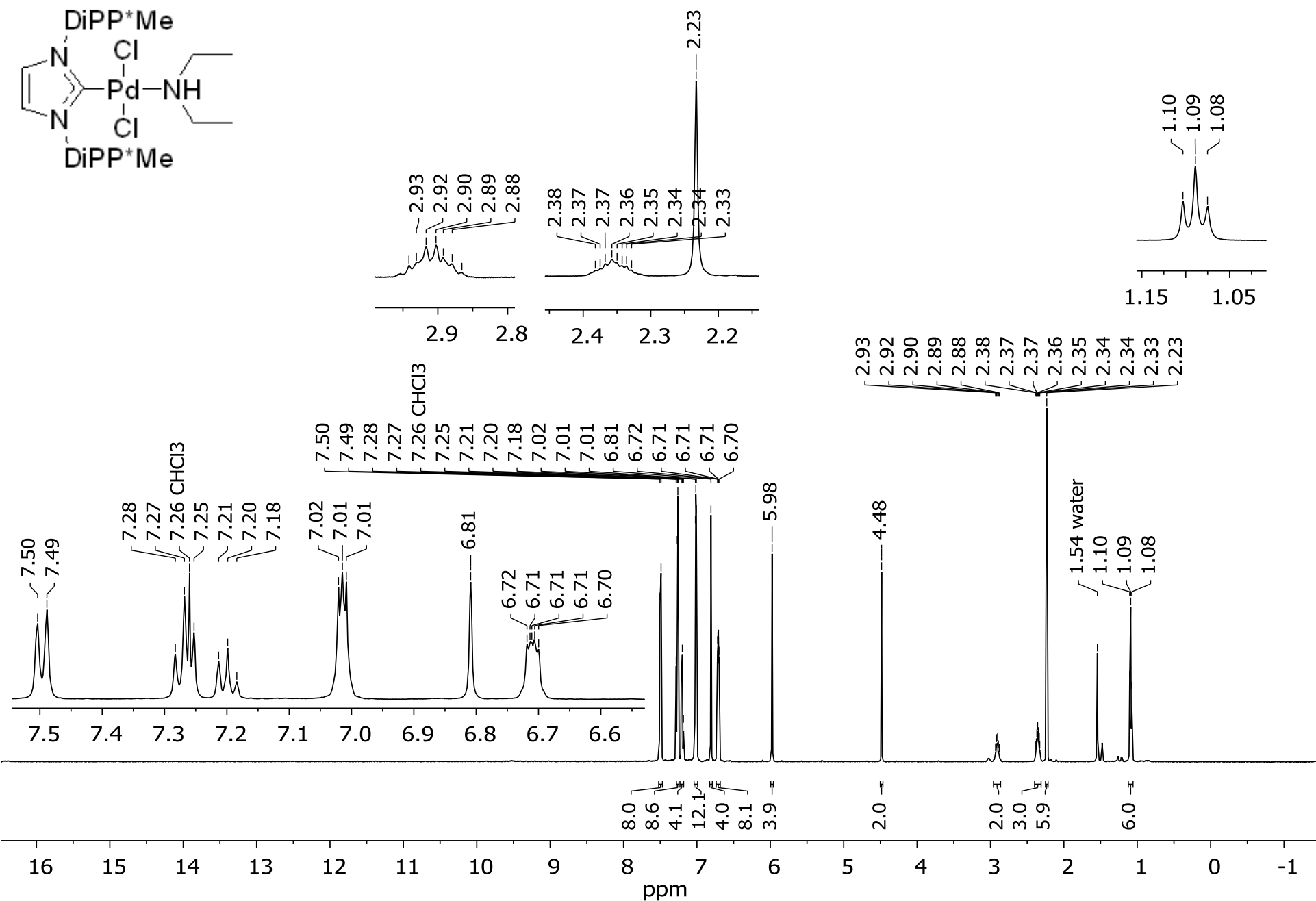


Figure S43. <sup>1</sup>H NMR spectrum of compound 2t ( $\text{CDCl}_3$ , 500 MHz)



**Figure S44.** <sup>13</sup>C NMR spectrum of compound **2t** ( $\text{CDCl}_3$ , 125 MHz)



**Figure S45.** <sup>1</sup>H NMR spectrum of compound **2u** ( $\text{CDCl}_3$ , 500 MHz)

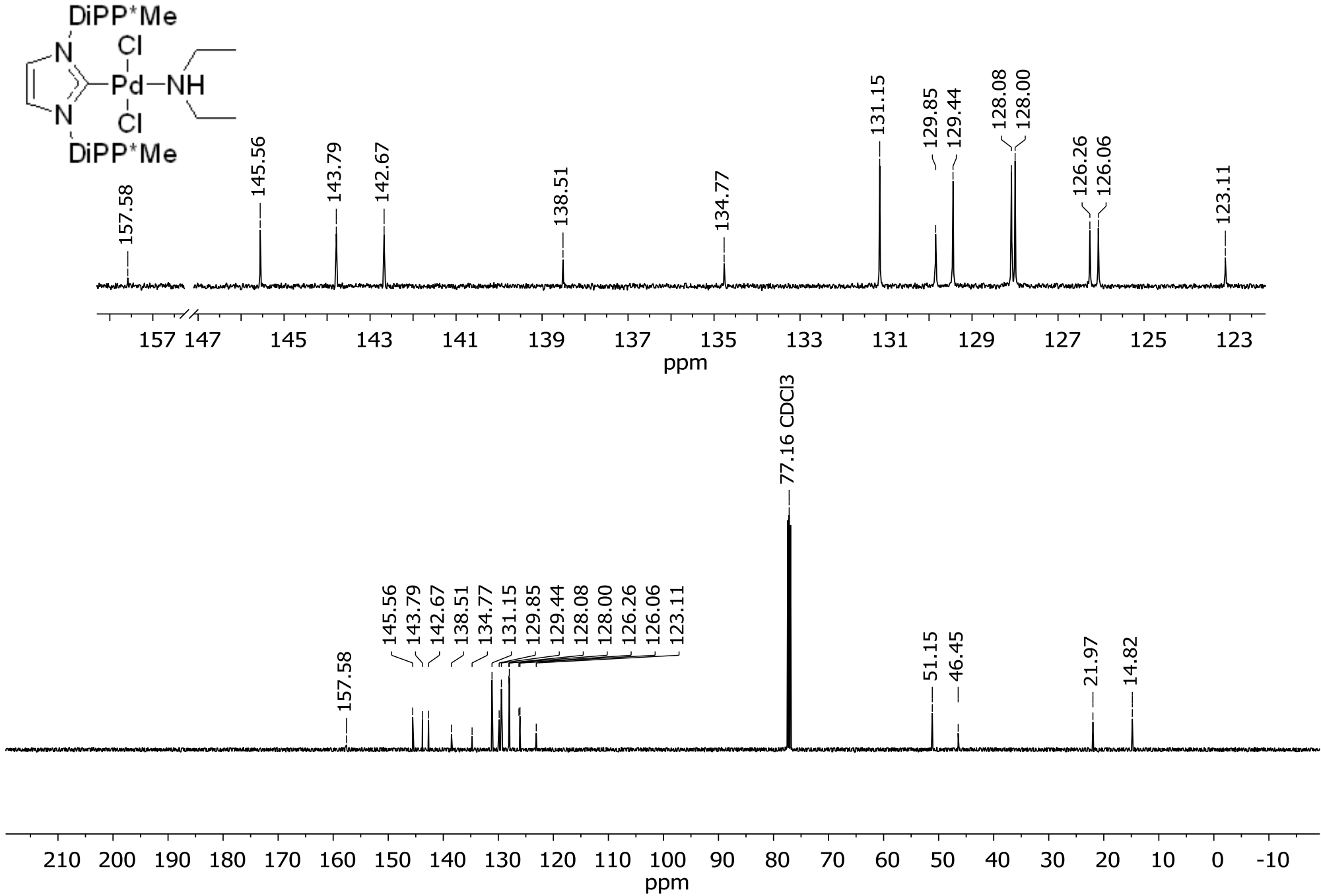


**Figure S46.** <sup>13</sup>C NMR spectrum of compound **2u** (CDCl<sub>3</sub>, 125 MHz)

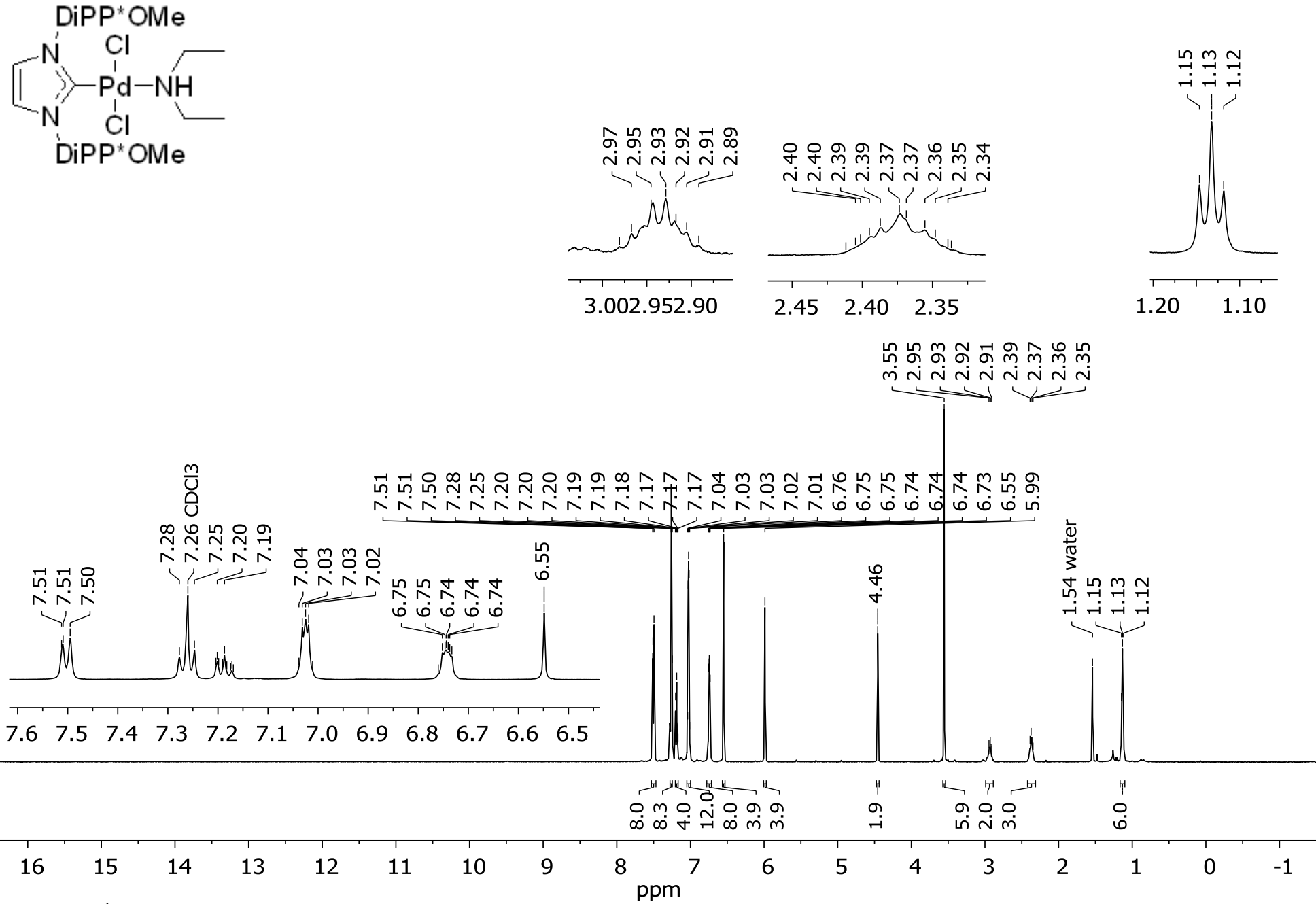


**Figure S47.** <sup>1</sup>H NMR spectrum of compound **2v** ( $\text{CDCl}_3$ , 500 MHz)

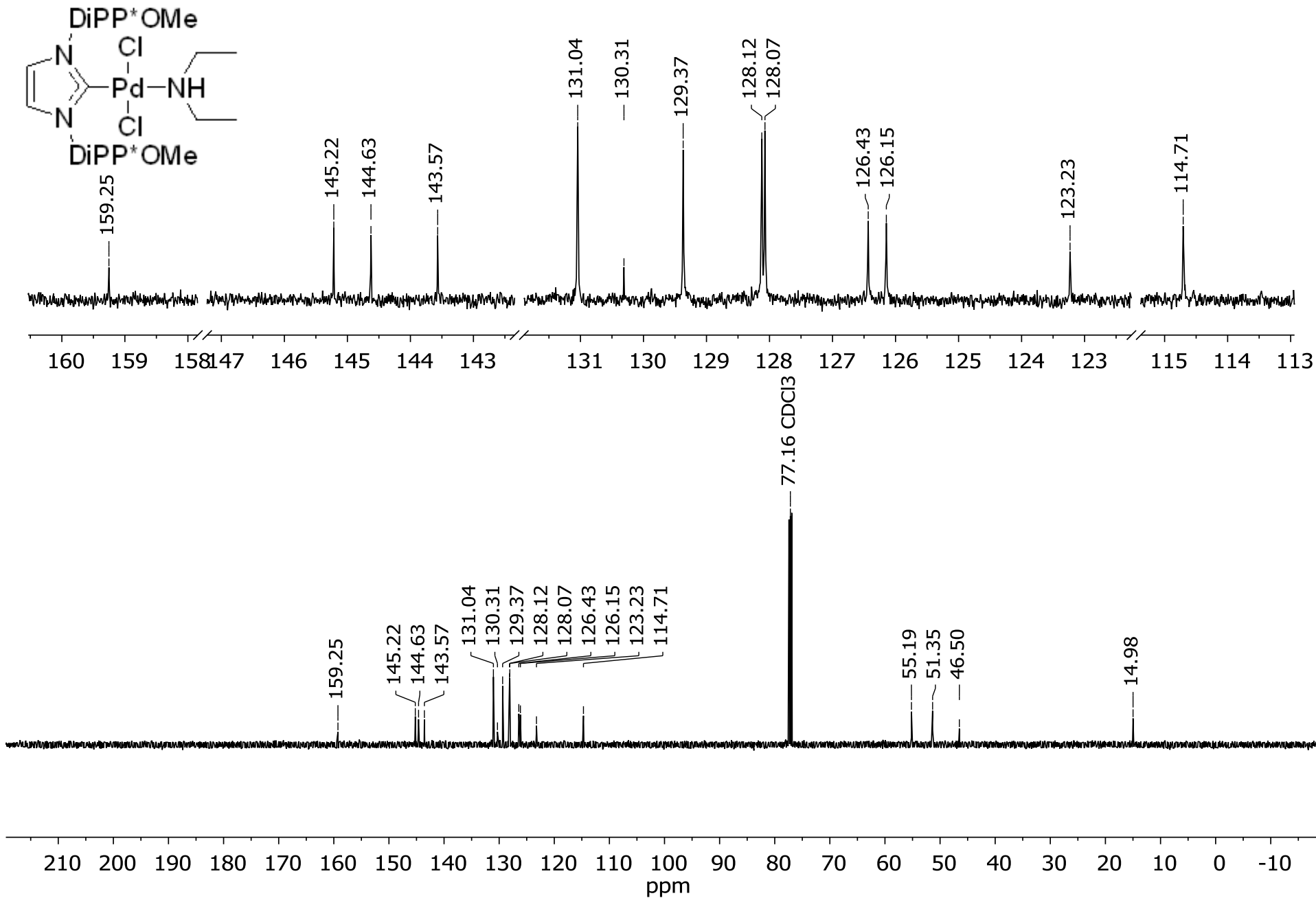


Figure S48.  $^{13}\text{C}$  NMR spectrum of compound **2v** (CDCl<sub>3</sub>, 125 MHz)

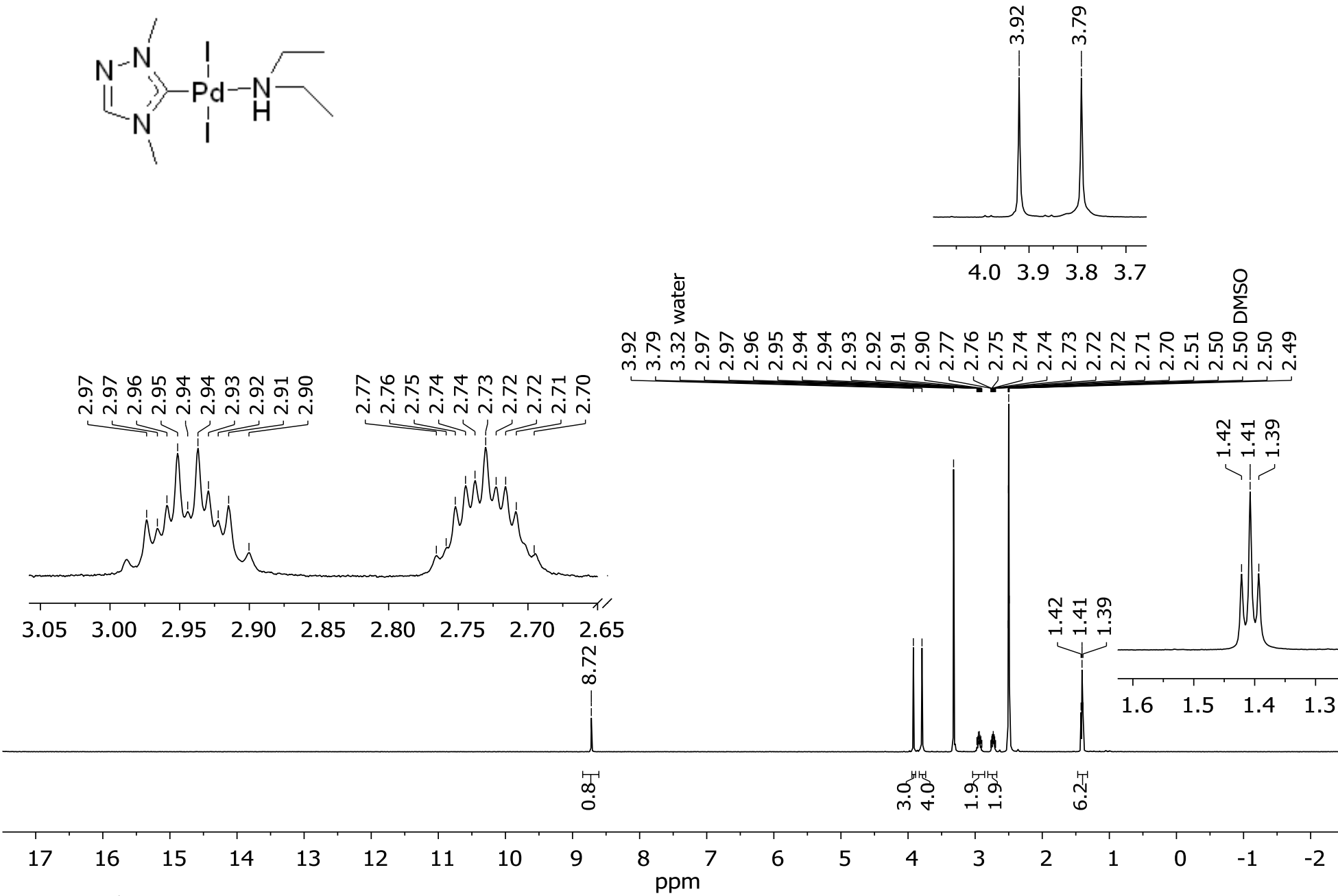


Figure S49. <sup>1</sup>H NMR spectrum of compound 2w (DMSO-*d*<sub>6</sub>, 500 MHz)

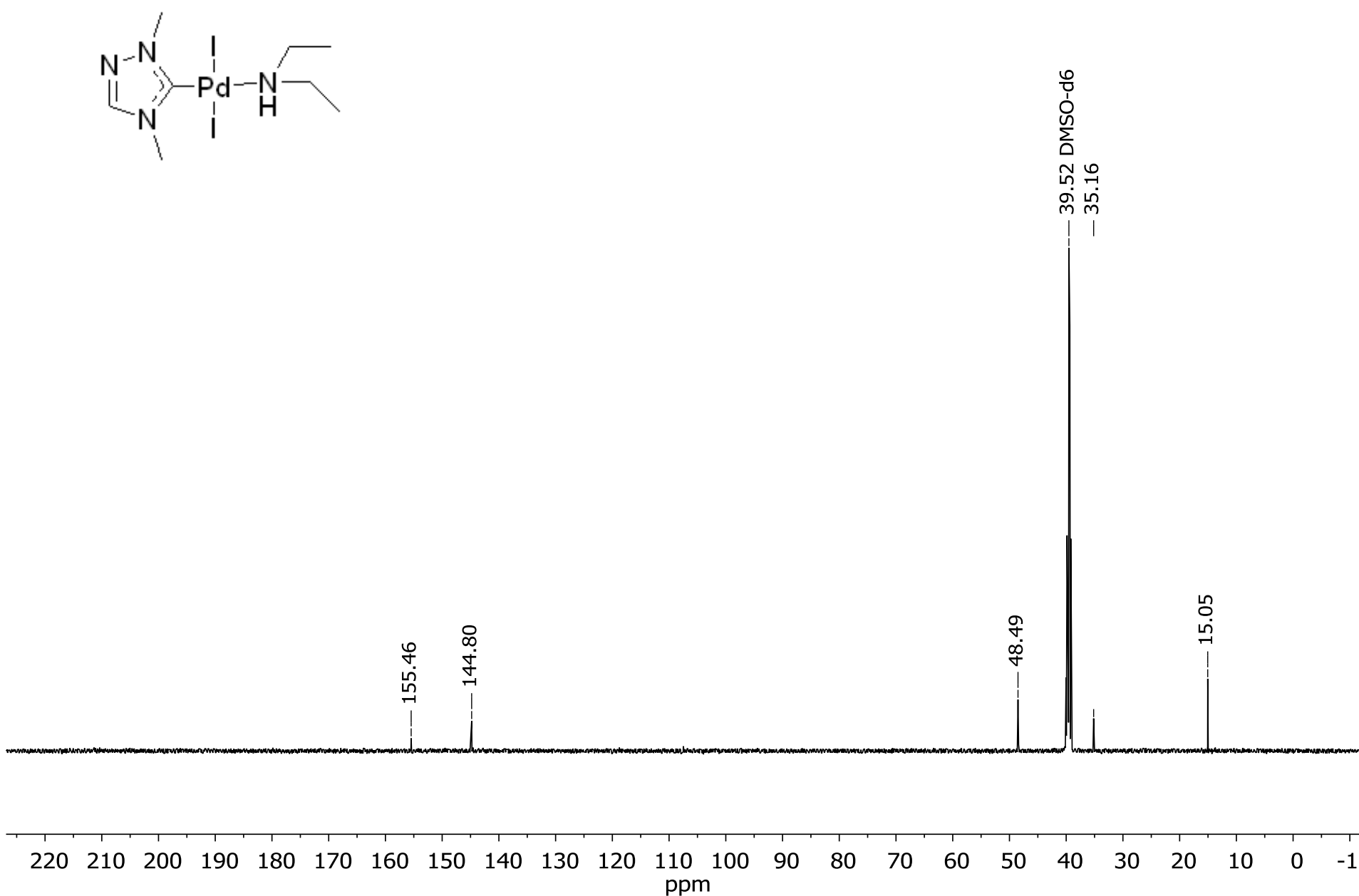
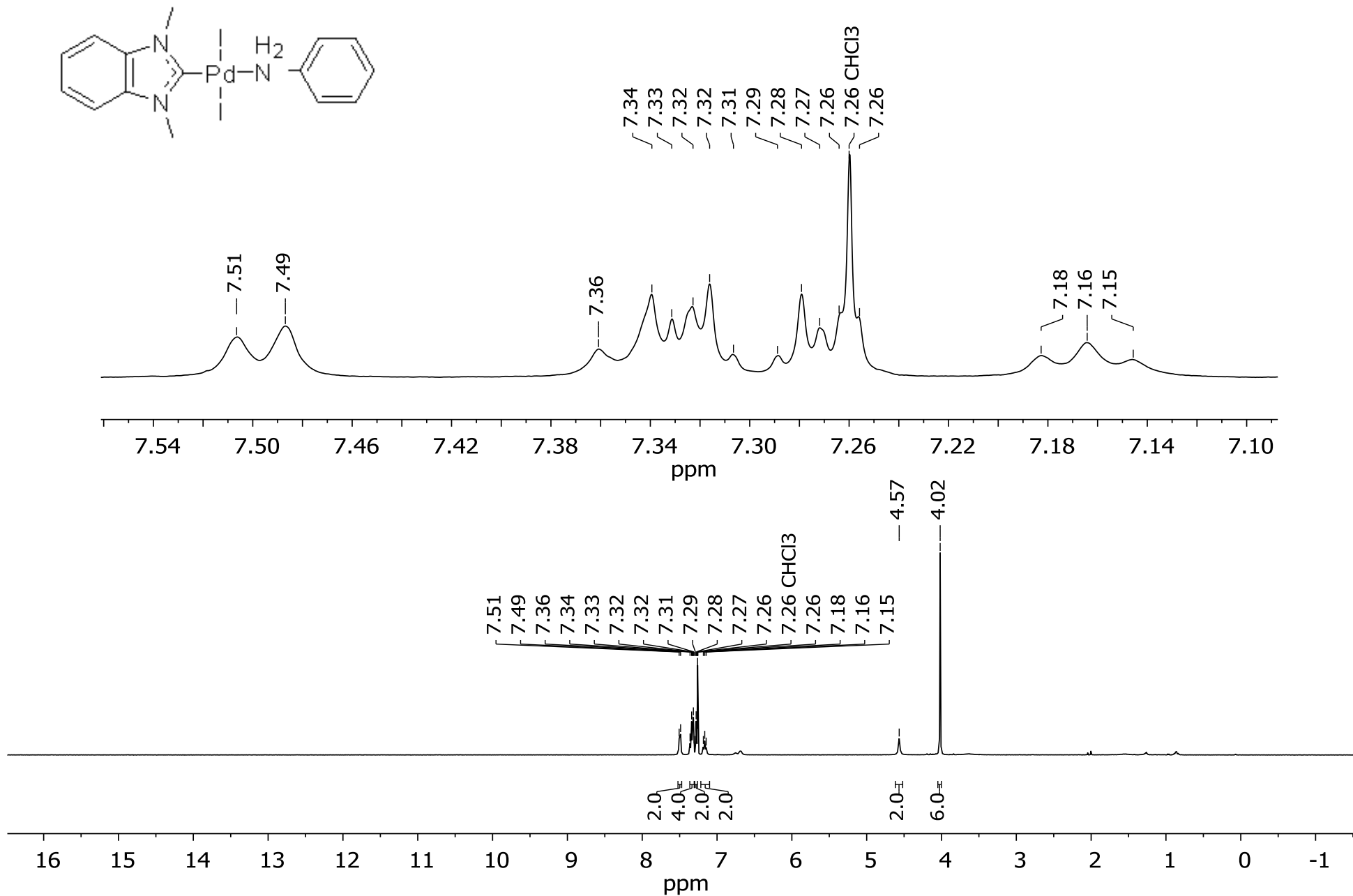


Figure S50. <sup>13</sup>C NMR spectrum of compound **2w** (DMSO-*d*<sub>6</sub>, 125 MHz)



**Figure S51.**  $^1\text{H}$  NMR spectrum of compound **2y** ( $\text{CDCl}_3$ , 500 MHz)

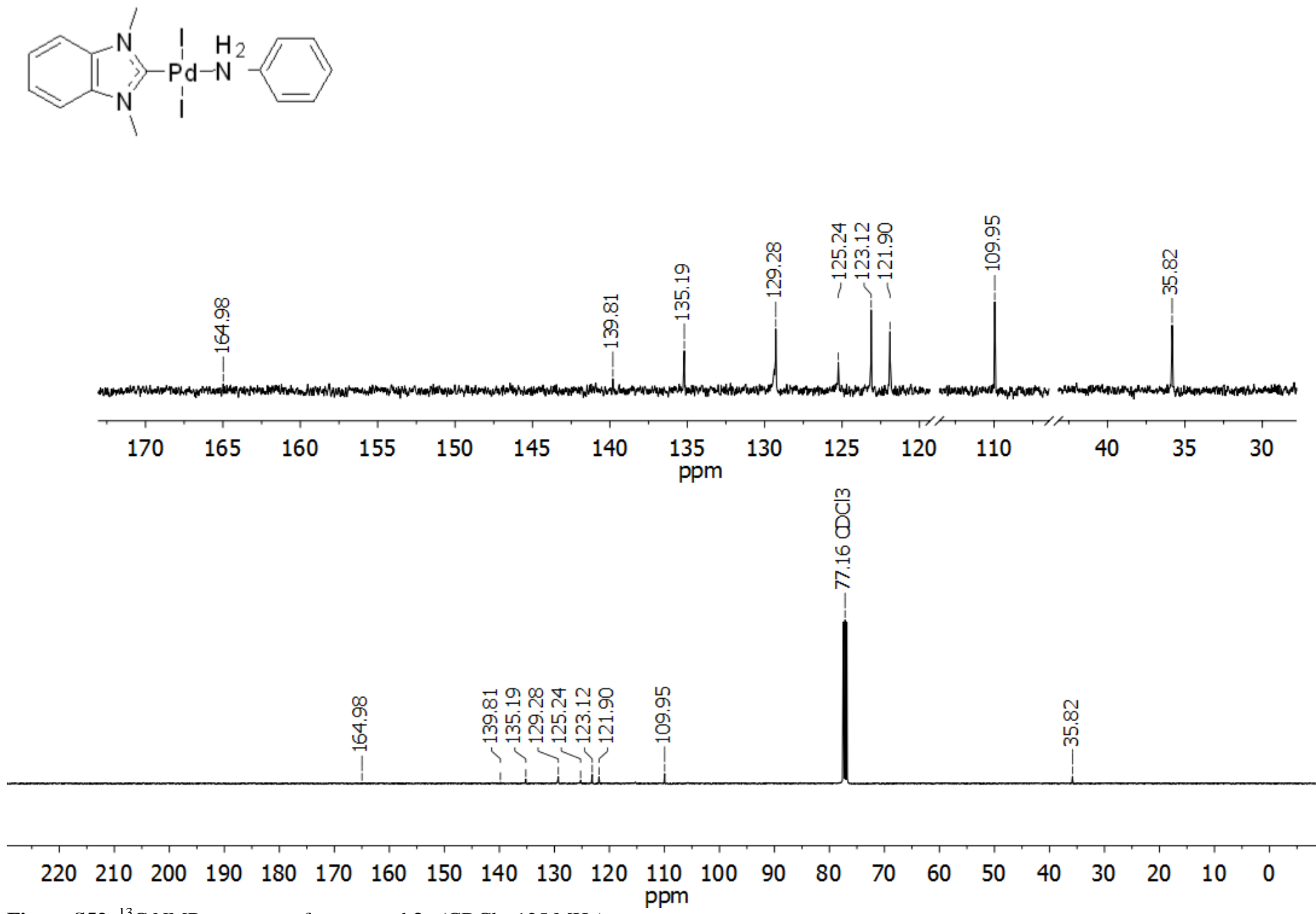
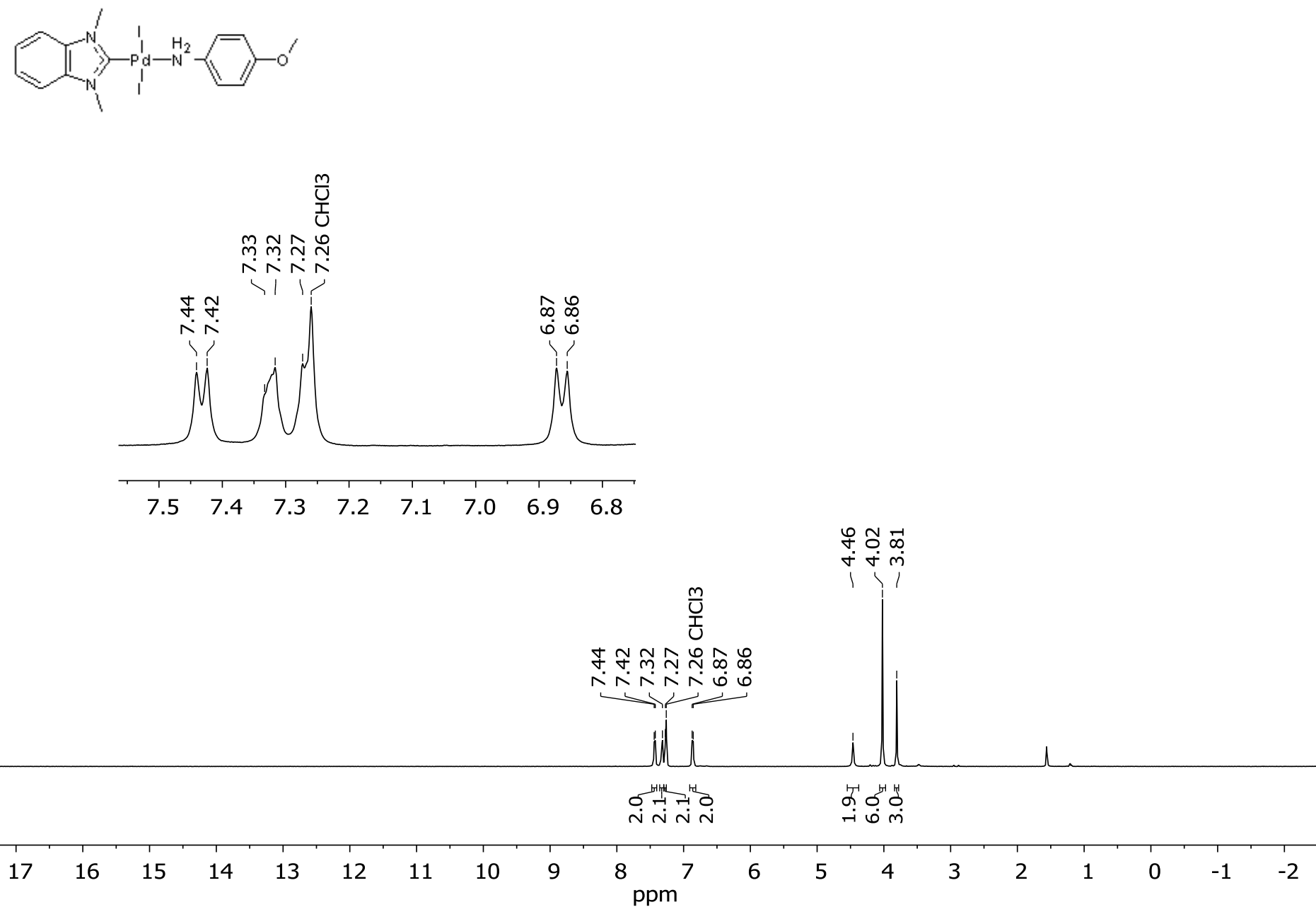
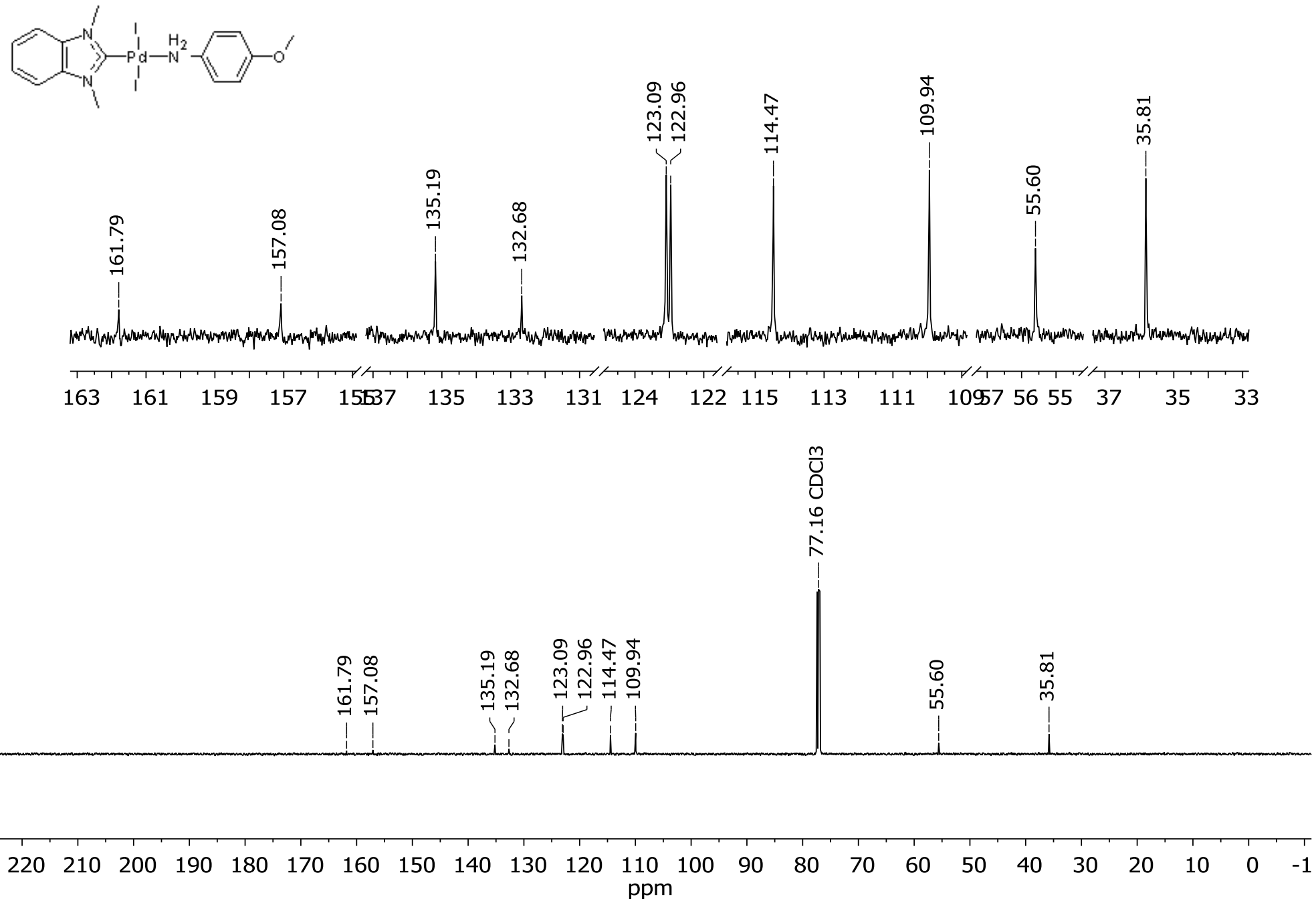


Figure S52.  $^{13}\text{C}$  NMR spectrum of compound **2y** ( $\text{CDCl}_3$ , 125 MHz)



**Figure S53.**  $^1\text{H}$  NMR spectrum of compound **2z** ( $\text{CDCl}_3$ , 500 MHz)



**Figure S54.** <sup>13</sup>C NMR spectrum of compound **2z** (CDCl<sub>3</sub>, 125 MHz)

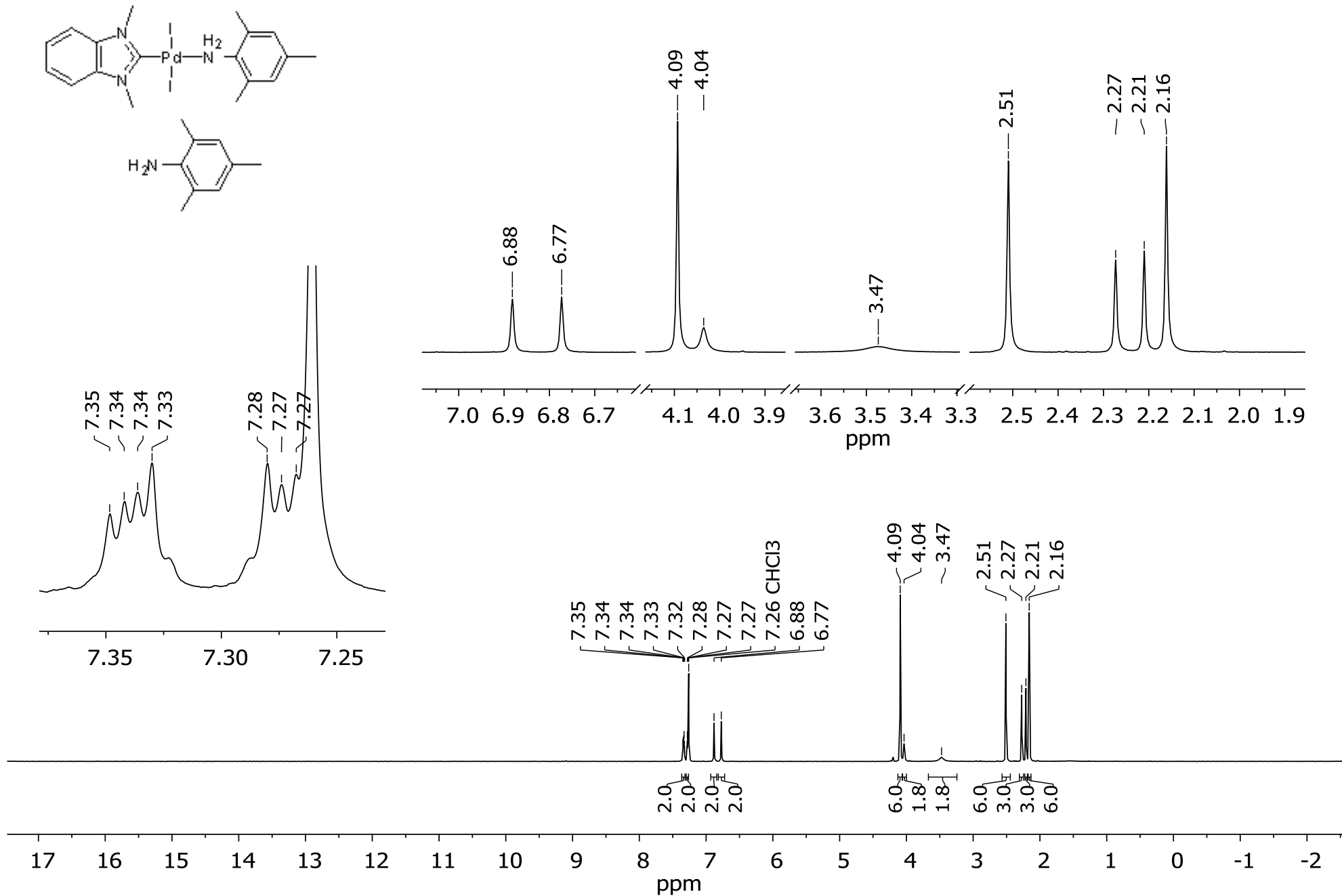
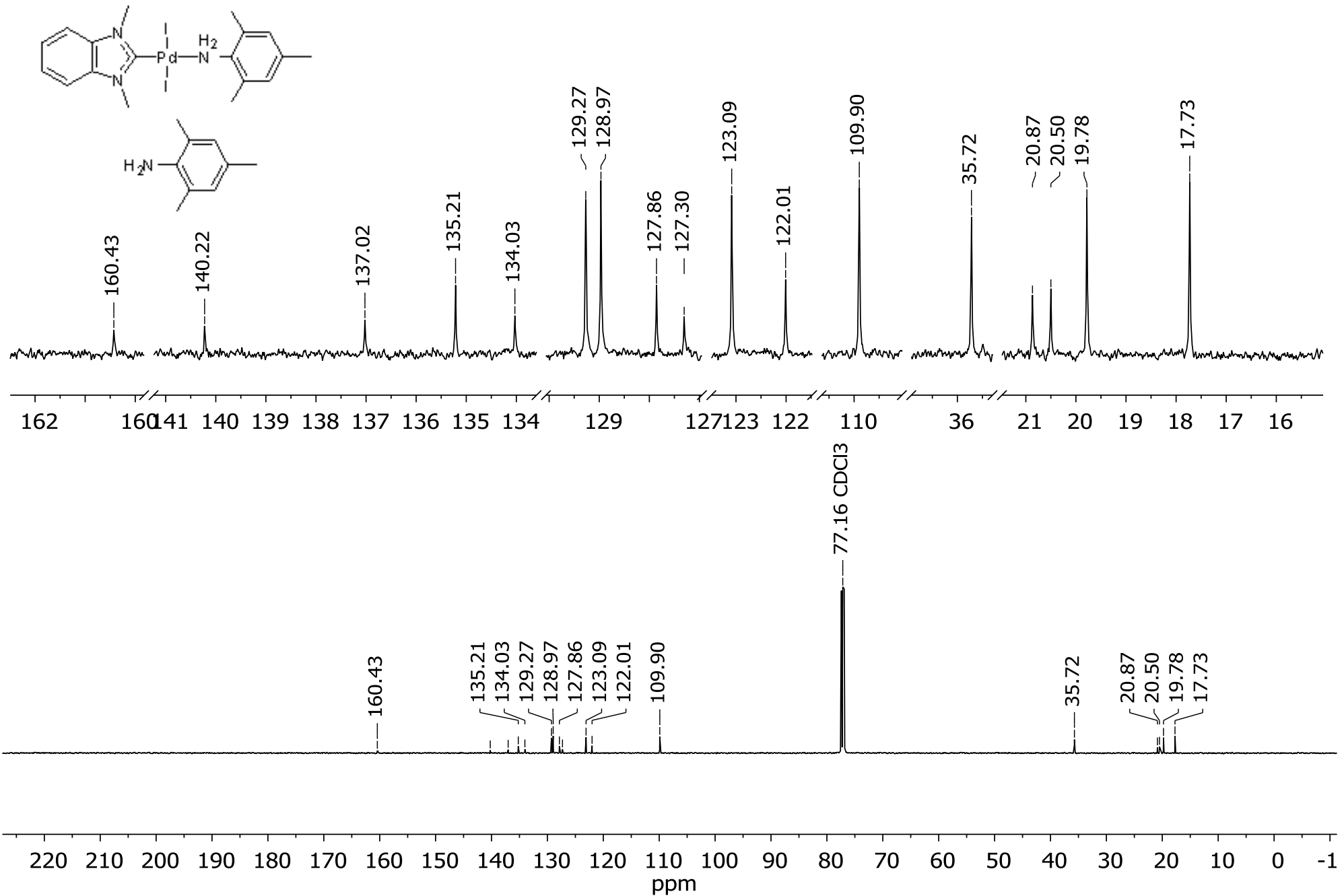
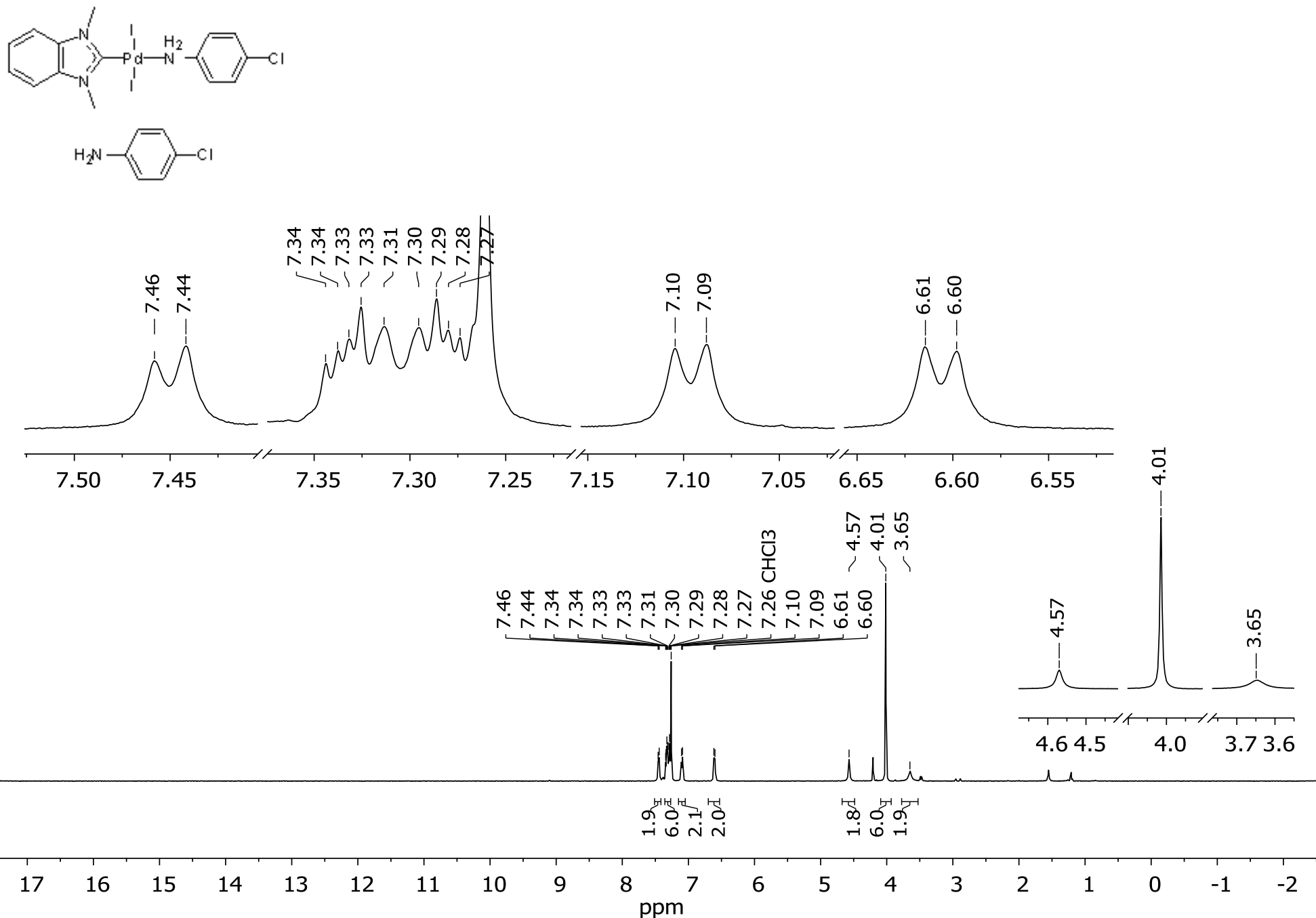


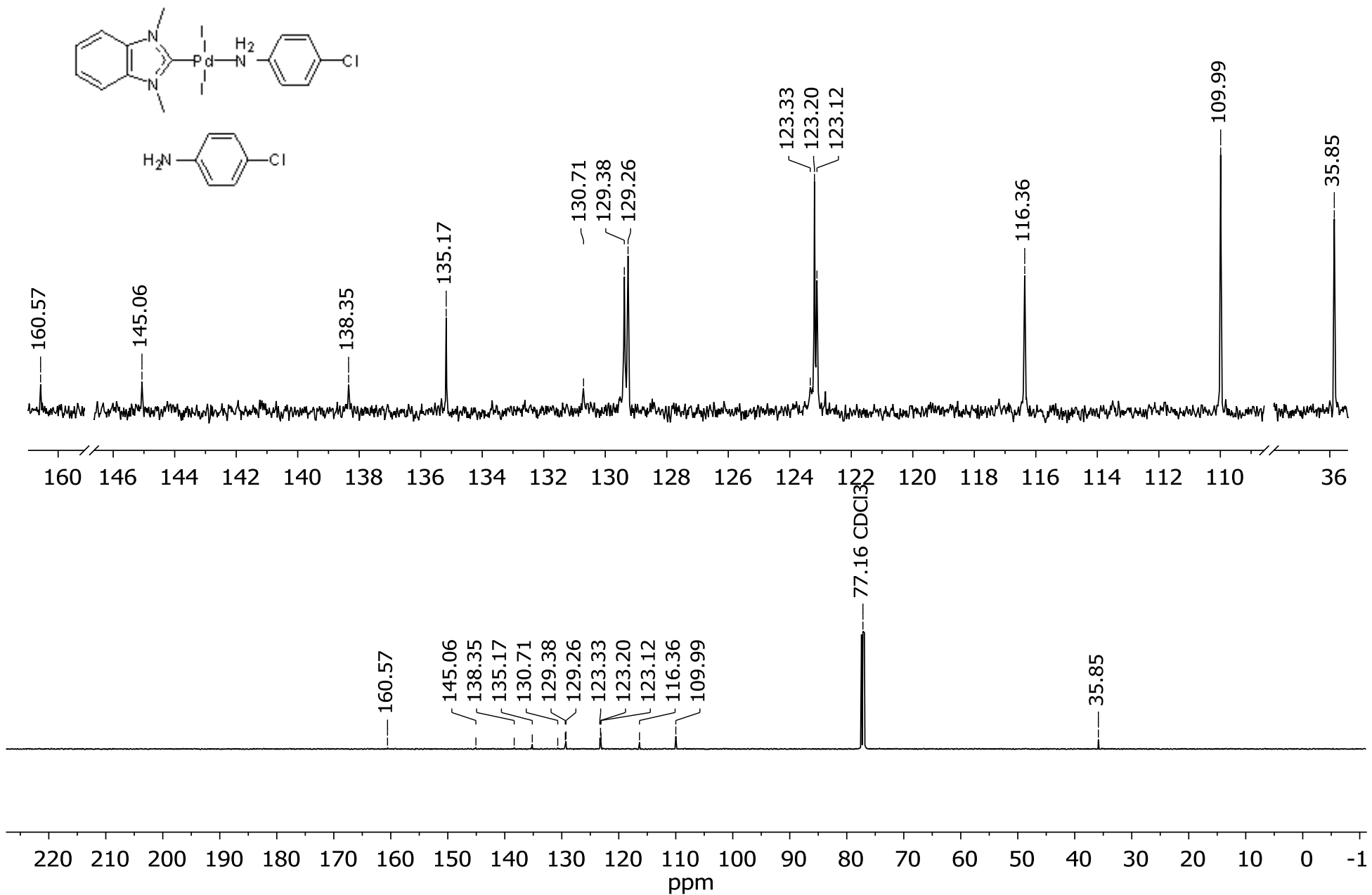
Figure S55. <sup>1</sup>H NMR spectrum of compound 2aa (CDCl<sub>3</sub>, 500 MHz)



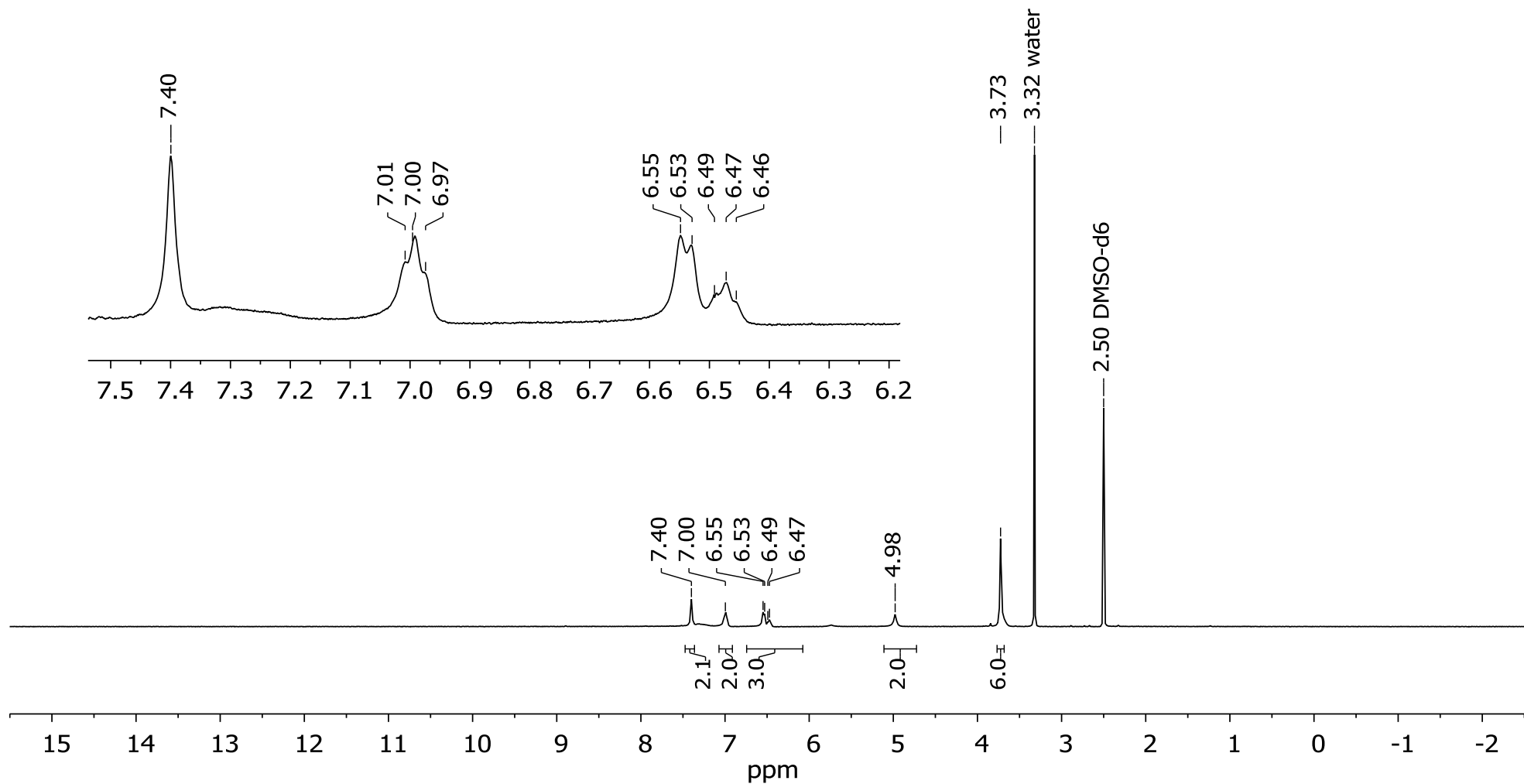
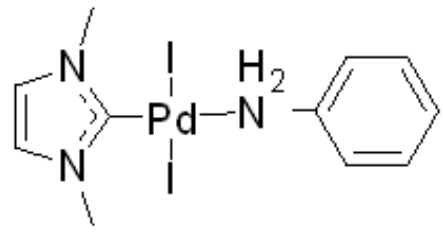
**Figure S56.**  $^{13}\text{C}$  NMR spectrum of compound **2aa** ( $\text{CDCl}_3$ , 125 MHz)



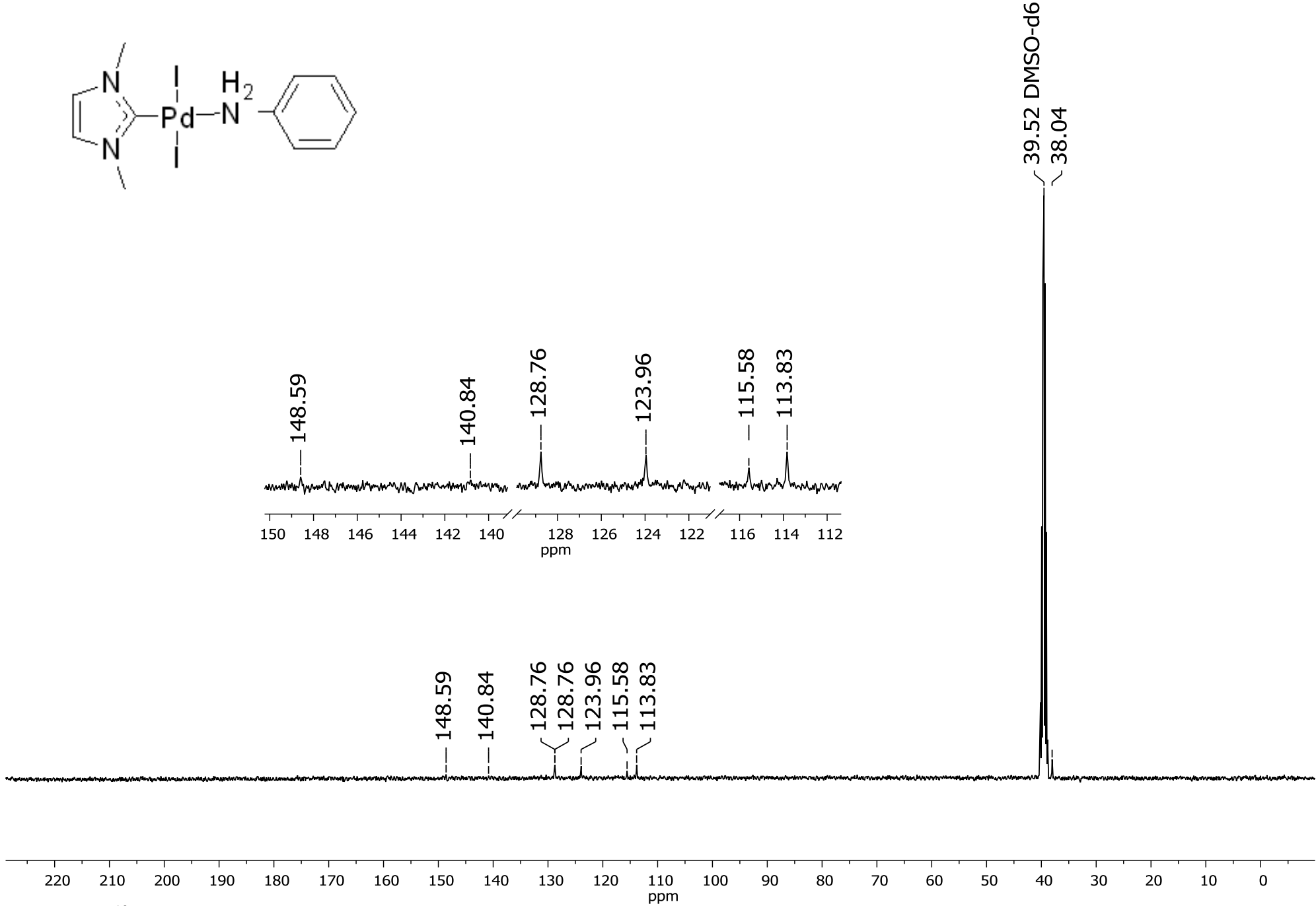
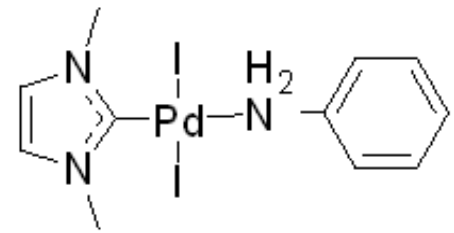
**Figure S57.**  $^1\text{H}$  NMR spectrum of compound **2ab** ( $\text{CDCl}_3$ , 500 MHz)



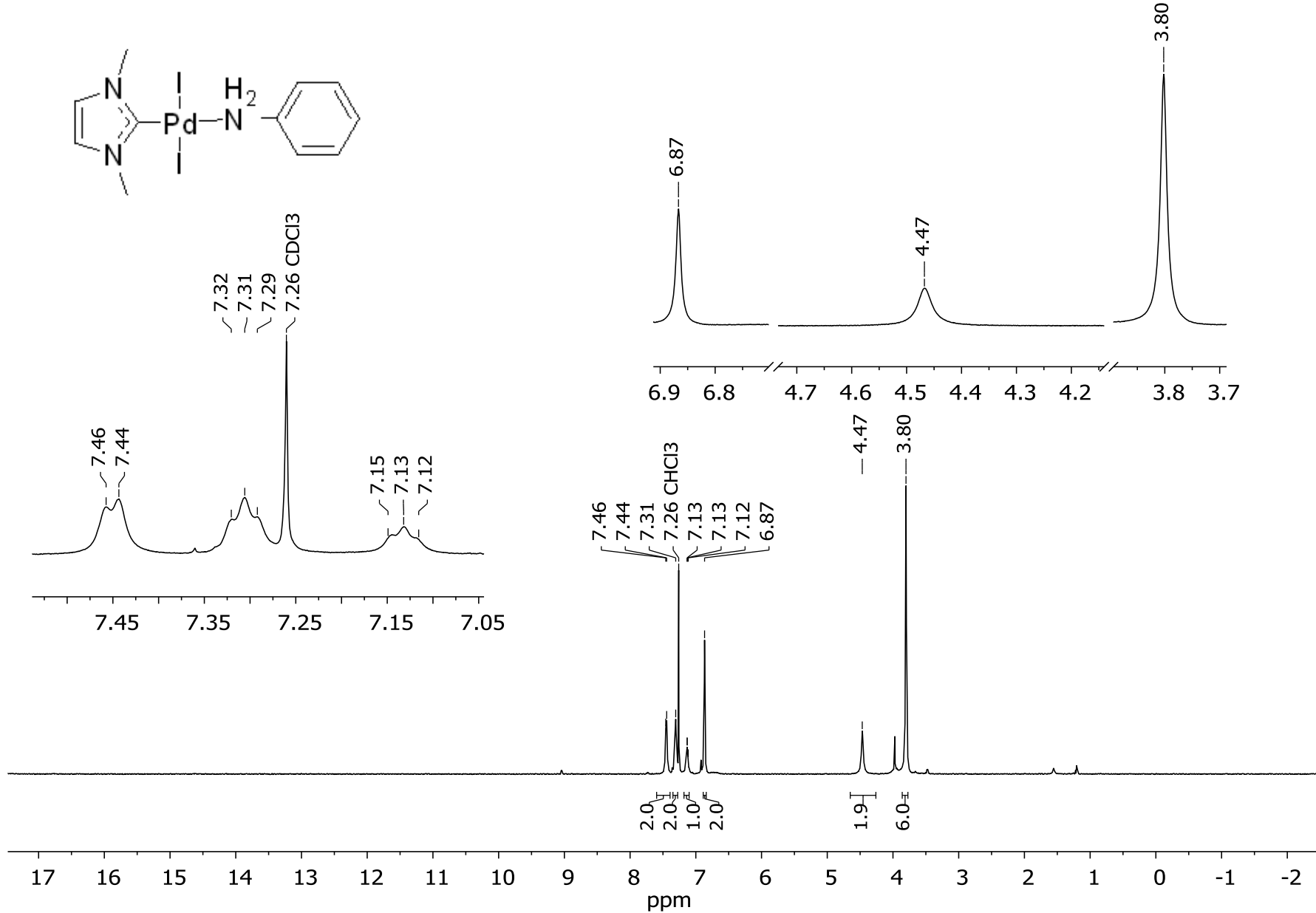
**Figure S58.**  $^{13}\text{C}$  NMR spectrum of compound **2ab** ( $\text{CDCl}_3$ , 125 MHz)



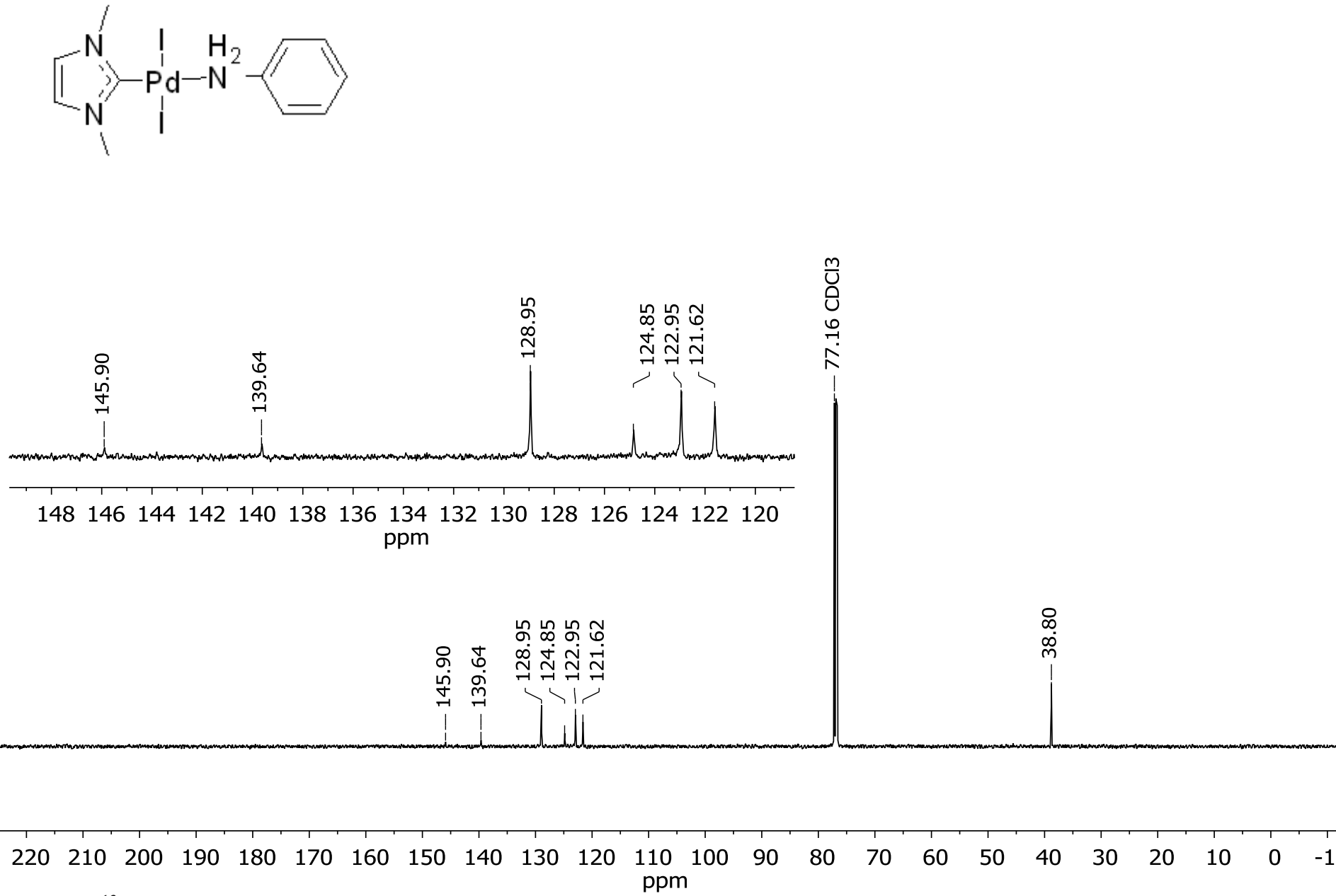
**Figure S59.** <sup>1</sup>H NMR spectrum of compound **2ac** (DMSO-*d*<sub>6</sub>, 500 MHz)



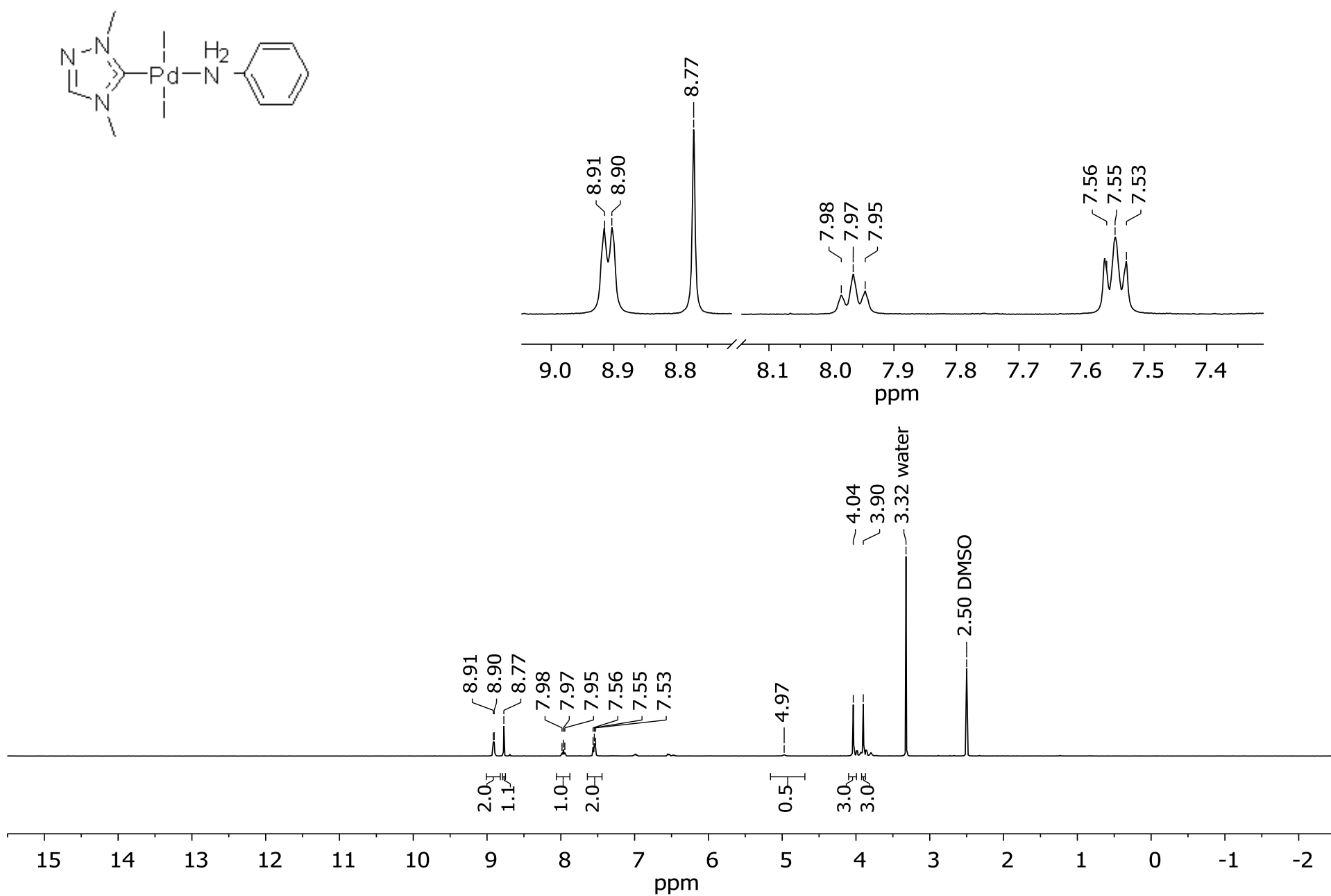
**Figure S60.** <sup>13</sup>C NMR spectrum of compound **2ac** (DMSO-*d*<sub>6</sub>, 125 MHz)



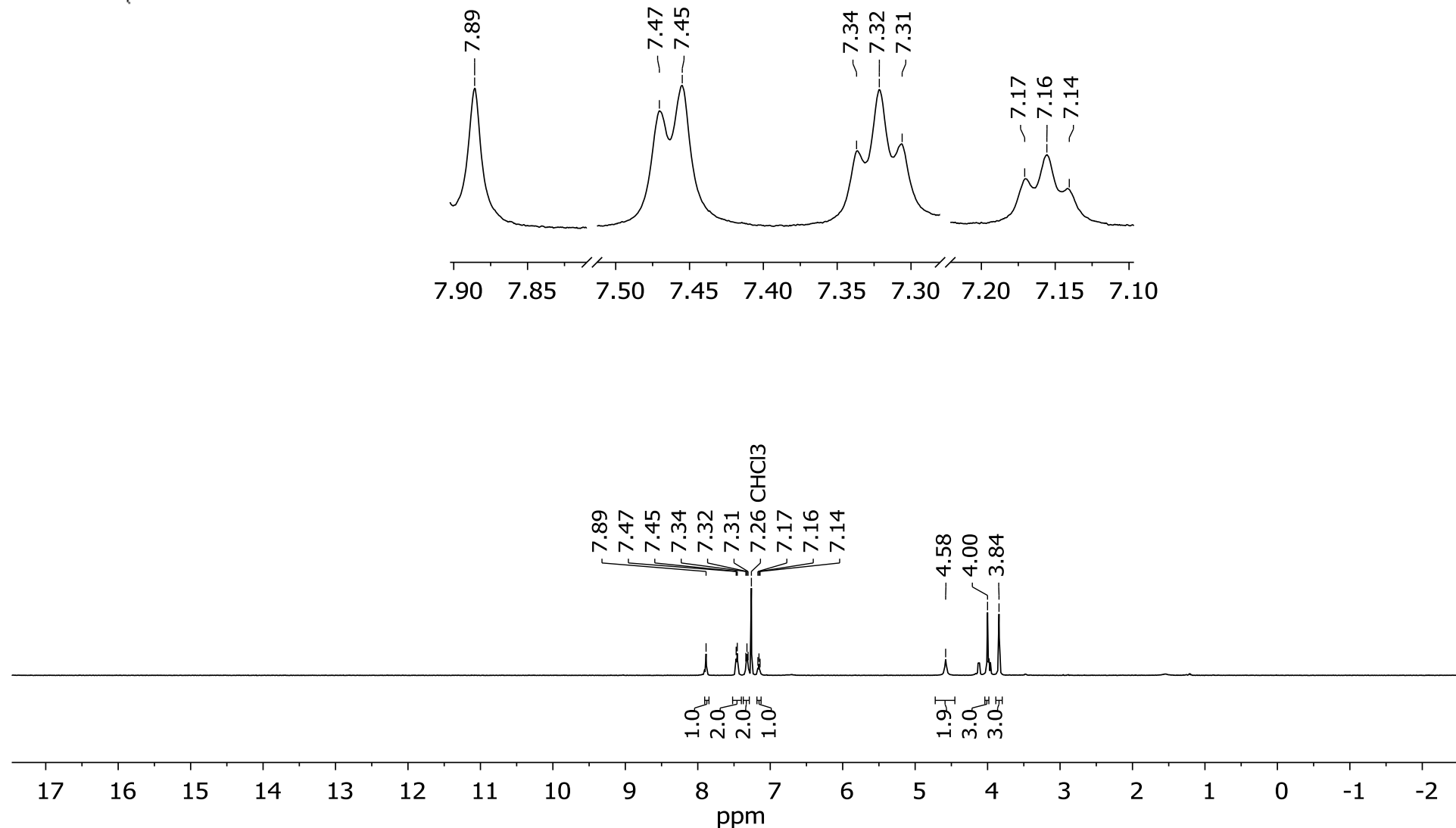
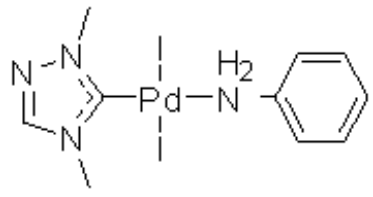
**Figure S61.** <sup>1</sup>H NMR spectrum of compound **2ac** (CDCl<sub>3</sub>, 500 MHz)



**Figure S62.**  $^{13}\text{C}$  NMR spectrum of compound **2ac** ( $\text{CDCl}_3$ , 125 MHz)



**Figure S63.**  $^1\text{H}$  NMR spectrum of compound **2ae** ( $\text{DMSO}-d_6$ , 500 MHz)



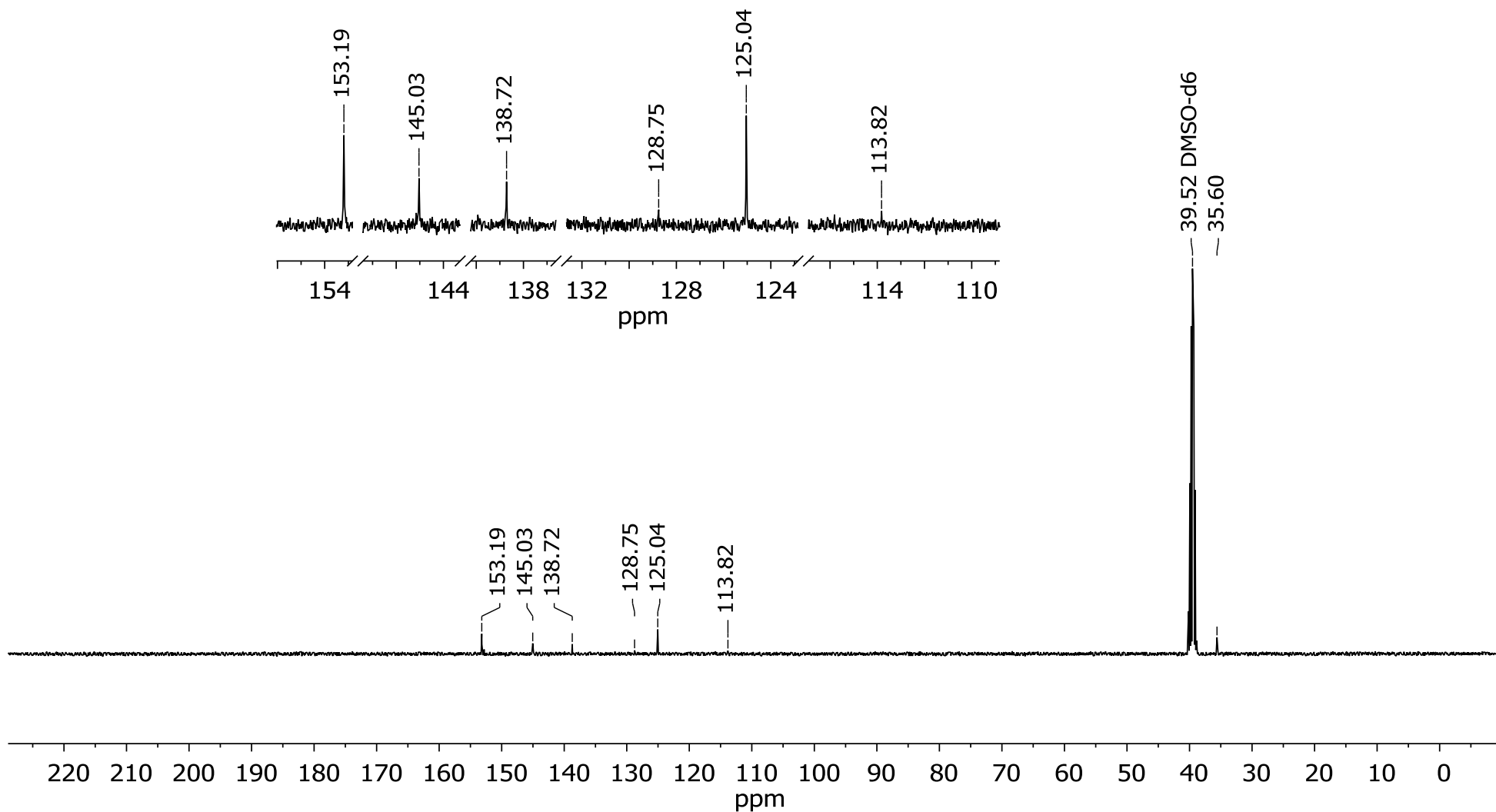
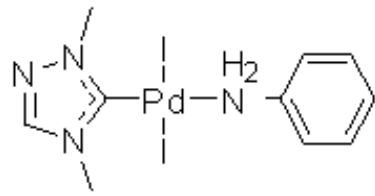


**Figure S65.**  $^{13}\text{C}$  NMR spectrum of compound **2ae** (DMSO-*d*<sub>6</sub>, 125 MHz)

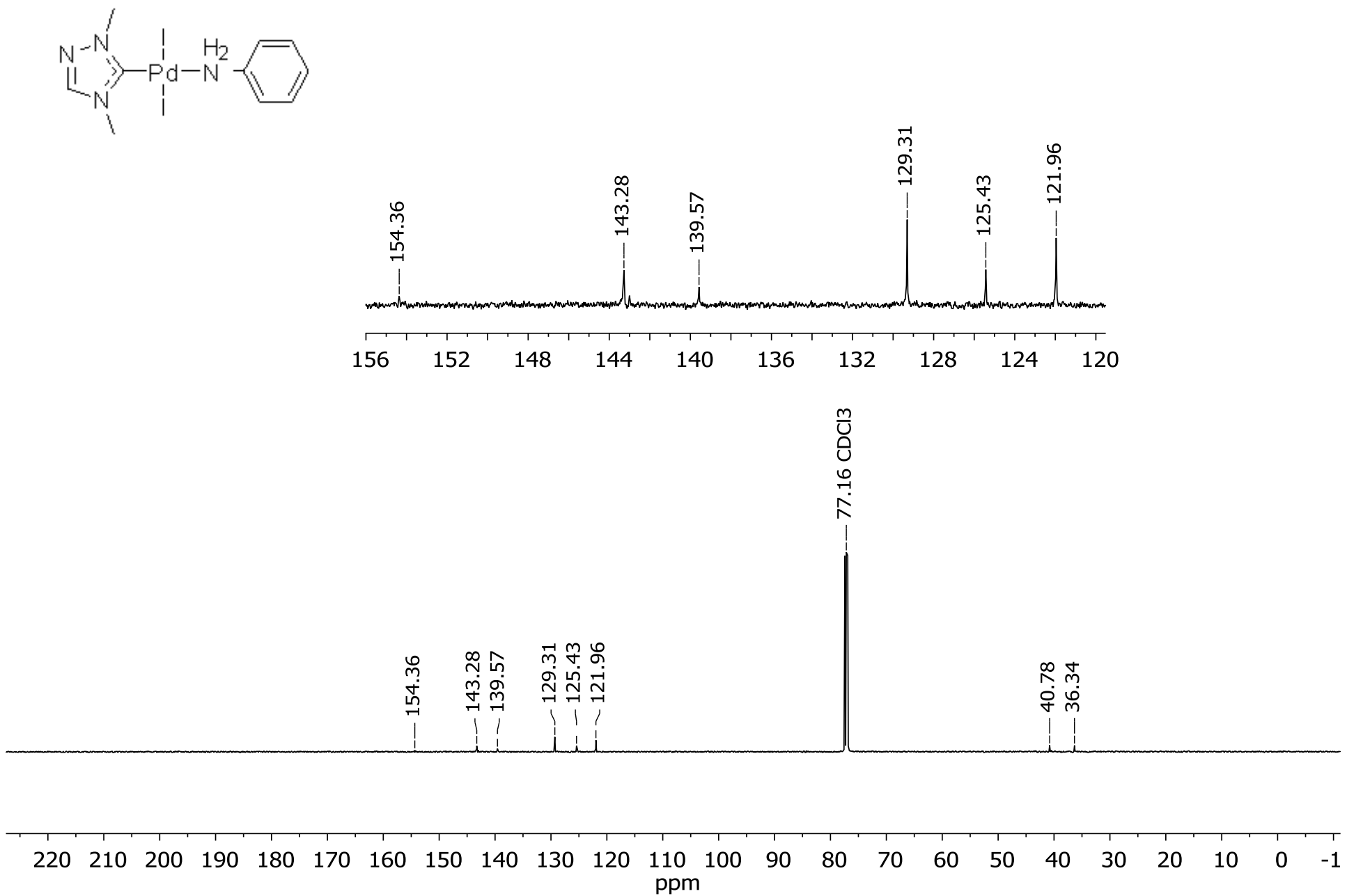


**Figure S66.**  $^{13}\text{C}$  NMR spectrum of compound **2ae** ( $\text{CDCl}_3$ , 125 MHz)

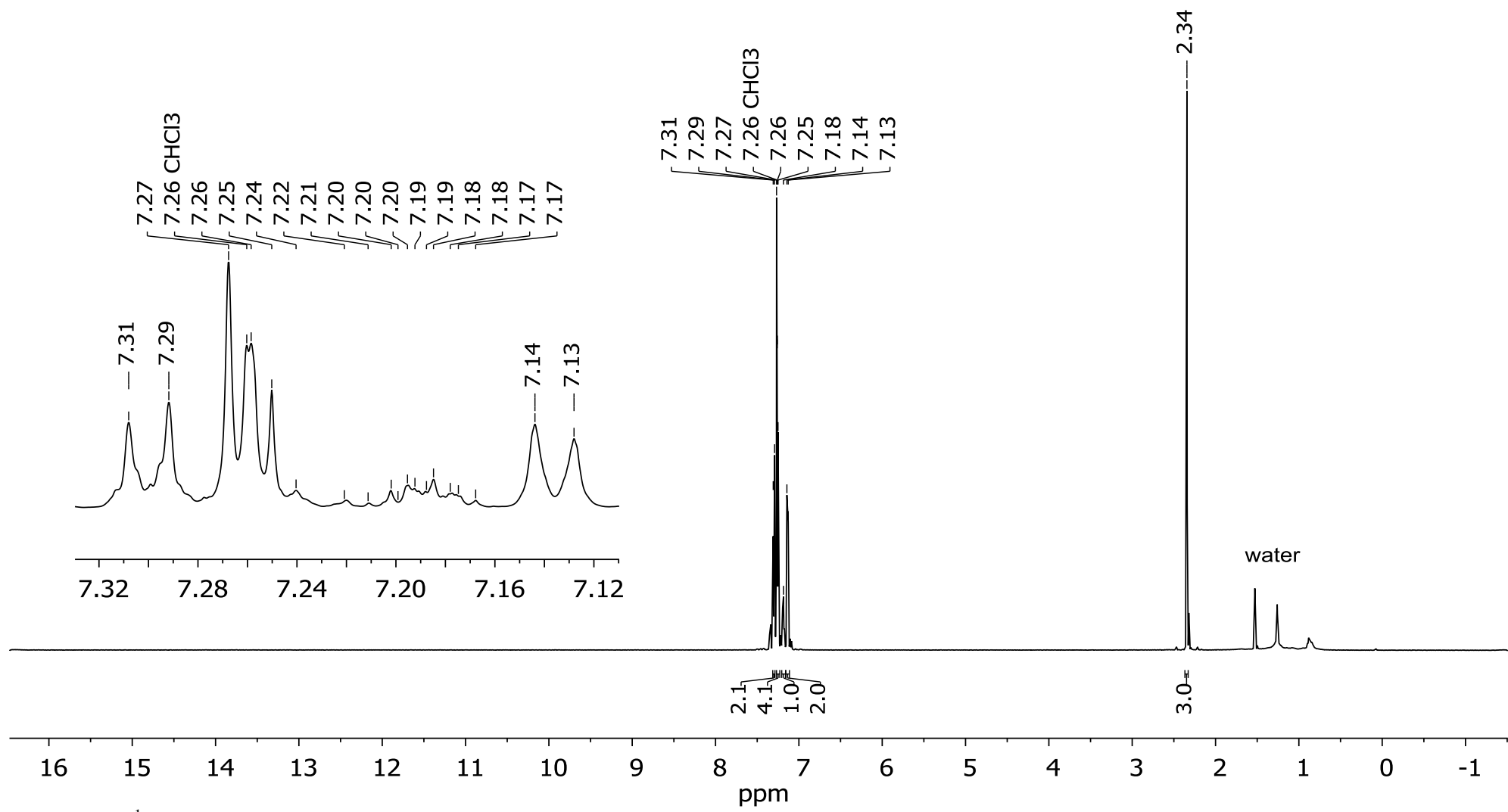
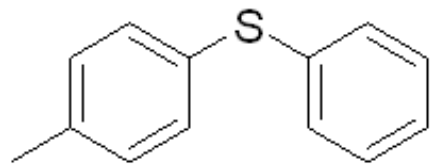
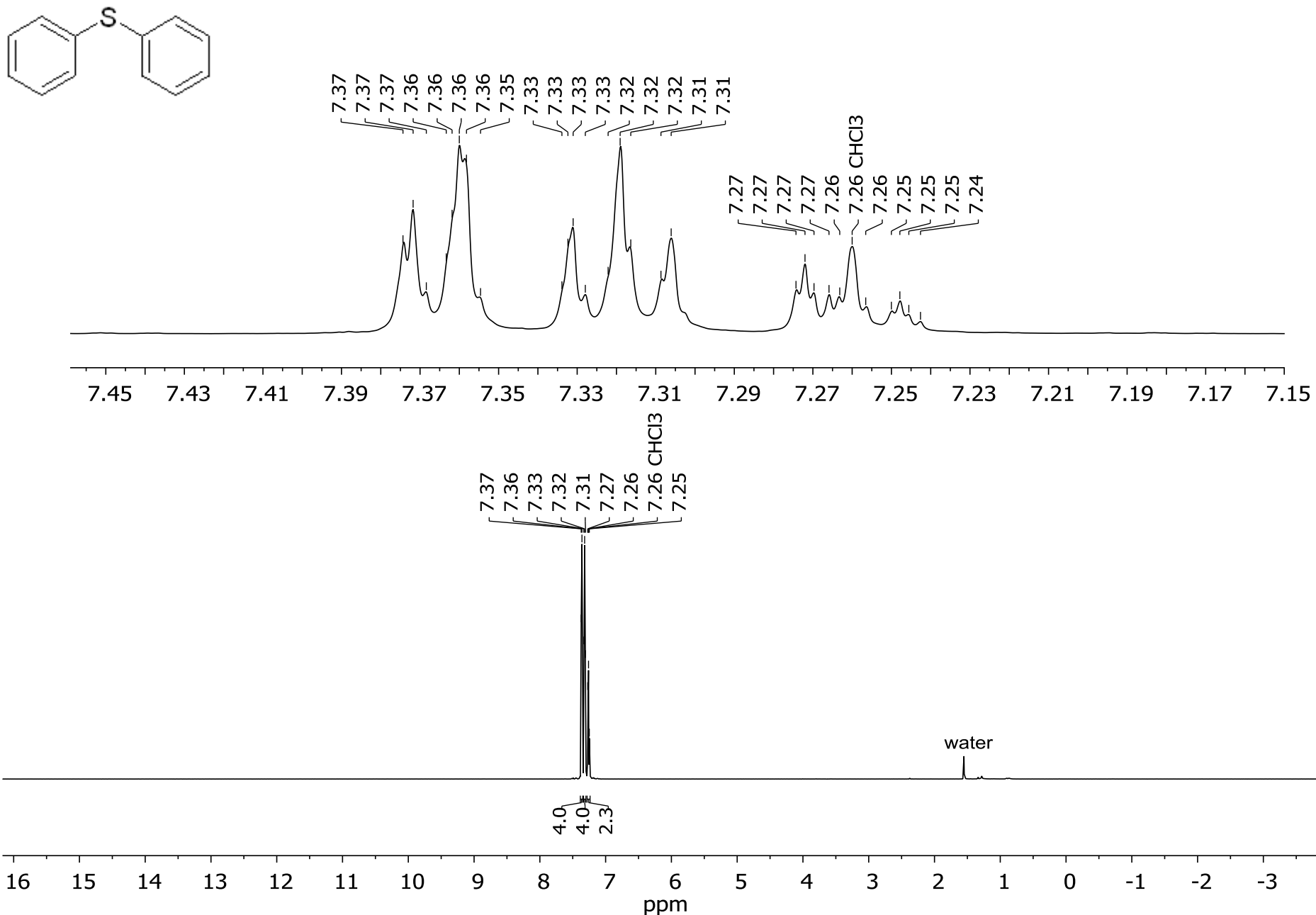
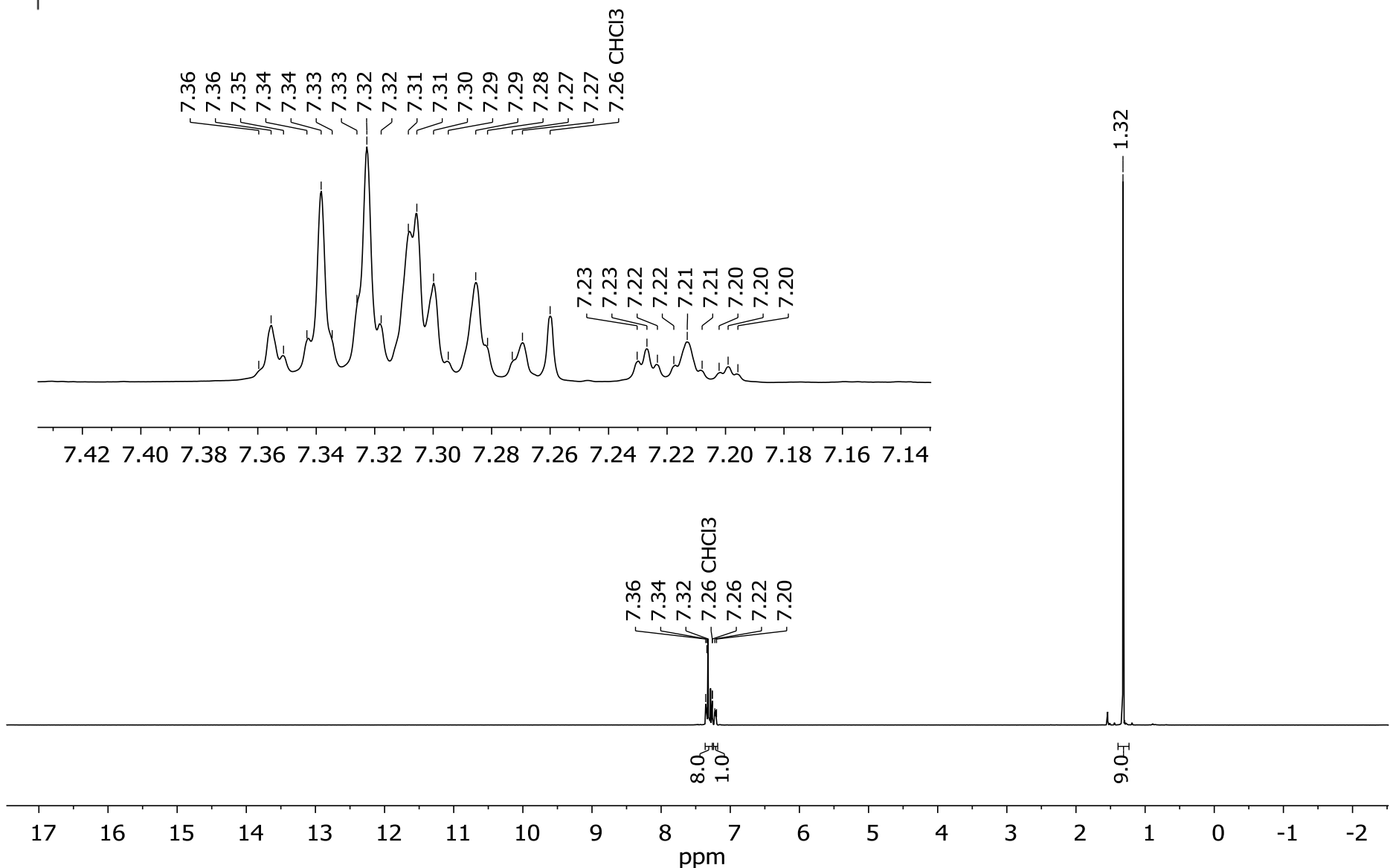
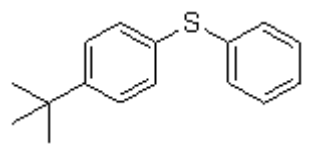


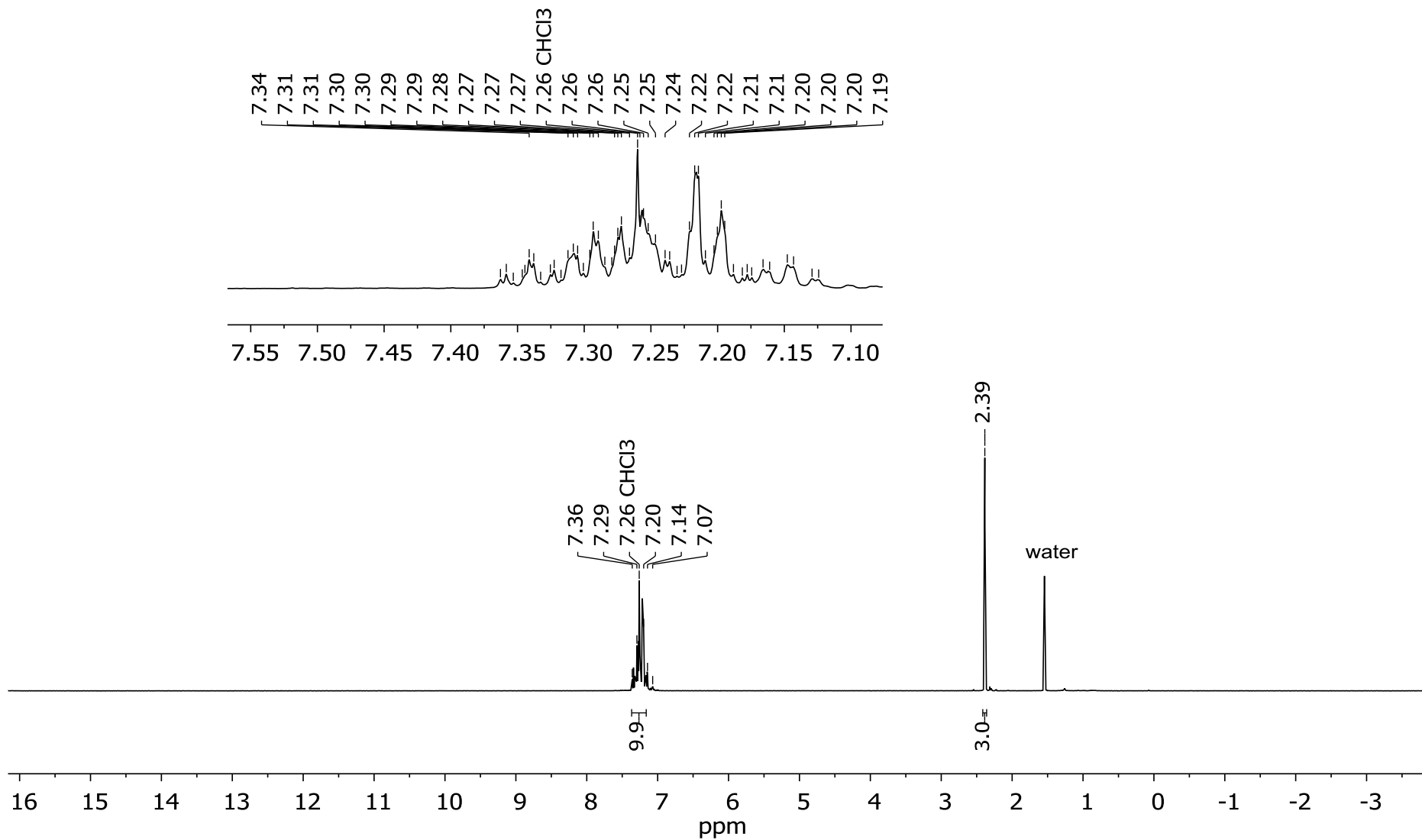
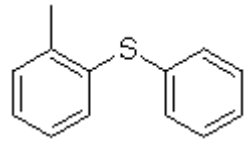
Figure S67.  $^1\text{H}$  NMR spectrum of compound **7a** ( $\text{CDCl}_3$ , 500 MHz)



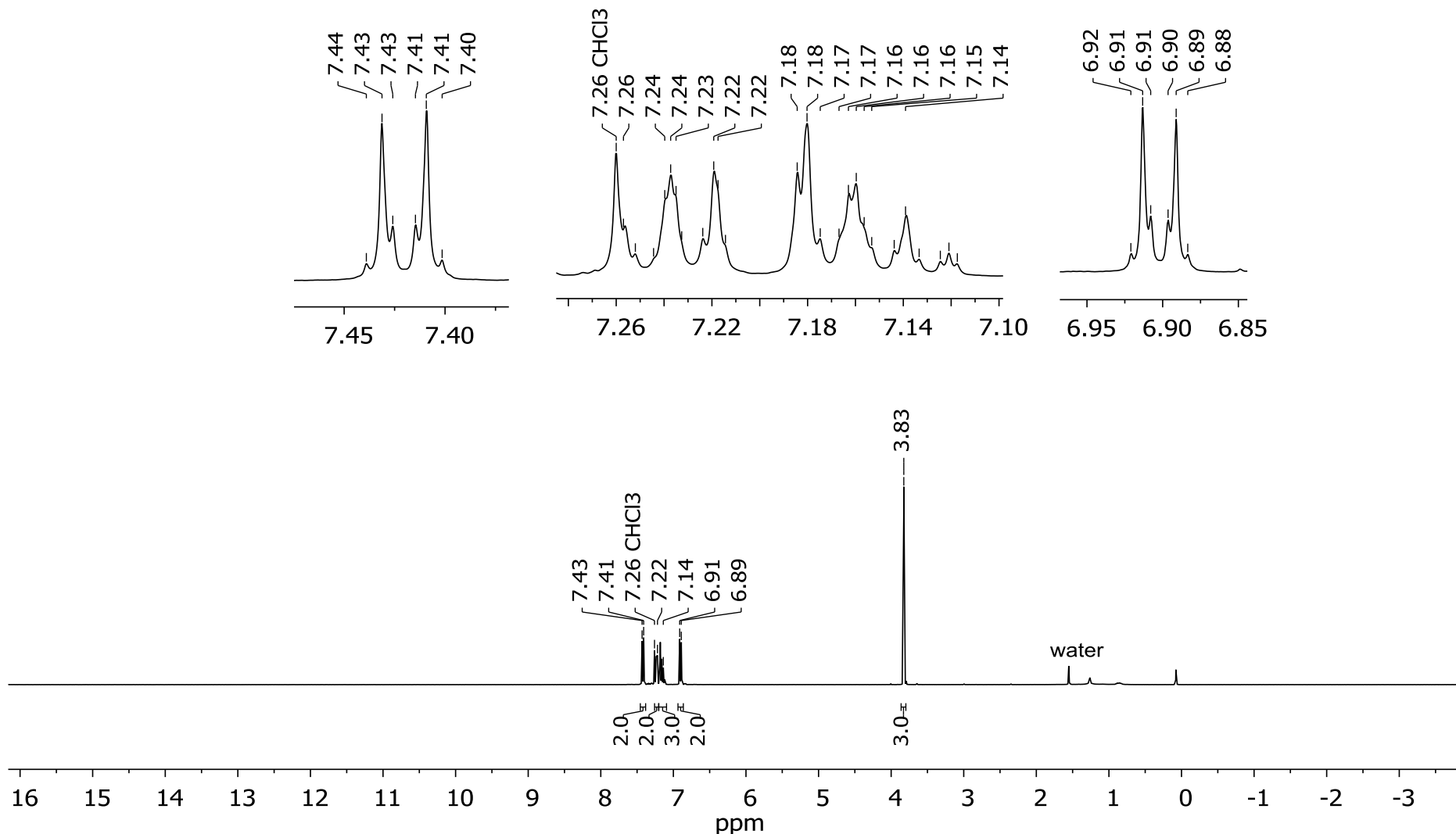
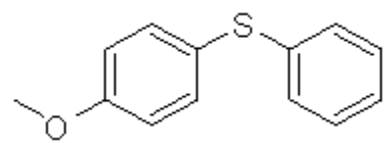
**Figure S68.**  $^1\text{H}$  NMR spectrum of compound **7c** ( $\text{CDCl}_3$ , 500 MHz)



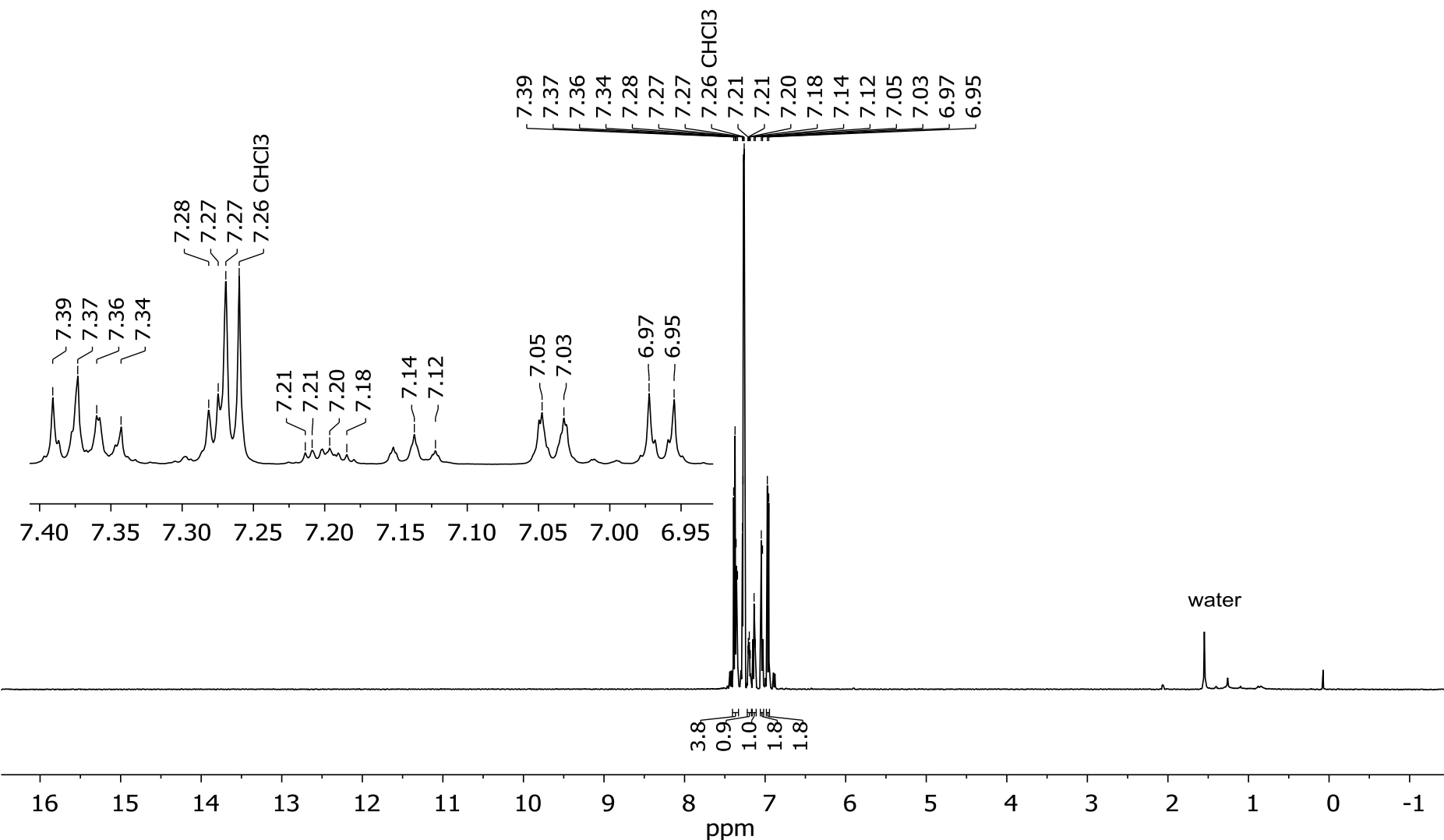
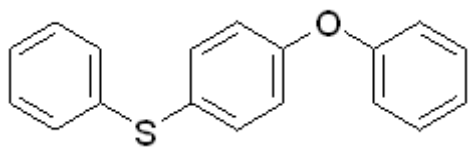
**Figure S69.** <sup>1</sup>H NMR spectrum of compound **7d** (CDCl<sub>3</sub>, 500 MHz)



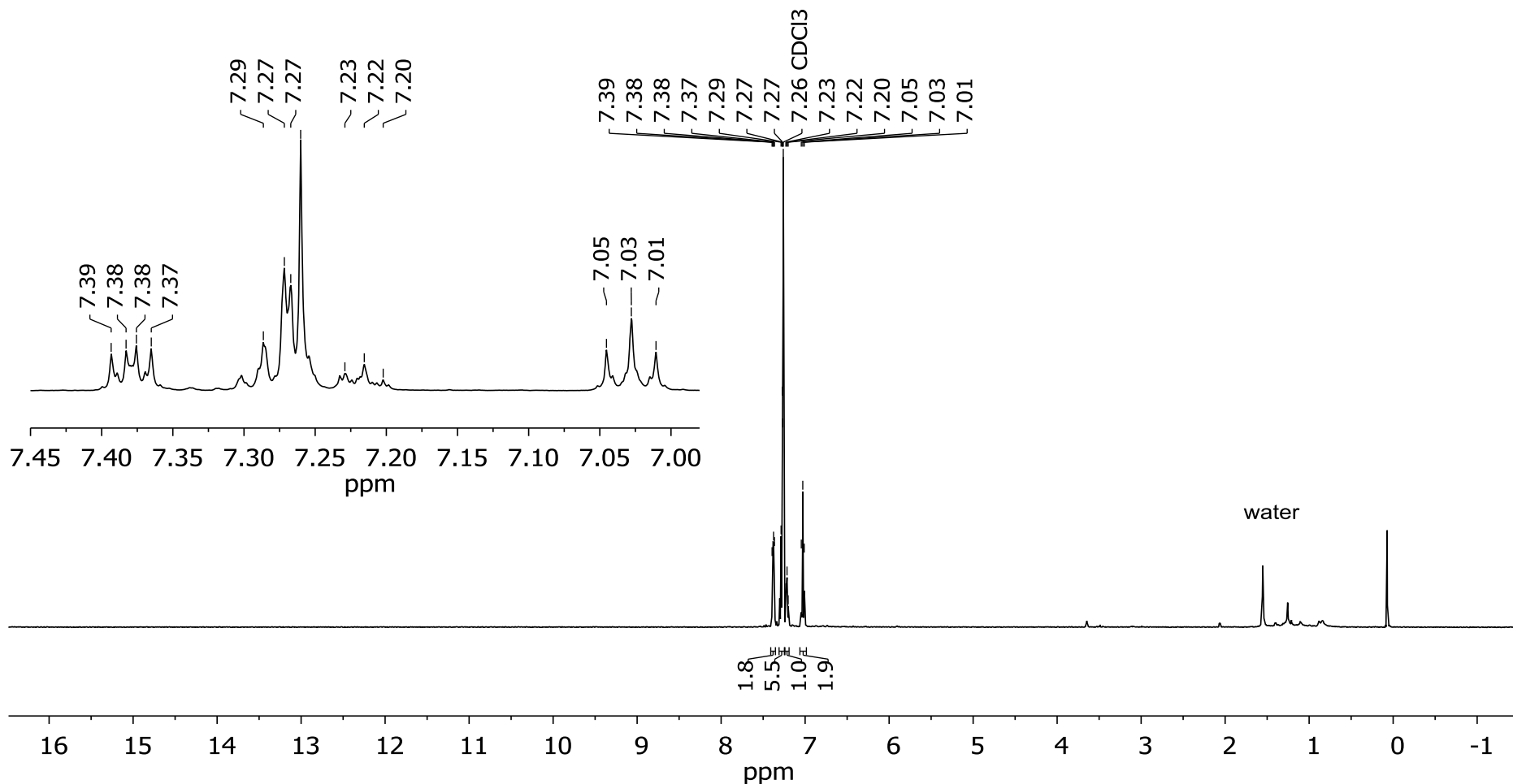
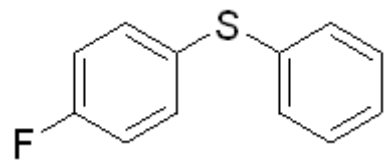
**Figure S70.**  $^1\text{H}$  NMR spectrum of compound **7e** ( $\text{CDCl}_3$ , 500 MHz)



**Figure S71.**  $^1\text{H}$  NMR spectrum of compound 7f (CDCl<sub>3</sub>, 500 MHz)



**Figure S72.** <sup>1</sup>H NMR spectrum of compound 7g ( $\text{CDCl}_3$ , 500 MHz)



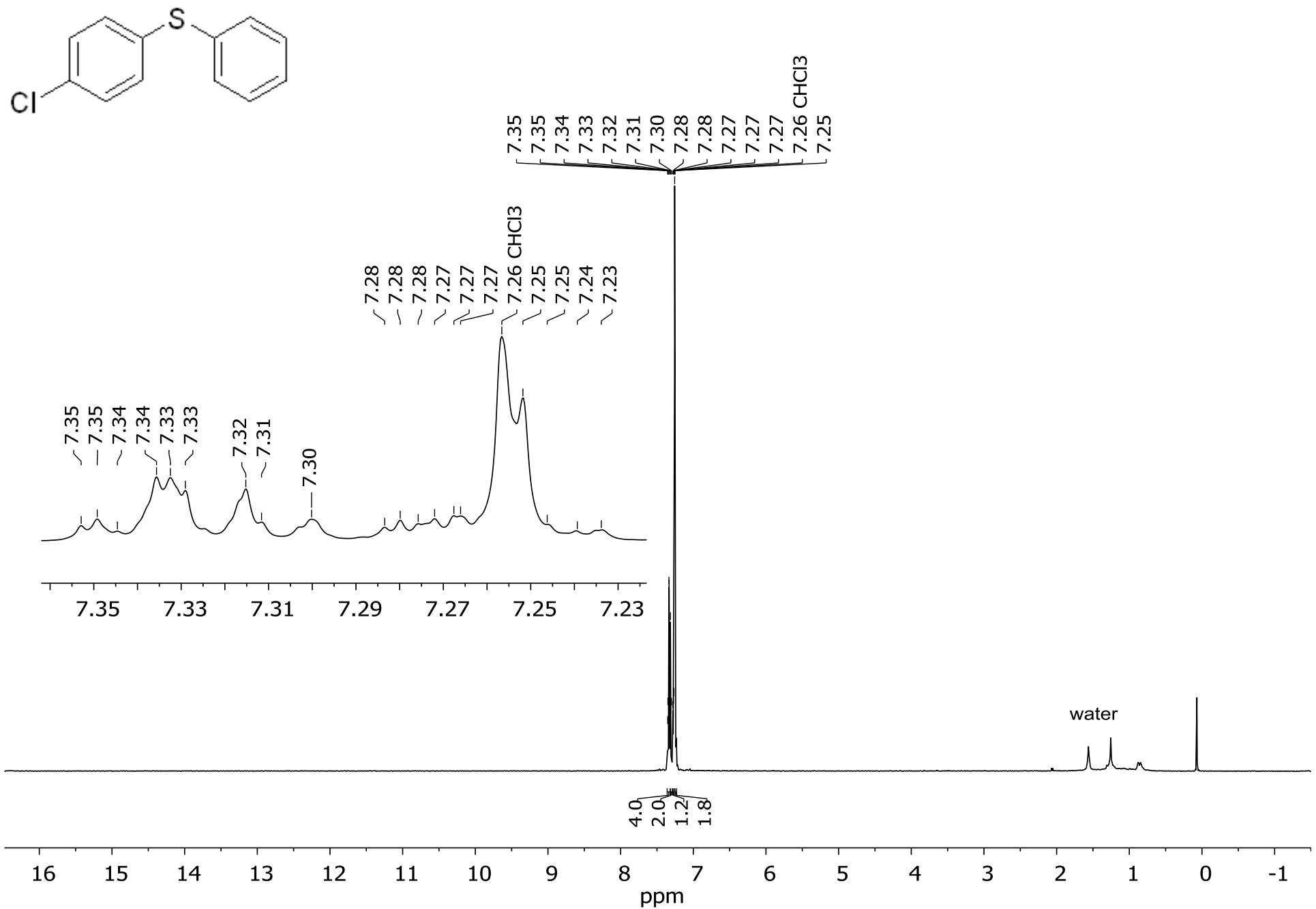


**Figure S74.**  $^1\text{H}$  NMR spectrum of compound **7i** ( $\text{CDCl}_3$ , 500 MHz)

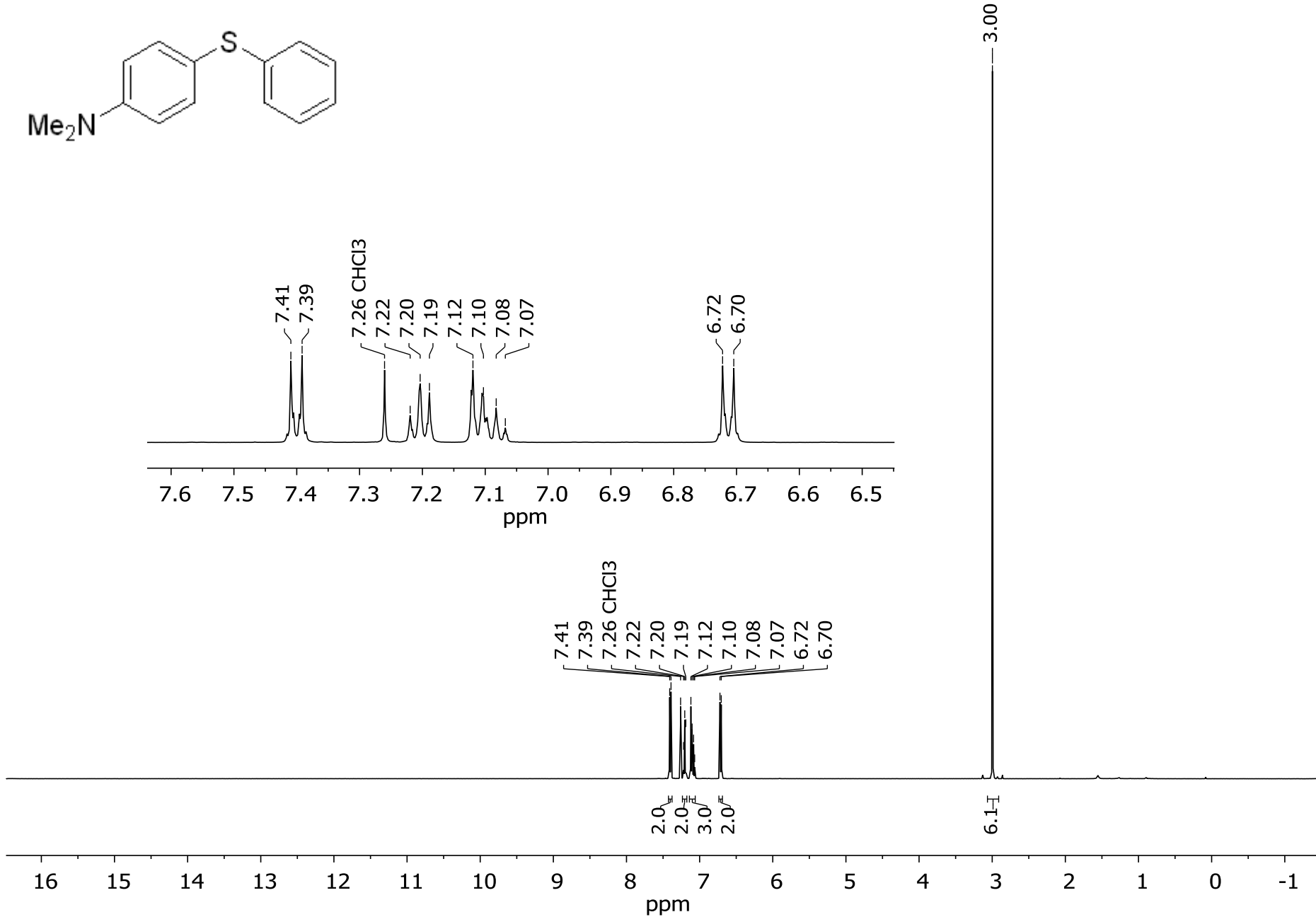
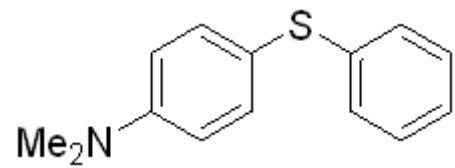


**Figure S75.**  $^1\text{H}$  NMR spectrum of compound **7j** ( $\text{CDCl}_3$ , 500 MHz)

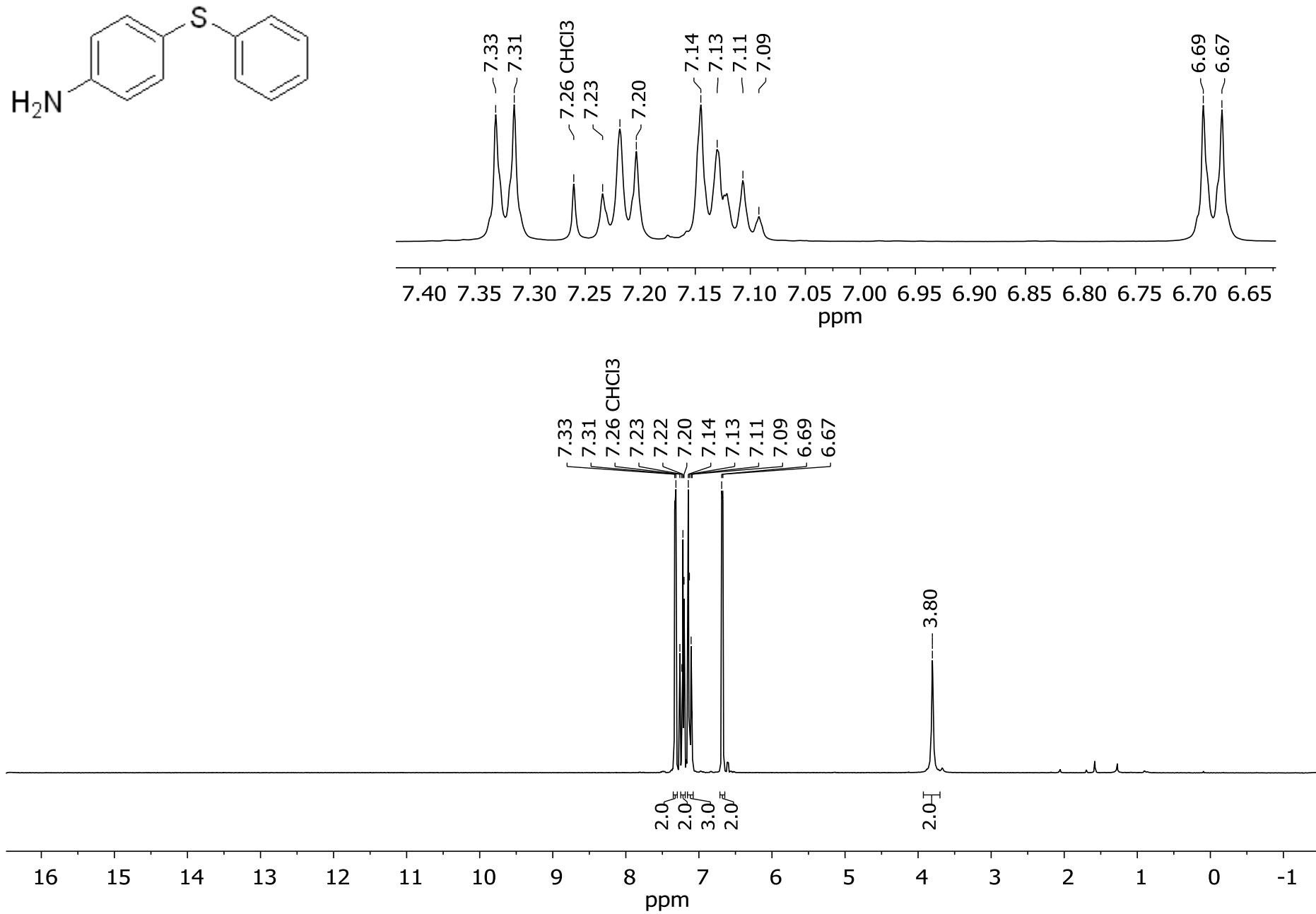


**Figure S76.**  $^1\text{H}$  NMR spectrum of compound **7k** ( $\text{CDCl}_3$ , 500 MHz)

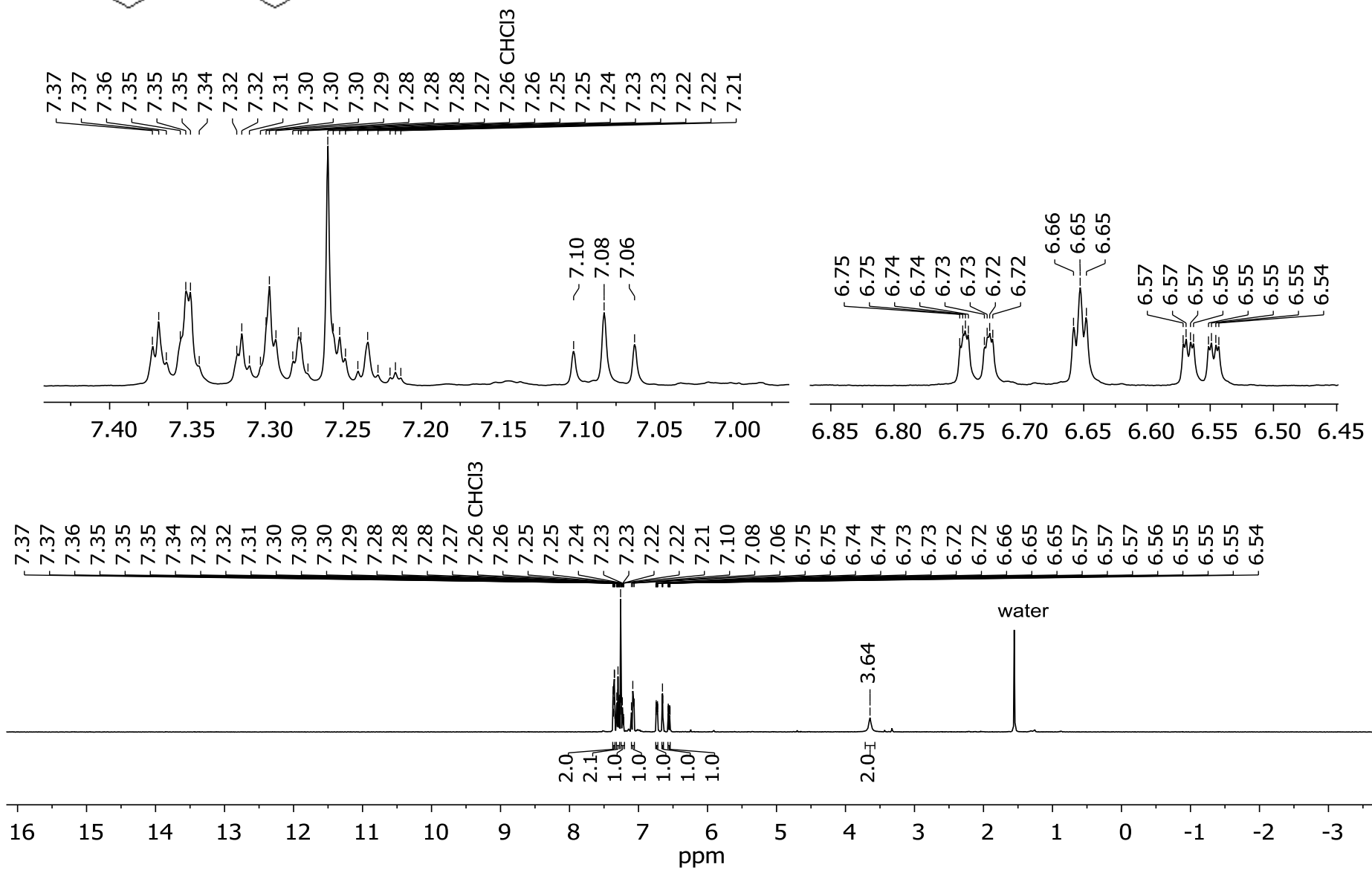
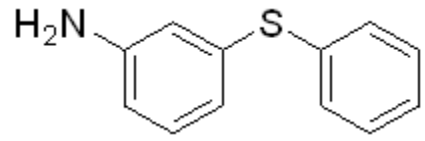
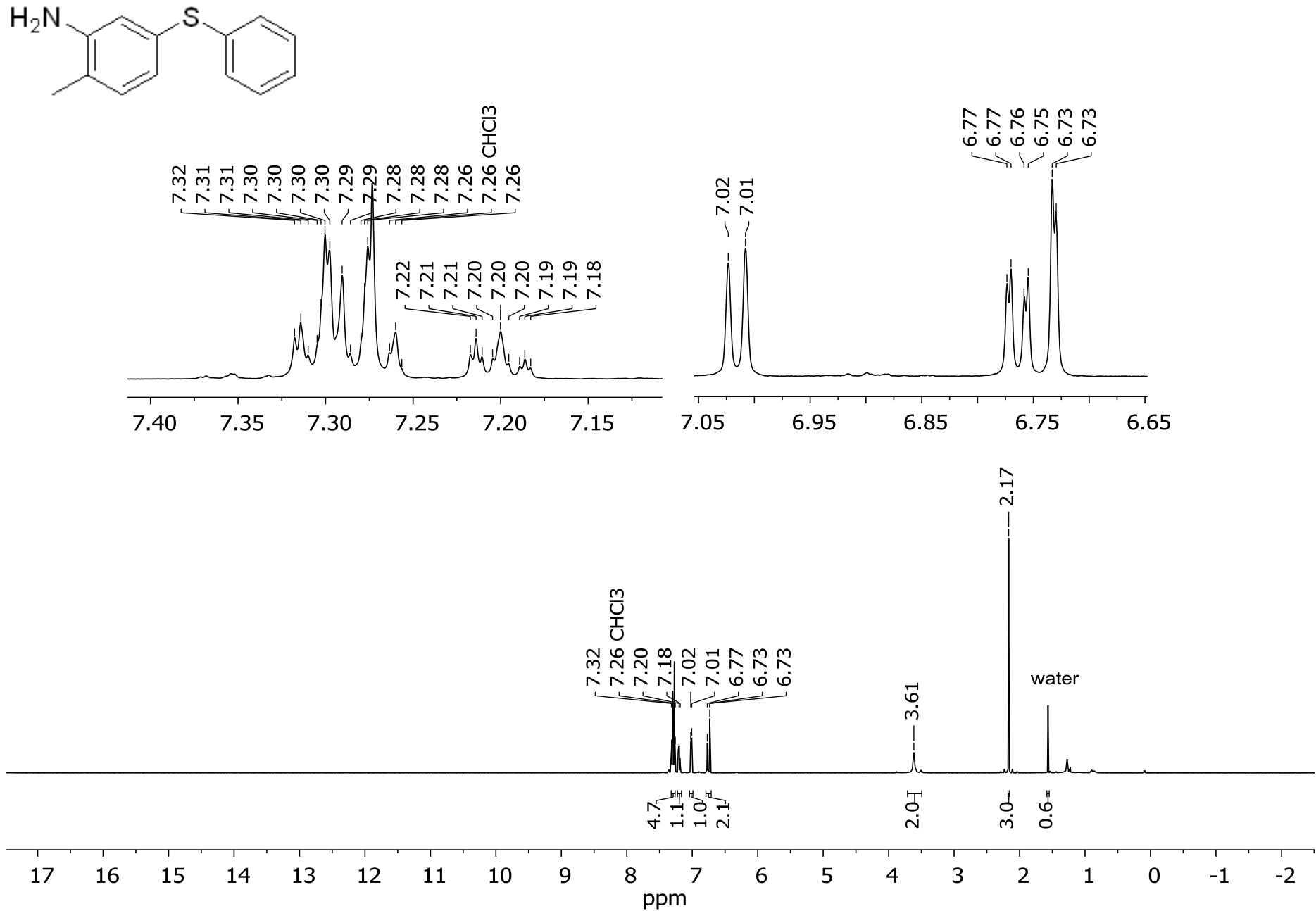
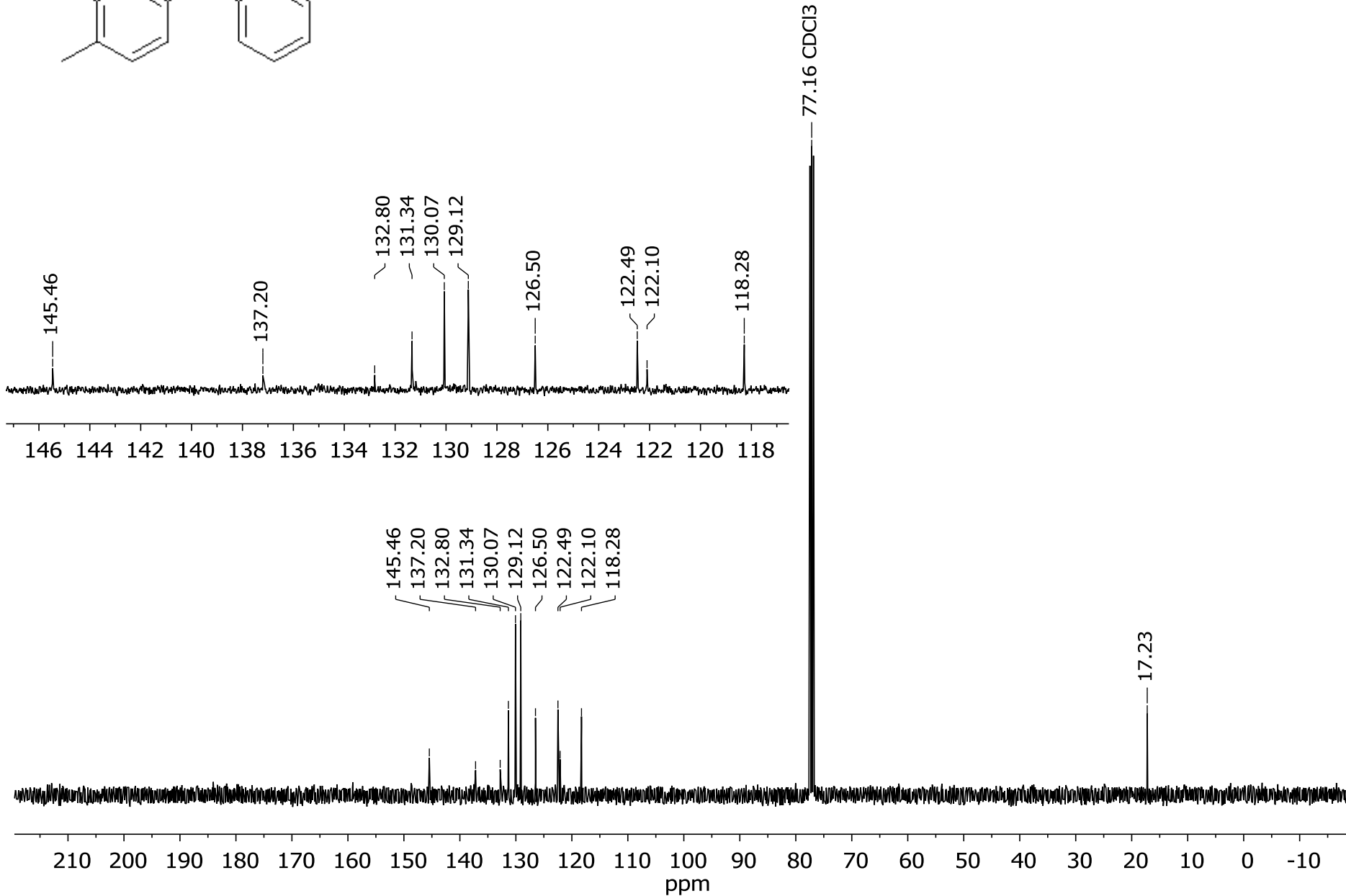
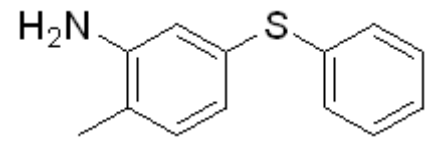


Figure S77. <sup>1</sup>H NMR spectrum of compound 7l (CDCl<sub>3</sub>, 500 MHz)



**Figure S78.**  $^1\text{H}$  NMR spectrum of compound **7m** ( $\text{CDCl}_3$ , 500 MHz)



**Figure S79.**  $^{13}\text{C}$  NMR spectrum of compound **7m** ( $\text{CDCl}_3$ , 125 MHz)

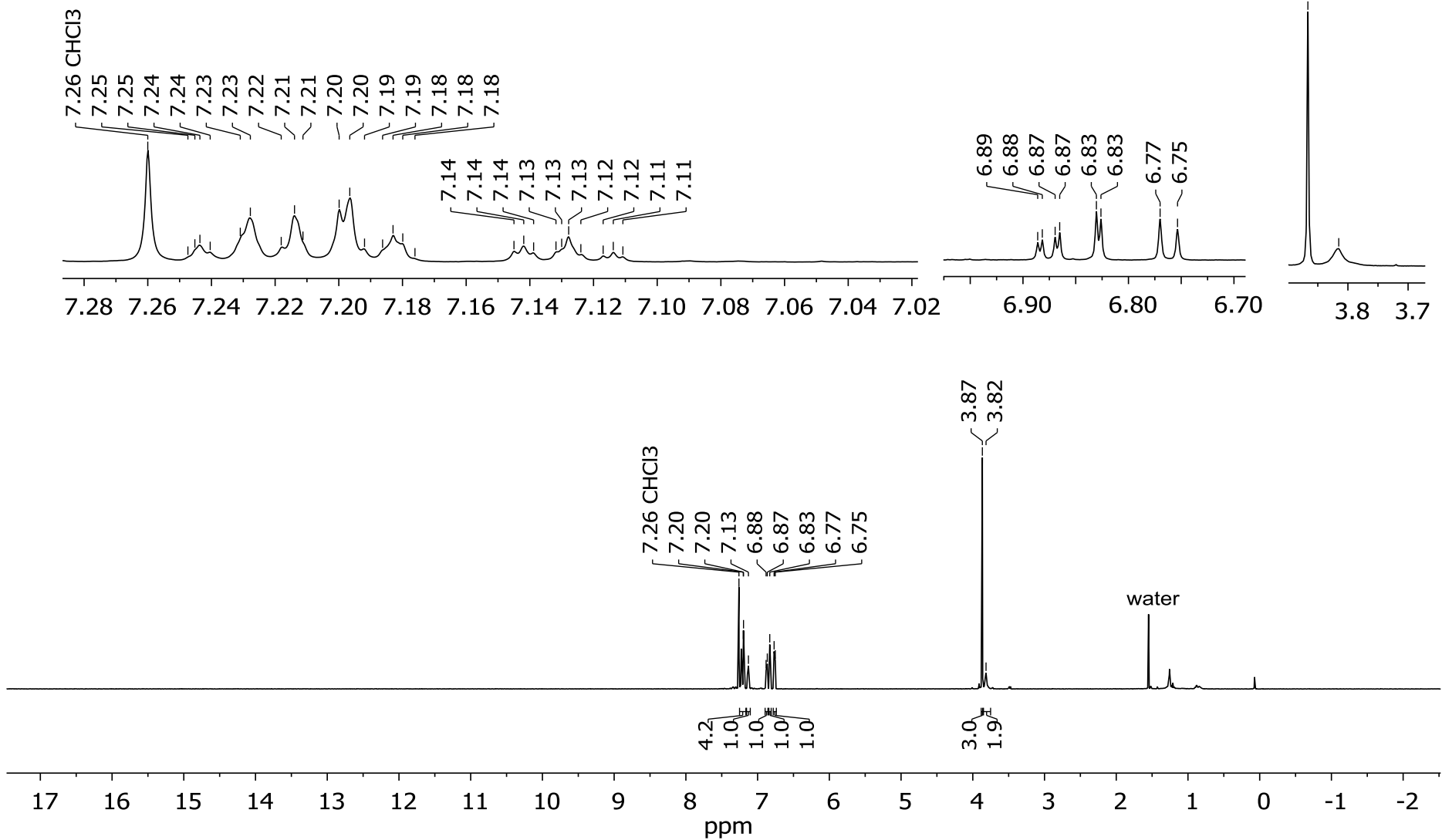
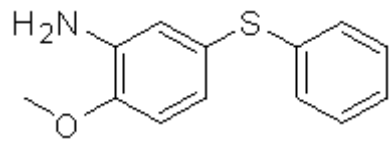


**Figure S80.**  $^1\text{H}$  NMR spectrum of compound **7n** ( $\text{CDCl}_3$ , 500 MHz)

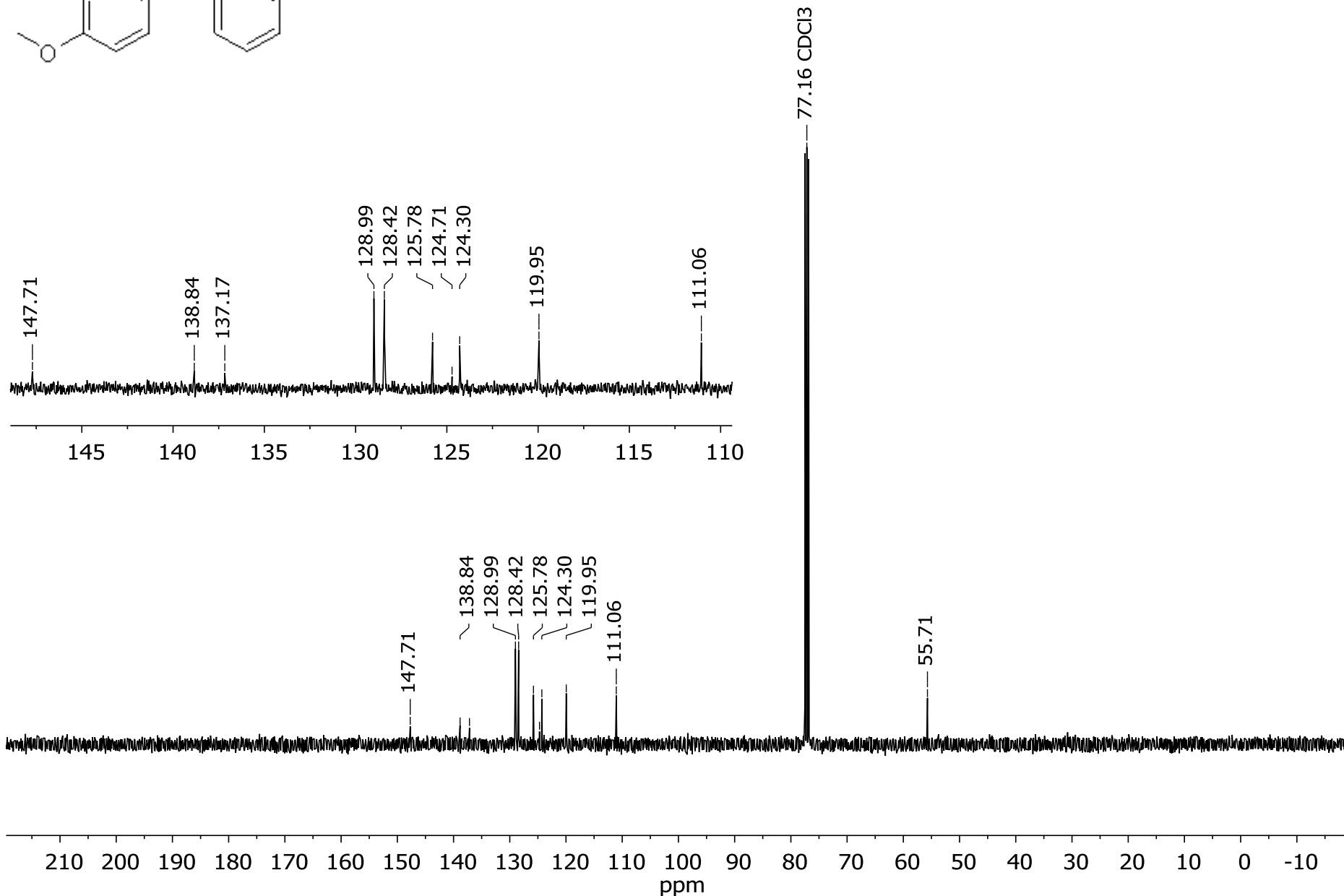
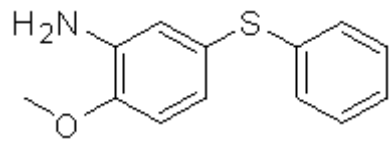


**Figure S81.**  $^{13}\text{C}$  NMR spectrum of compound **7n** (CDCl<sub>3</sub>, 125 MHz)

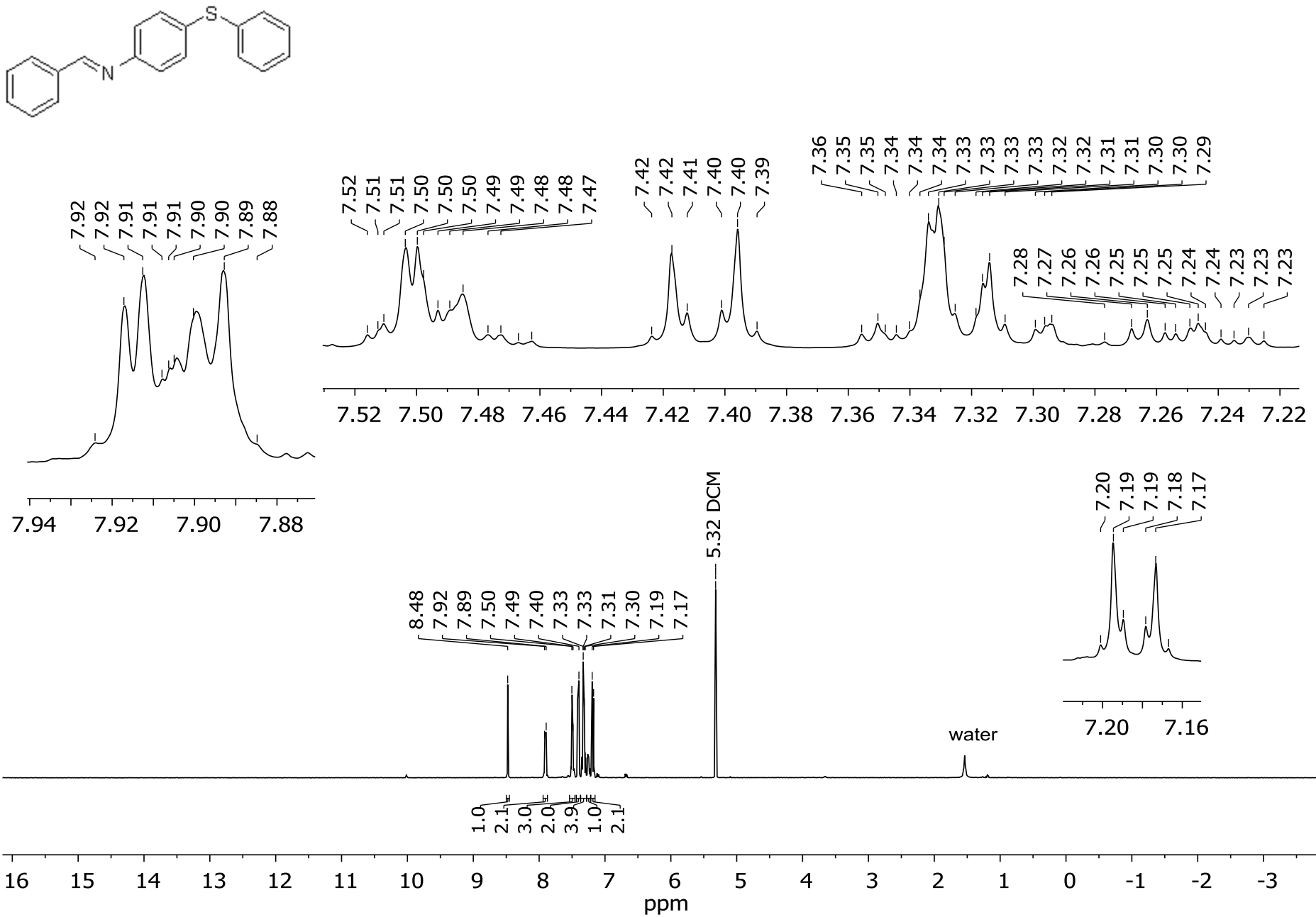


**Figure S82.** <sup>1</sup>H NMR spectrum of compound **7o** (CD<sub>2</sub>Cl<sub>2</sub>, 500 MHz)

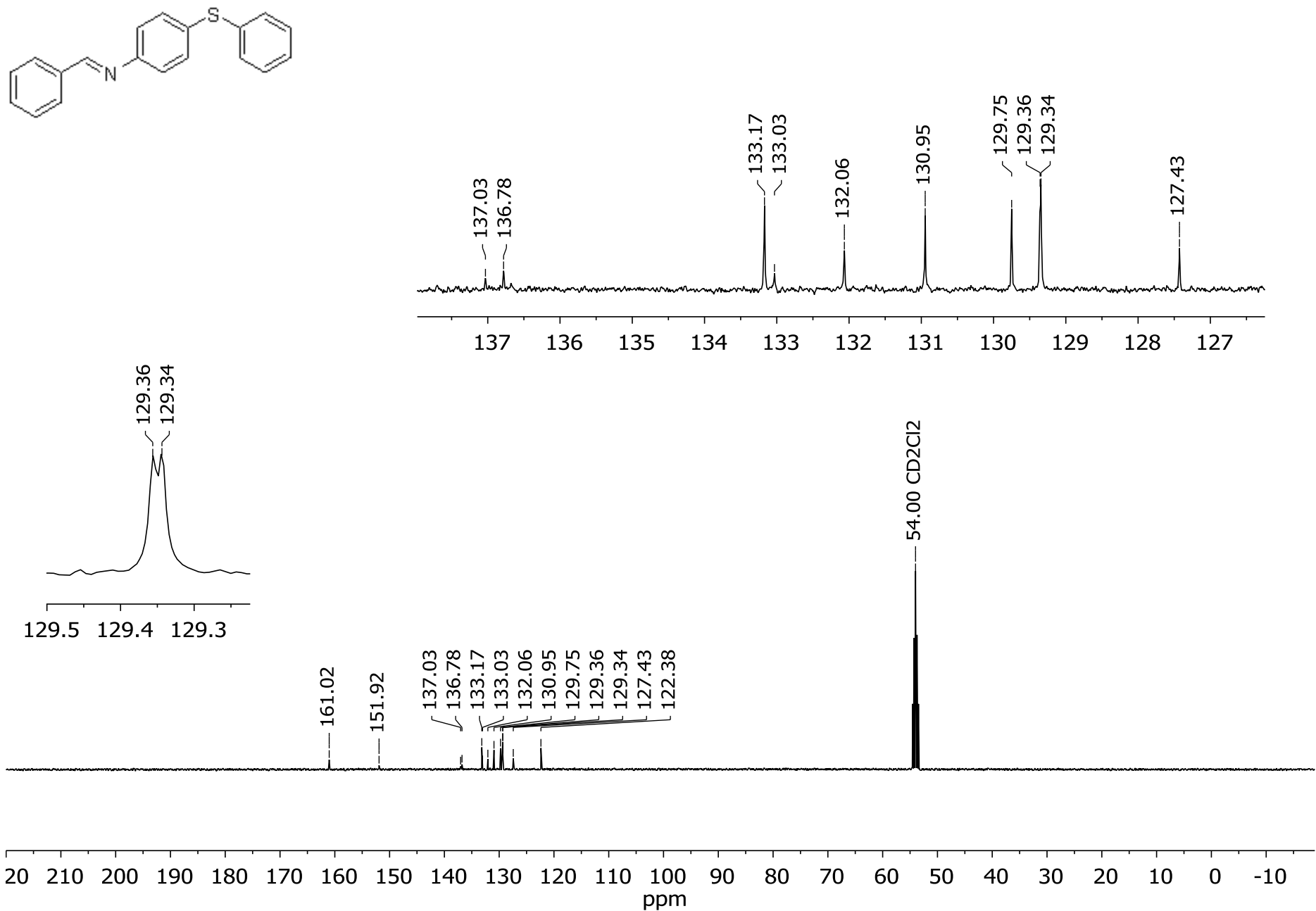


**Figure S83.**  $^{13}\text{C}$  NMR spectrum of compound **7o** ( $\text{CD}_2\text{Cl}_2$ , 125 MHz)

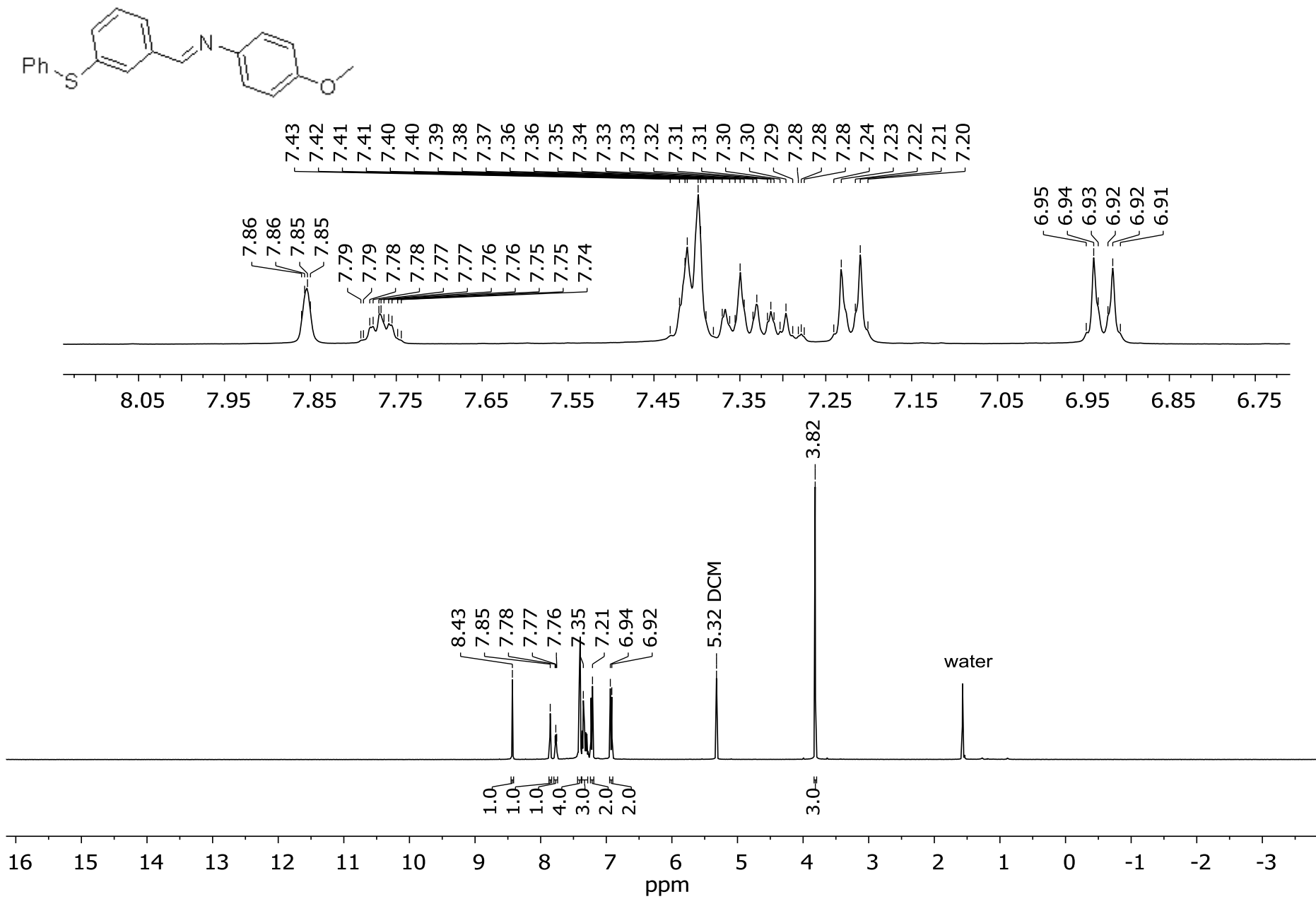


**Figure S84.**  $^1\text{H}$  NMR spectrum of compound **7p** ( $\text{CD}_2\text{Cl}_2$ , 500 MHz)

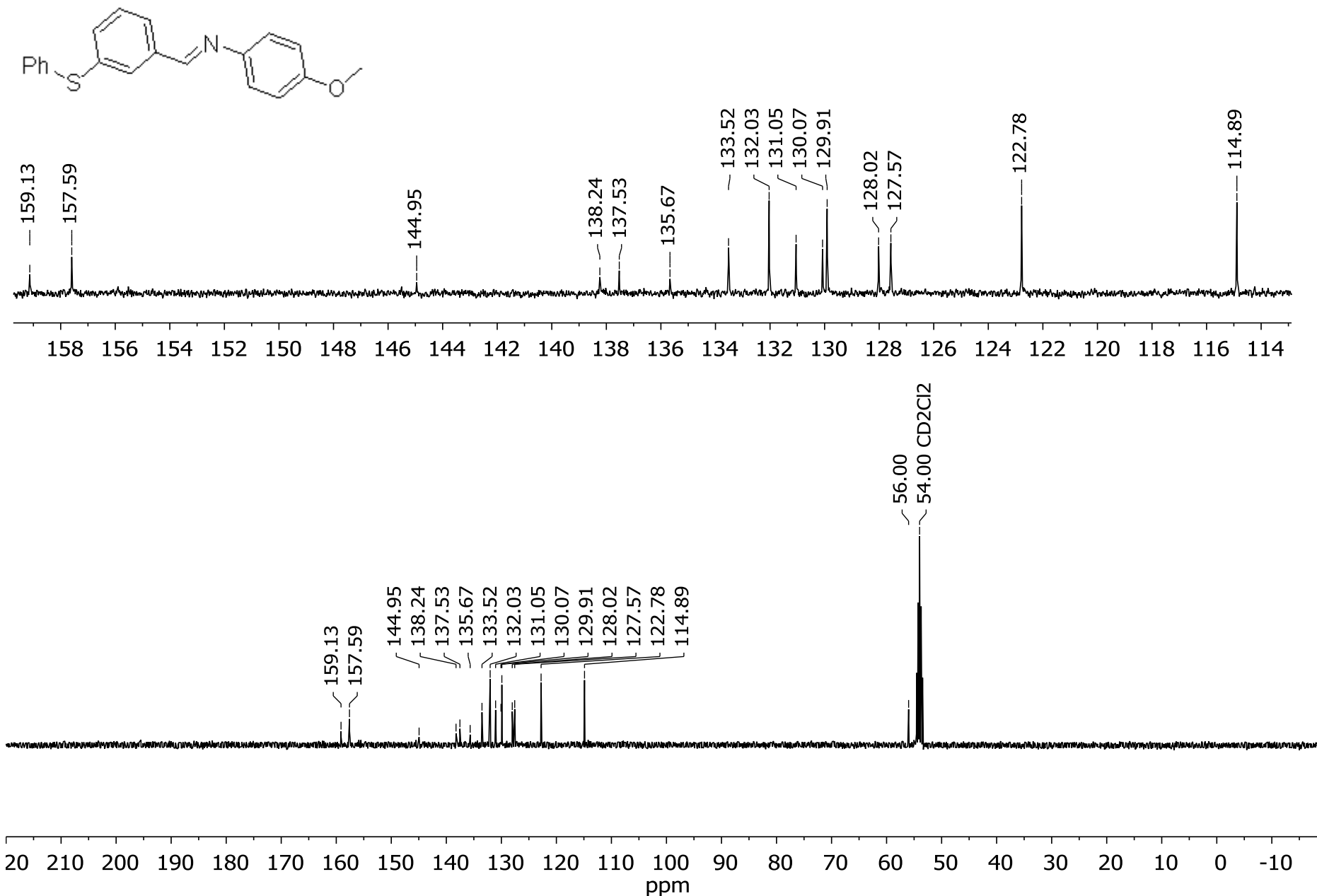


**Figure S85.**  $^{13}\text{C}$  NMR spectrum of compound **7p** ( $\text{CD}_2\text{Cl}_2$ , 125 MHz)

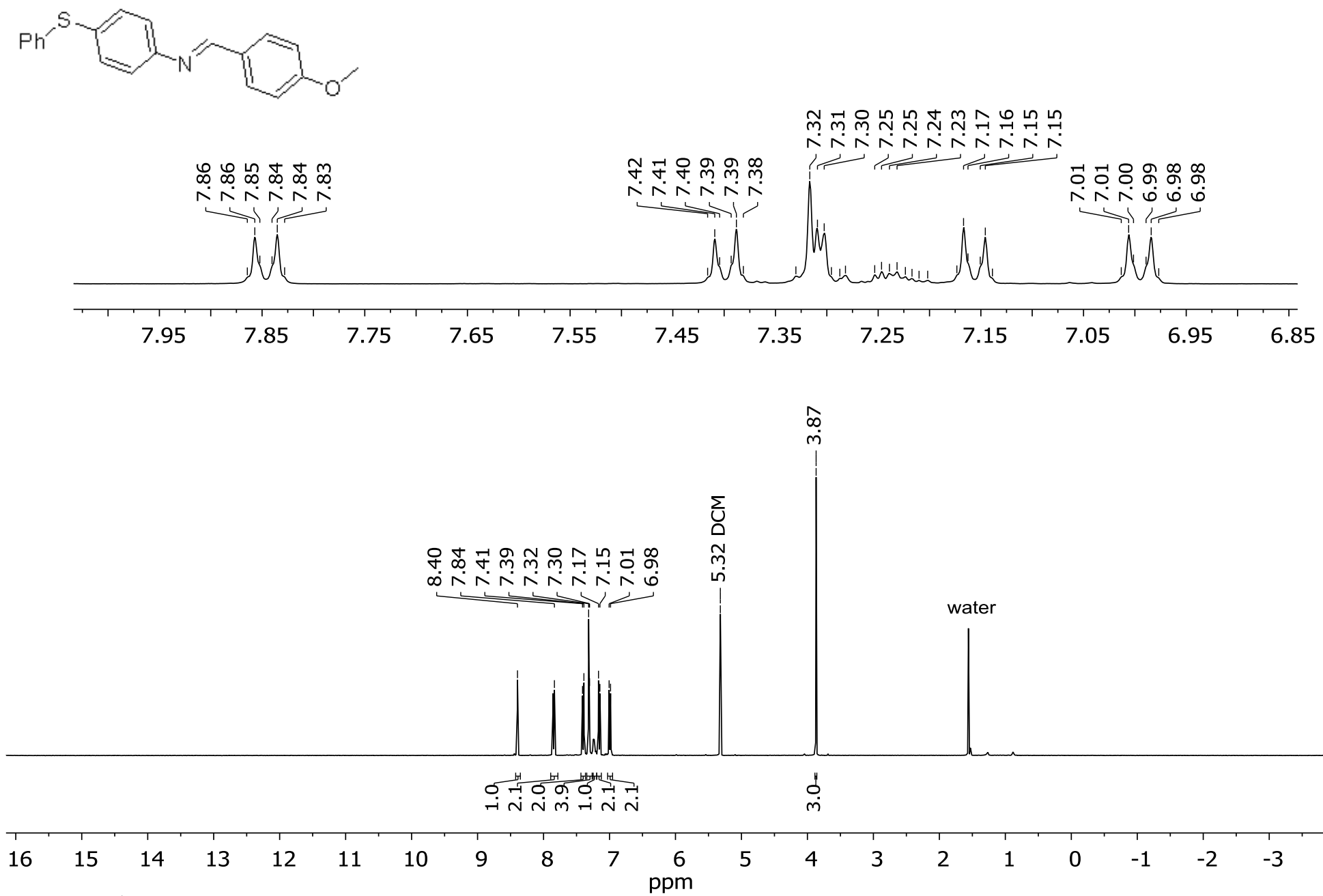


**Figure S86.**  $^1\text{H}$  NMR spectrum of compound **7r** ( $\text{CD}_2\text{Cl}_2$ , 500 MHz)

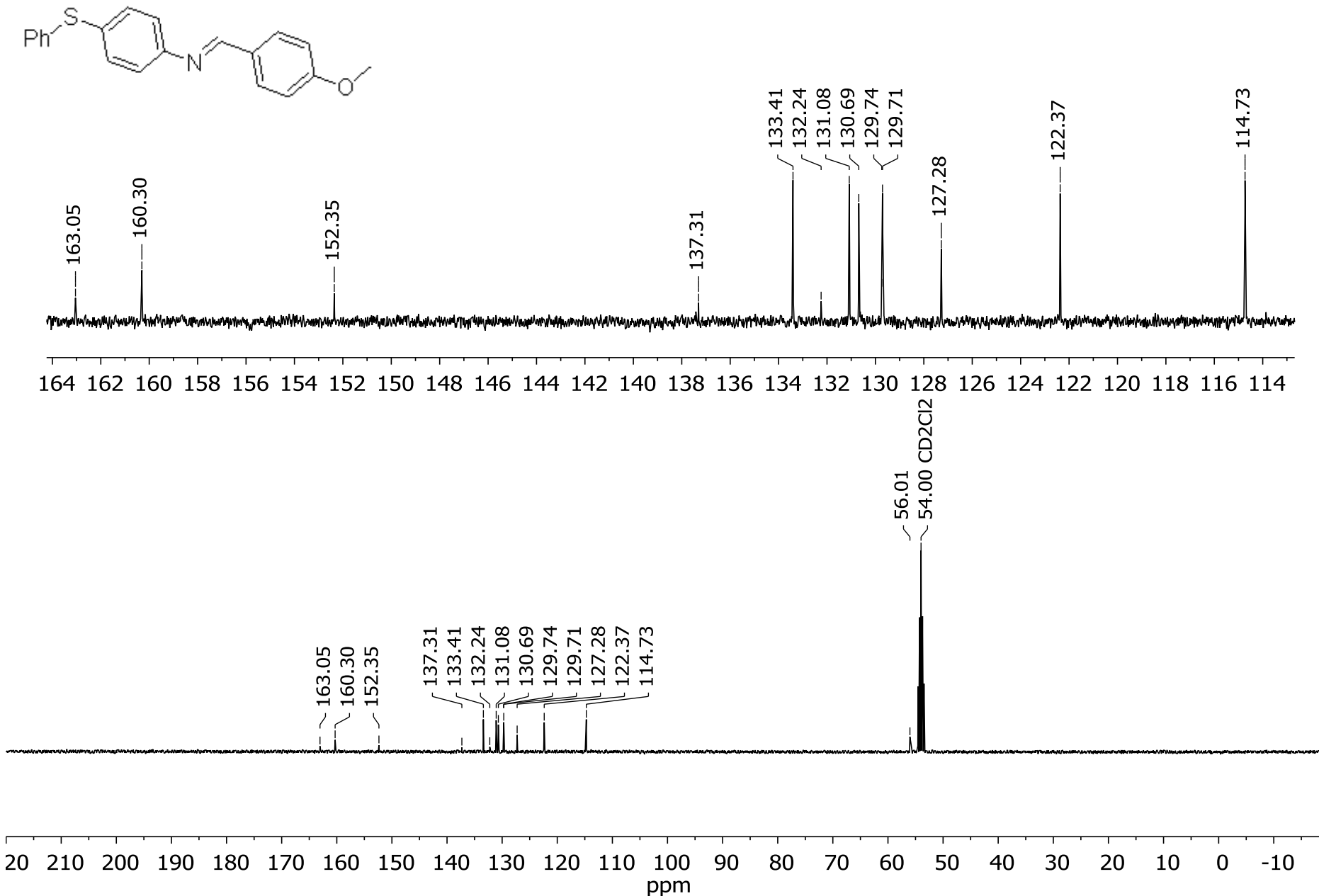


**Figure S87.**  $^{13}\text{C}$  NMR spectrum of compound **7r** ( $\text{CD}_2\text{Cl}_2$ , 125 MHz)

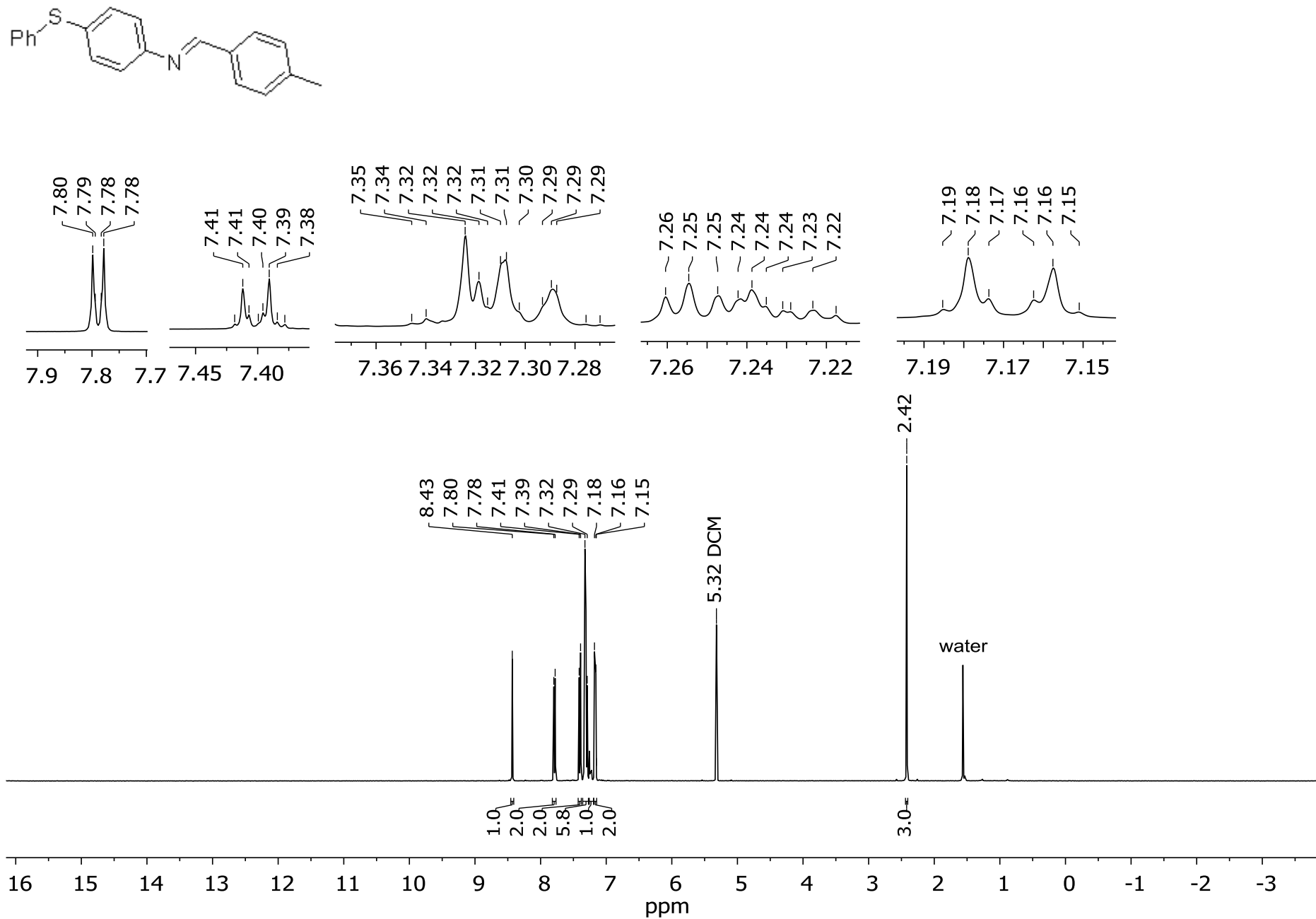


**Figure S88.**  $^1\text{H}$  NMR spectrum of compound 7s ( $\text{CD}_2\text{Cl}_2$ , 500 MHz)

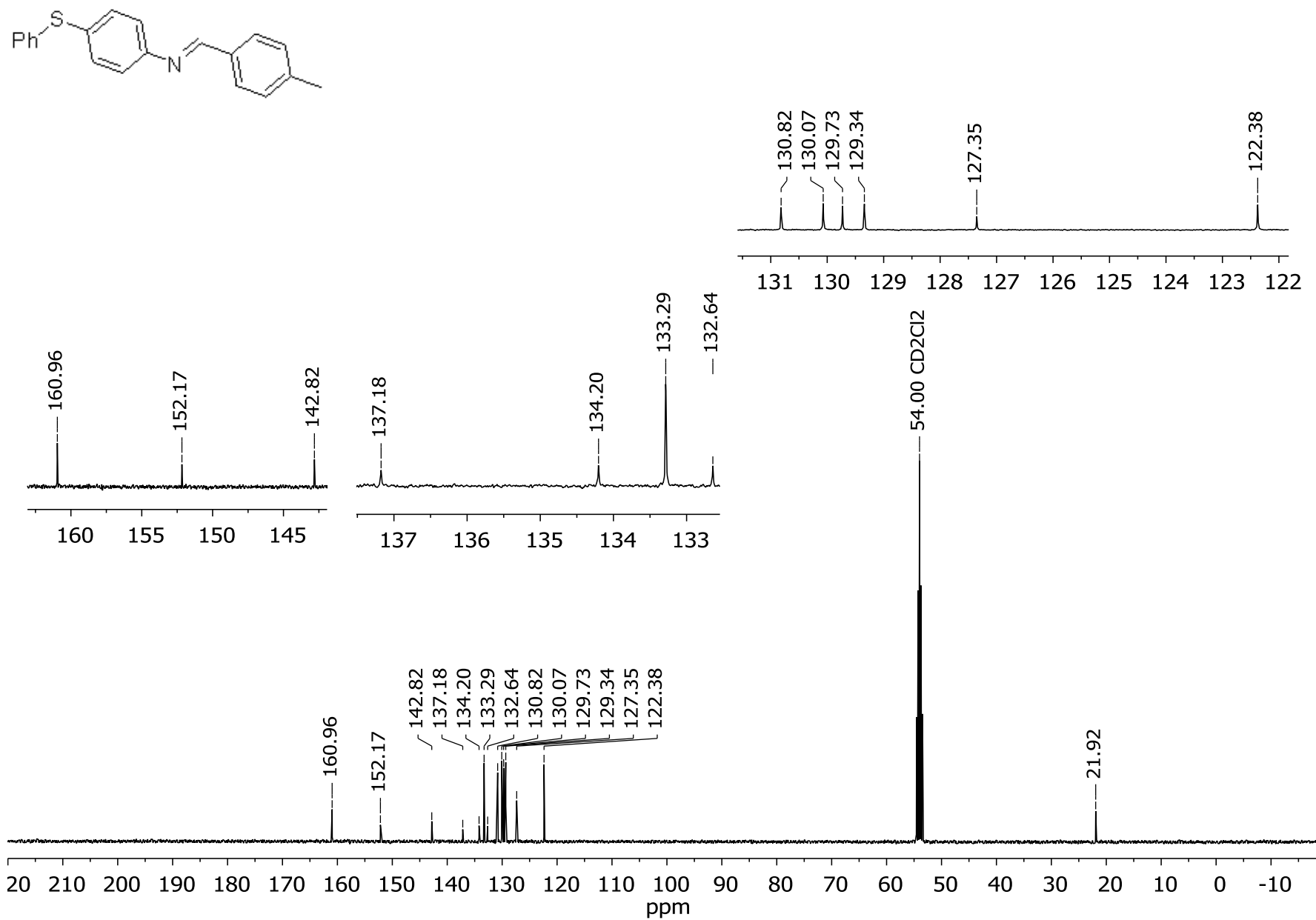


**Figure S89.**  $^{13}\text{C}$  NMR spectrum of compound **7s** ( $\text{CD}_2\text{Cl}_2$ , 125 MHz)

## S4. Single Crystal X-Ray Diffraction Data

### Experimental

X-ray diffraction data were collected on the STOE STADIVARI Pilatus 100K diffractometer using CuKa radiation provided by a GeniX3D HF generator equipped with a microfocus X-ray tube and combined with a Xenocs FOX3D HF multilayer thin-film ellipsoidal monochromator. Data collection, determination and refinement of the unit cell parameters were preformed using STOE X-Area software package (STOE & Cie GmbH, Germany). Intensity data were scaled with LANA (part of X-Area) in order to minimize differences in intensities of the symmetry-equivalent reflections (multi-scan method). The structures were determined by direct method and refined by full-matrix least squares technique on  $F^2$  with anisotropic displacement parameters for non-hydrogen atoms. All hydrogen atoms were placed in calculated positions and refined within the riding model with fixed isotropic displacement parameters ( $U_{\text{iso}}(\text{H}) = 1.5U_{\text{eq}}(\text{C})$  for the  $\text{CH}_3$ -groups and  $U_{\text{iso}}(\text{H}) = 1.2U_{\text{eq}}(\text{C})$  for the other groups). All calculations were carried out using the *SHELXTL* program.<sup>1</sup> Crystallographic data for **2a**, **2g**, **2k** and **2y** have been deposited in the Cambridge Crystallographic Data Center. CCDC 1867867 (**2a**), CCDC 1867865 (**2k**), CCDC 1867866 (**2g**), and CCDC 1907428 (**2y**) contain the supplementary crystallographic data for this paper. These data can be obtained free of charge from the Director, CCDC, 12 Union Road, Cambridge CB2 1EZ, UK (Fax: +44 1223 336033; e-mail: deposit@ccdc.cam.ac.uk or [www.ccdc.cam.ac.uk](http://www.ccdc.cam.ac.uk)).

### References

- (1) Sheldrick, G. SHELXT - Integrated space-group and crystal-structure determination. *Acta Crystallographica Section A* **2015**, *71*, 3-8.

## Compound 2a

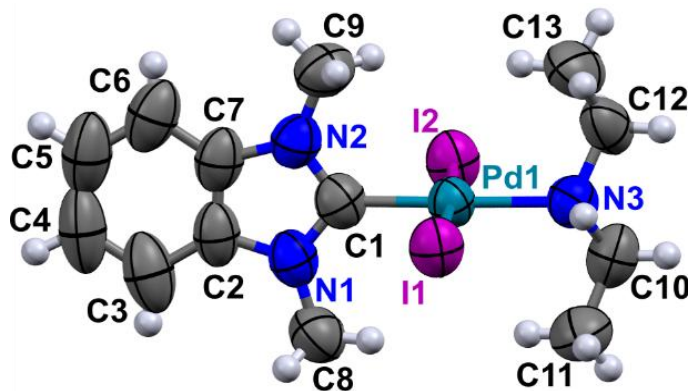


**Figure S90.** The molecular structure of compound **2a** according to single-crystal X-ray diffraction data. Thermal ellipsoids are shown at 50 % probability.

Table S6. Crystal data for compound **2a**

C <sub>13</sub> H <sub>21</sub> I <sub>2</sub> N <sub>3</sub> Pd	<i>F</i> (000) = 1088
Mr = 579.53	<i>Dx</i> = 2.083 Mg m <sup>-3</sup>
Monoclinic, P2 <sub>1</sub> /c	<i>Cu K</i> <sub>a</sub> radiation, $\lambda$ = 1.54186 Å
<i>a</i> = 17.5721 (7) Å	Cell parameters from 2334 reflections
<i>b</i> = 12.5994 (8) Å	$\theta$ = 4.5–70.5°
<i>c</i> = 8.4655 (4) Å	$\mu$ = 34.26 mm <sup>-1</sup>
$\beta$ = 99.550 (3)°	<i>T</i> = 295 K
<i>V</i> = 1848.27 (16) Å <sup>3</sup>	Block, yellow
Z = 4	0.17 × 0.14 × 0.13 mm

Table S7. Data collection for compound **2a**

STOE diffractometer	3573 independent reflections
Radiation source: Cu GeniX 3D	2389 reflections with $I > 2\sigma(I)$
None monochromator	$R_{\text{int}}$ = 0.097
Detector resolution: 5.81 pixels mm <sup>-1</sup>	$\theta_{\max}$ = 73.3°, $\theta_{\min}$ = 4.3°
rotation method scans	
Absorption correction: part of the refinement model (ΔF) (See: Walker, N. & Stuart, D. (1983) Acta Cryst. A39, 158-166)	
$T_{\min}$ = 0.327, $T_{\max}$ = 0.702	
3573 measured reflections	

Table S8. Refinement for compound **2a**

Refinement on $F^2$	Hydrogen site location: inferred from neighbouring sites
Least-squares matrix: full	H-atom parameters constrained
$R[F^2 > 2\sigma(F^2)] = 0.063$	$w = 1/[\sigma^2(F_o^2) + (0.1309P)^2]$ where $P = (F_o^2 + 2F_c^2)/3$
$wR(F^2) = 0.186$	$(\Delta/\sigma)_{\max} = 0.001$
S = 0.95	$\Delta\rho_{\max} = 0.96 \text{ e } \text{\AA}^{-3}$
3573 reflections	$\Delta\rho_{\min} = -1.18 \text{ e } \text{\AA}^{-3}$
176 parameters	
0 restraints	

Table S9. Geometric parameters ( $\text{\AA}$ ) for compound **2a**

Pd1—C1	1.944 (11)	C6—C7	1.408 (16)
Pd1—N3	2.125 (9)	C6—H6	0.9300
Pd1—I1	2.5949 (8)	C8—H8A	0.9600
Pd1—I2	2.6101 (9)	C8—H8B	0.9600
N1—C1	1.352 (14)	C8—H8C	0.9600
N1—C2	1.409 (13)	C9—H9A	0.9600
N1—C8	1.446 (16)	C9—H9B	0.9600
N2—C1	1.339 (14)	C9—H9C	0.9600
N2—C7	1.393 (14)	C10—C11	1.503 (19)
N2—C9	1.440 (15)	C10—H10A	0.9700
N3—C10	1.449 (16)	C10—H10B	0.9700
N3—C12	1.486 (14)	C11—H11A	0.9600
N3—H31	0.9800	C11—H11B	0.9600
C2—C7	1.370 (18)	C11—H11C	0.9600
C2—C3	1.392 (18)	C12—C13	1.49 (2)
C3—C4	1.39 (3)	C12—H12A	0.9700
C3—H3	0.9300	C12—H12B	0.9700
C4—C5	1.39 (3)	C13—H13A	0.9600
C4—H4	0.9300	C13—H13B	0.9600
C5—C6	1.36 (3)	C13—H13C	0.9600
C5—H5	0.9300		

*Special details (Geometry):*

All e.s.d.'s (except the e.s.d. in the dihedral angle between two l.s. planes) are estimated using the full covariance matrix. The cell e.s.d.'s are taken into account individually in the estimation of e.s.d.'s in distances, angles and torsion angles; correlations between e.s.d.'s in cell parameters are only used when they are defined by crystal symmetry. An approximate (isotropic) treatment of cell e.s.d.'s is used for estimating e.s.d.'s involving l.s. planes.

## Compound 2g

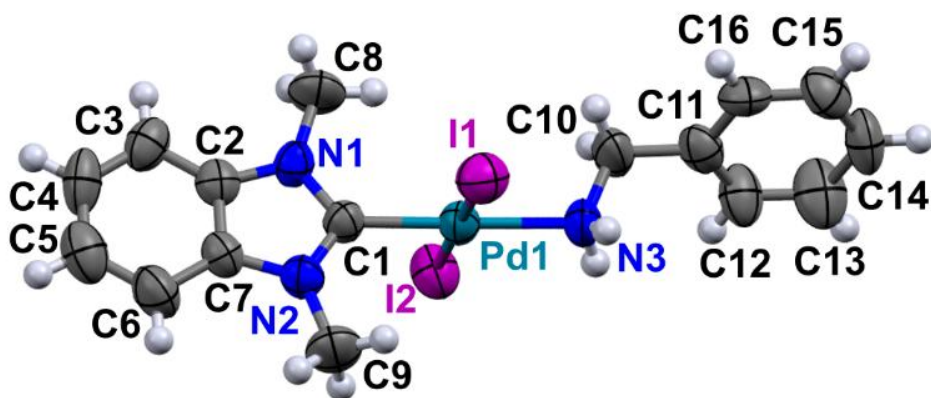


**Figure S91.** The molecular structure of compound **2g** according to single-crystal X-ray diffraction data. Thermal ellipsoids are shown at 50 % probability.

Table S10. Crystal data for compound **2g**

C <sub>16</sub> H <sub>19</sub> I <sub>2</sub> N <sub>3</sub> Pd	Z = 2
Mr = 613.54	<i>F</i> (000) = 576
Triclinic, <i>P</i> <sub>-1</sub>	<i>D</i> <sub>x</sub> = 2.086 Mg m <sup>-3</sup>
<i>a</i> = 9.5333 (7) Å	<i>Cu K</i> α radiation, $\lambda$ = 1.54186 Å
<i>b</i> = 10.9640 (8) Å	Cell parameters from 1876 reflections
<i>c</i> = 11.3716 (7) Å	$\theta$ = 4–60°
$\alpha$ = 62.480 (5)°	$\mu$ = 32.47 mm <sup>-1</sup>
$\beta$ = 79.571 (5)°	<i>T</i> = 295 K
$\gamma$ = 67.896 (5)°	Block, yellow
<i>V</i> = 976.59 (13) Å <sup>3</sup>	0.18 × 0.13 × 0.1 mm

Table S11. Data collection for compound **2g**

STOE diffractometer	3696 independent reflections
Radiation source: Cu GeniX 3D	2442 reflections with $I > 2\sigma(I)$
	$R_{\text{int}} = 0.086$
	$\theta_{\max} = 73.3^\circ$ , $\theta_{\min} = 4.4^\circ$
rotation method scans	
Absorption correction: part of the refinement model ( $\Delta F$ ) (See: Walker, N. & Stuart, D. (1983) Acta Cryst. A39, 158-166)	
$T_{\min} = 0.327$ , $T_{\max} = 0.702$	

Table S12. Refinement for compound **2g**

Refinement on $F^2$	Hydrogen site location: inferred from neighbouring sites
Least-squares matrix: full	H-atom parameters constrained
$R[F^2 > 2\sigma(F^2)] = 0.064$	$w = 1/[\sigma^2(F_o^2) + (0.1433P)^2]$ where $P = (F_o^2 + 2F_c^2)/3$
$wR(F^2) = 0.217$	$(\Delta/\sigma)_{\max} = 0.001$
$S = 1.05$	$\Delta\rho_{\max} = 1.08 \text{ e } \text{\AA}^{-3}$
3696 reflections	$\Delta\rho_{\min} = -1.90 \text{ e } \text{\AA}^{-3}$
201 parameters	Extinction correction: <i>SHELXL</i> , $F_c^* = kF_c[1 + 0.001xF_c^2\lambda^3/\sin(2\theta)]^{-1/4}$
0 restraint	Extinction coefficient: 0.0026 (2)
Primary atom site location: difference Fourier map	

Table S13. Geometric parameters ( $\text{\AA}$ ) for compound **2g**

Pd1—C1	1.971 (9)	C6—H6	0.9300
Pd1—N3	2.110 (8)	C8—H8A	0.9600
Pd1—I2	2.5933 (10)	C8—H8B	0.9600
Pd1—I1	2.6032 (10)	C8—H8C	0.9600
N1—C1	1.347 (12)	C9—H9A	0.9600
N1—C2	1.382 (12)	C9—H9B	0.9600
N1—C8	1.448 (12)	C9—H9C	0.9600
N2—C1	1.309 (11)	C10—C11	1.496 (15)
N2—C7	1.405 (13)	C10—H10A	0.9700
N2—C9	1.457 (14)	C10—H10B	0.9700
N3—C10	1.437 (13)	C11—C12	1.369 (18)
N3—H3A	0.8900	C11—C16	1.385 (16)
N3—H3B	0.8900	C12—C13	1.345 (18)
C2—C3	1.367 (15)	C12—H12	0.9300
C2—C7	1.385 (14)	C13—C14	1.38 (2)
C3—C4	1.360 (17)	C13—H13	0.9300
C3—H3	0.9300	C14—C15	1.38 (2)
C4—C5	1.36 (2)	C14—H14	0.9300
C4—H4	0.9300	C15—C16	1.384 (17)
C5—C6	1.40 (2)	C15—H15	0.9300
C5—H5	0.9300	C16—H16	0.9300
C6—C7	1.389 (14)		

*Special details (Geometry):*

All e.s.d.'s (except the e.s.d. in the dihedral angle between two l.s. planes) are estimated using the full covariance matrix. The cell e.s.d.'s are taken into account individually in the estimation of e.s.d.'s in distances, angles and torsion angles; correlations between e.s.d.'s in cell parameters are only used when they are defined by crystal symmetry. An approximate (isotropic) treatment of cell e.s.d.'s is used for estimating e.s.d.'s involving l.s. planes.

## Compound 2k

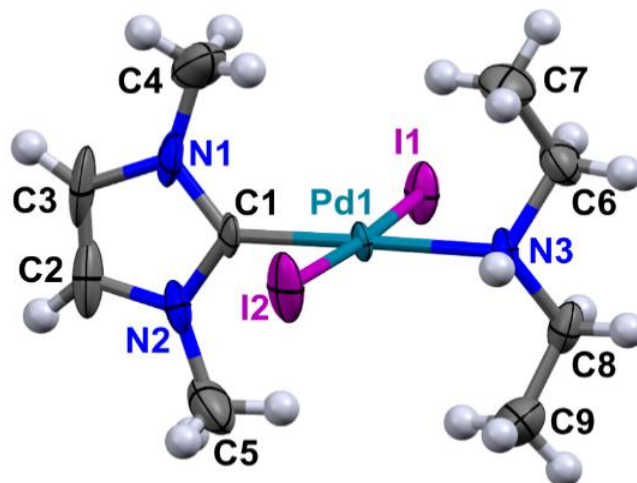


**Figure S92.** The molecular structure of compound **2k** according to single-crystal X-ray diffraction data. Thermal ellipsoids are shown at 50 % probability.

Table S14. Crystal data for compound **2k**

C <sub>9</sub> H <sub>19</sub> I <sub>2</sub> N <sub>3</sub> Pd	<i>F</i> (000) = 1968
Mr = 529.47	<i>D</i> x = 2.236 Mg m <sup>-3</sup>
Monoclinic, C2/c	<i>Cu K</i> $\alpha$ radiation, $\lambda$ = 1.54186 Å
<i>a</i> = 14.7908 (9) Å	Cell parameters from 2564 reflections
<i>b</i> = 7.8079 (3) Å	$\theta$ = 3.5–65°
<i>c</i> = 27.592 (1) Å	$\mu$ = 40.17 mm <sup>-1</sup>
$\beta$ = 99.197 (3)°	<i>T</i> = 295 K
V = 3145.5 (3) Å <sup>3</sup>	Block, yellow
Z = 8	0.22 × 0.16 × 0.13 mm

Table S15. Data collection for compound **2k**

STOE diffractometer	3032 independent reflections
Radiation source: Cu GeniX 3D	2384 reflections with $I > 2\sigma(I)$
None monochromator	$R_{\text{int}} = 0.070$
Detector resolution: 5.81 pixels mm <sup>-1</sup>	$\theta_{\text{max}} = 73.1^\circ$ , $\theta_{\text{min}} = 6.1^\circ$
rotation method scans	
Absorption correction: part of the refinement model (See: Walker, N. & Stuart, D. (1983) Acta Cryst. A39, 158-166)	
$T_{\text{min}} = 0.327$ , $T_{\text{max}} = 0.702$	
3032 measured reflections	

Table S16. Refinement for compound **2k**

Refinement on $F^2$	Hydrogen site location: inferred from neighbouring sites
Least-squares matrix: full	H-atom parameters constrained
$R[F^2 > 2\sigma(F^2)] = 0.067$	$w = 1/[\sigma^2(F_o^2) + (0.1343P)^2]$ where $P = (F_o^2 + 2F_c^2)/3$
$wR(F^2) = 0.182$	$(\Delta/\sigma)_{\max} = 0.003$
S = 0.97	$\Delta\rho_{\max} = 2.63 \text{ e \AA}^{-3}$
3032 reflections	$\Delta\rho_{\min} = -2.33 \text{ e \AA}^{-3}$
140 parameters	
0 restraints	

Table S17. Geometric parameters ( $\text{\AA}$ ) for compound **2k**

I1—Pd1	2.5982 (8)	C4—H4B	0.9600
I2—Pd1	2.5932 (8)	C4—H4C	0.9600
Pd1—C1	1.953 (9)	C5—H5A	0.9600
Pd1—N3	2.124 (7)	C5—H5B	0.9600
N1—C1	1.350 (13)	C5—H5C	0.9600
N1—C3	1.390 (17)	C6—C7	1.530 (19)
N1—C4	1.42 (2)	C6—H6A	0.9700
N2—C1	1.332 (13)	C6—H6B	0.9700
N2—C2	1.377 (15)	C7—H7A	0.9600
N2—C5	1.47 (2)	C7—H7B	0.9600
N3—C6	1.472 (14)	C7—H7C	0.9600
N3—C8	1.476 (14)	C8—C9	1.476 (19)
N3—H3	0.9800	C8—H8A	0.9700
C2—C3	1.33 (3)	C8—H8B	0.9700
C2—H2	0.9300	C9—H9A	0.9600
C3—H3A	0.9300	C9—H9B	0.9600
C4—H4A	0.9600	C9—H9C	0.9600

*Special details (Geometry):*

All e.s.d.'s (except the e.s.d. in the dihedral angle between two l.s. planes) are estimated using the full covariance matrix. The cell e.s.d.'s are taken into account individually in the estimation of e.s.d.'s in distances, angles and torsion angles; correlations between e.s.d.'s in cell parameters are only used when they are defined by crystal symmetry. An approximate (isotropic) treatment of cell e.s.d.'s is used for estimating e.s.d.'s involving l.s. planes.

## Compound 2y

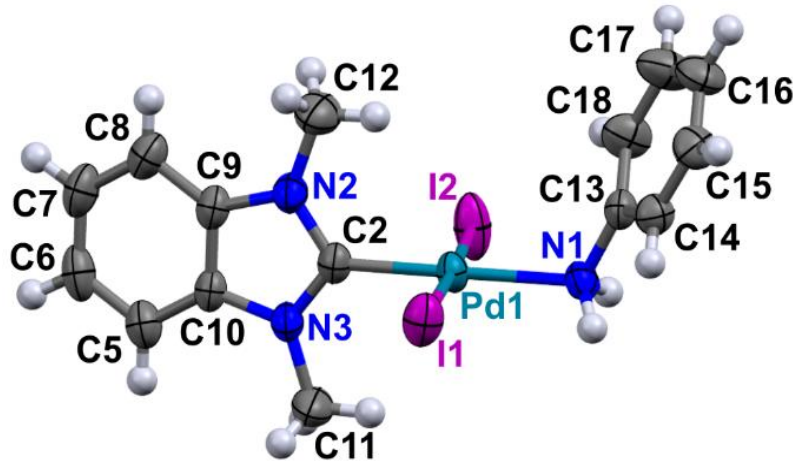


**Figure S93.** The molecular structure of compound **2y** according to single-crystal X-ray diffraction data. Thermal ellipsoids are shown at 50 % probability.

Table S18. Crystal data for compound **2y**

C <sub>15</sub> H <sub>17</sub> I <sub>2</sub> N <sub>3</sub> Pd	$F(000) = 2240$
Mr = 599.52	$Dx = 2.116 \text{ Mg m}^{-3}$
Monoclinic, C2/c	<i>Mo K<math>\alpha</math> radiation, <math>\lambda = 0.71073 \text{ \AA}</math></i>
$a = 21.6545 (7) \text{ \AA}$	<i>Cell parameters from 5734 reflections</i>
$b = 8.6570 (2) \text{ \AA}$	$\theta = 4\text{--}25^\circ$
$c = 20.1671 (8) \text{ \AA}$	$\mu = 4.26 \text{ mm}^{-1}$
$\beta = 95.408 (3)^\circ$	$T = 295 \text{ K}$
$V = 3763.8 (2) \text{ \AA}^3$	<i>Block, brown</i>
Z = 8	$0.29 \times 0.20 \times 0.17 \text{ mm}$

Table S19. Data collection for compound **2y**

STOE diffractometer	4989 independent reflections
Radiation source: Mo LFF Sealed Tube	3075 reflections with $I > 2\sigma(I)$
Plane graphite monochromator	$R_{\text{int}} = 0.048$
Detector resolution: 5.81 pixels mm <sup>-1</sup>	$\theta_{\text{max}} = 29.2^\circ, \theta_{\text{min}} = 3.7^\circ$
rotation method scans	$h = -29 \rightarrow 29$
Absorption correction: multi-scan [c.f. r.h. blessing, acta cryst. (1995), a51, 33-38]	$k = -11 \rightarrow 11$
$T_{\text{min}} = 0.211, T_{\text{max}} = 0.609$	$l = -26 \rightarrow 27$
35708 measured reflections	

Table S20. Refinement for compound **2y**

Refinement on $F^2$	Hydrogen site location: inferred from neighbouring sites
Least-squares matrix: full	H-atom parameters constrained
$R[F^2 > 2\sigma(F^2)] = 0.031$	$w = 1/[\sigma^2(F_o^2) + (0.0234P)^2]$ where $P = (F_o^2 + 2F_c^2)/3$
$wR(F^2) = 0.058$	$(\Delta/\sigma)_{\max} = 0.046$
$S = 0.85$	$\Delta\rho_{\max} = 0.99 \text{ e } \text{\AA}^{-3}$
4989 reflections	$\Delta\rho_{\min} = -0.91 \text{ e } \text{\AA}^{-3}$
193 parameters	Extinction correction: <i>SHELXL2014/7</i> (Sheldrick 2014, $F_c^* = kF_c[1+0.001xF_c^2\lambda^3/\sin(2\theta)]^{-1/4}$ )
0 restraint	Extinction coefficient: 0.00096 (3)

Table S21. Selected Geometric parameters ( $\text{\AA}$ ) for compound **2y**

Pd1—C2	1.957 (4)	C8—C9	1.394 (5)
Pd1—N1	2.132 (3)	C8—H8	0.9300
Pd1—I1	2.5868 (4)	C9—C10	1.383 (5)
Pd1—I2	2.5977 (4)	C11—H11A	0.9600
N1—C13	1.433 (4)	C11—H11B	0.9600
N1—H1A	0.8900	C11—H11C	0.9600
N1—H1B	0.8900	C12—H12A	0.9600
N2—C2	1.349 (4)	C12—H12B	0.9600
N2—C9	1.392 (4)	C12—H12C	0.9600
N2—C12	1.448 (5)	C13—C18	1.377 (5)
N3—C2	1.341 (4)	C13—C14	1.374 (5)
N3—C10	1.395 (4)	C14—C15	1.372 (5)
N3—C11	1.457 (5)	C14—H14	0.9300
C5—C10	1.371 (5)	C15—C16	1.360 (6)
C5—C6	1.379 (6)	C15—H15	0.9300
C5—H5	0.9300	C16—C17	1.362 (6)
C6—C7	1.372 (6)	C16—H16	0.9300
C6—H6	0.9300	C17—C18	1.371 (6)
C7—C8	1.374 (6)	C17—H17	0.9300
C7—H7	0.9300	C18—H18	0.9300

*Special details (Geometry):*

All e.s.d.'s (except the e.s.d. in the dihedral angle between two l.s. planes) are estimated using the full covariance matrix. The cell e.s.d.'s are taken into account individually in the estimation of e.s.d.'s in distances, angles and torsion angles; correlations between e.s.d.'s in cell parameters are only used when they are defined by crystal symmetry. An approximate (isotropic) treatment of cell e.s.d.'s is used for estimating e.s.d.'s involving l.s. planes.

## S5. Data of the QTAIM (quantum theory of atoms in molecules) analysis of molecular structures of compounds **2a**, **2g**, **2k**, **2y**

Atomic coordinates used for the QTAIM analyses were obtained from the X-ray diffraction data (Section S4). The topological parameters of the CP (3, -1) were calculated by means of the AIMAll software package<sup>1</sup>. Analysis of the electron density topology by means of "atoms in molecules" theory revealed no a bond path connecting H and I atoms and a (3,-1) critical point between H and I in the structures **2a**, **2g**, **2k** and **2y** (Figures S94-S97).

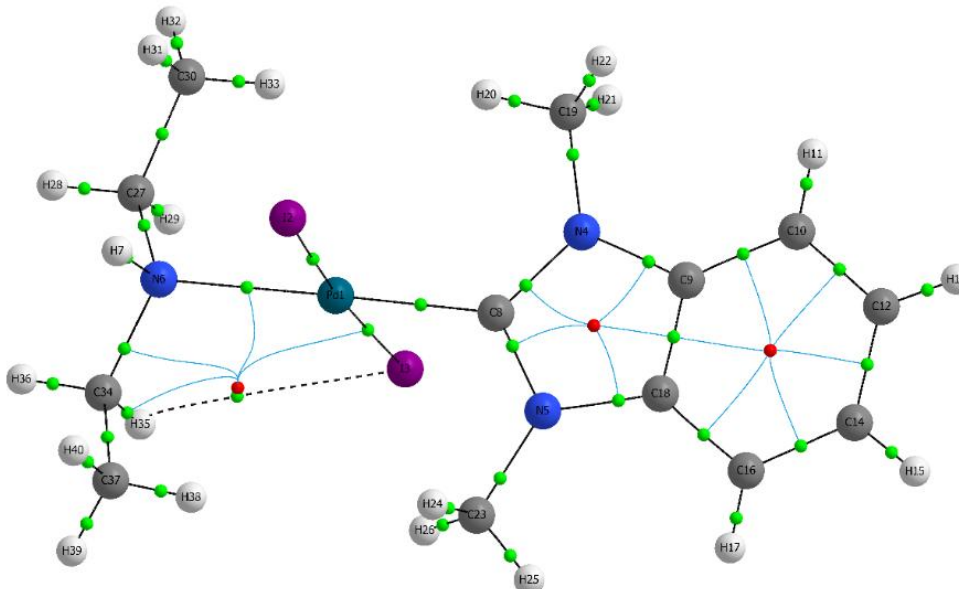


**Figure S94.** Molecular graph (AIMALL representation) of the compound **2a**.

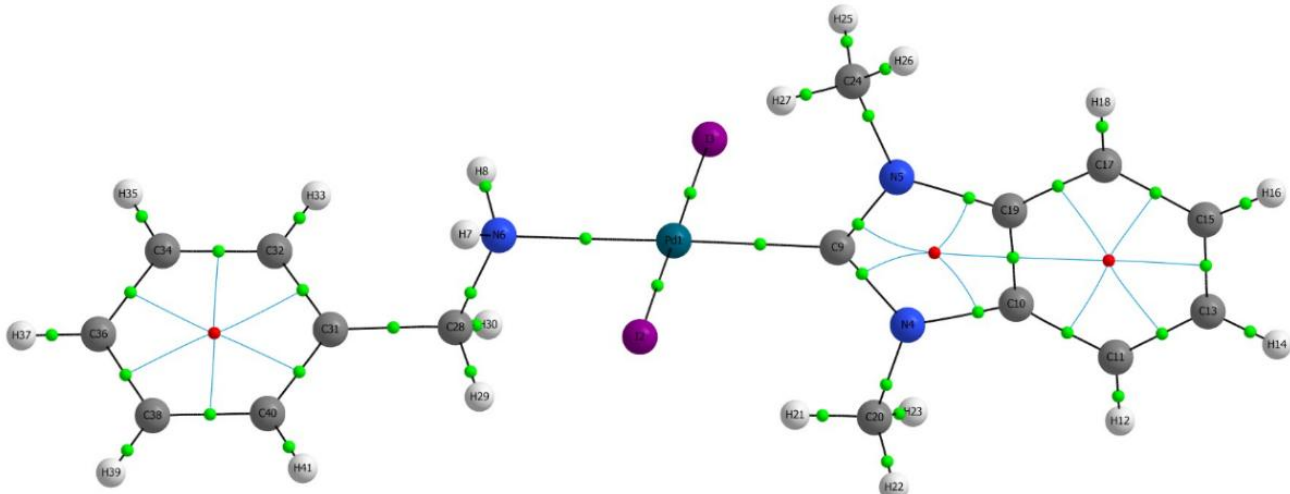


**Figure S95.** Molecular graph (AIMALL representation) of the compound **2g**.

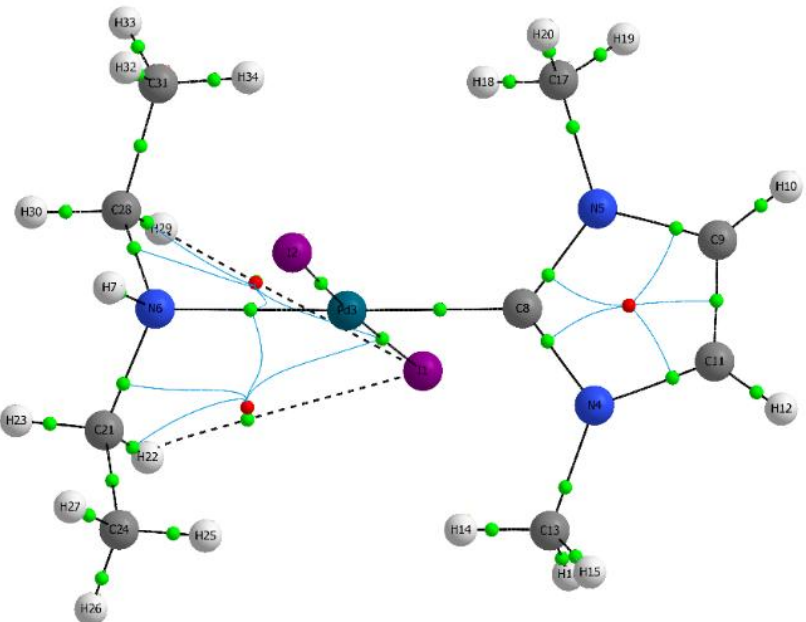


**Figure S96.** Molecular graph (AIMALL representation) of the compound **2k**.

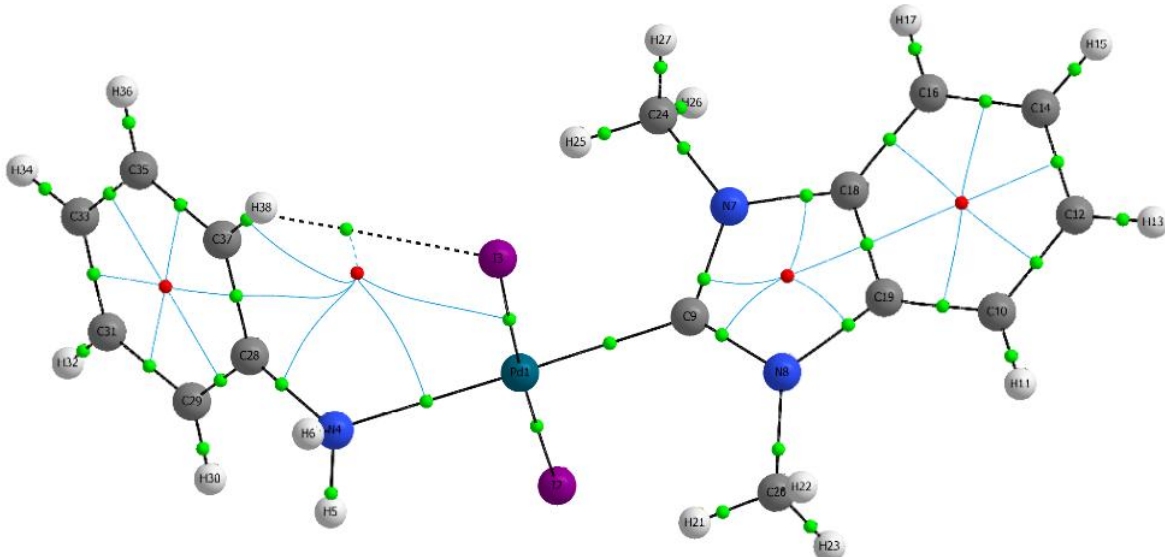


**Figure S97.** Molecular graph (AIMALL representation) of the compound **2y**.

## References

- (1) AIMAll (Version 19.02.13), Todd A. Keith, TK Gristmill Software, Overland Park KS, USA, 2019 ([aim.tkgristmill.com](http://aim.tkgristmill.com))

## S6. TEM, FE-SEM/EDS data

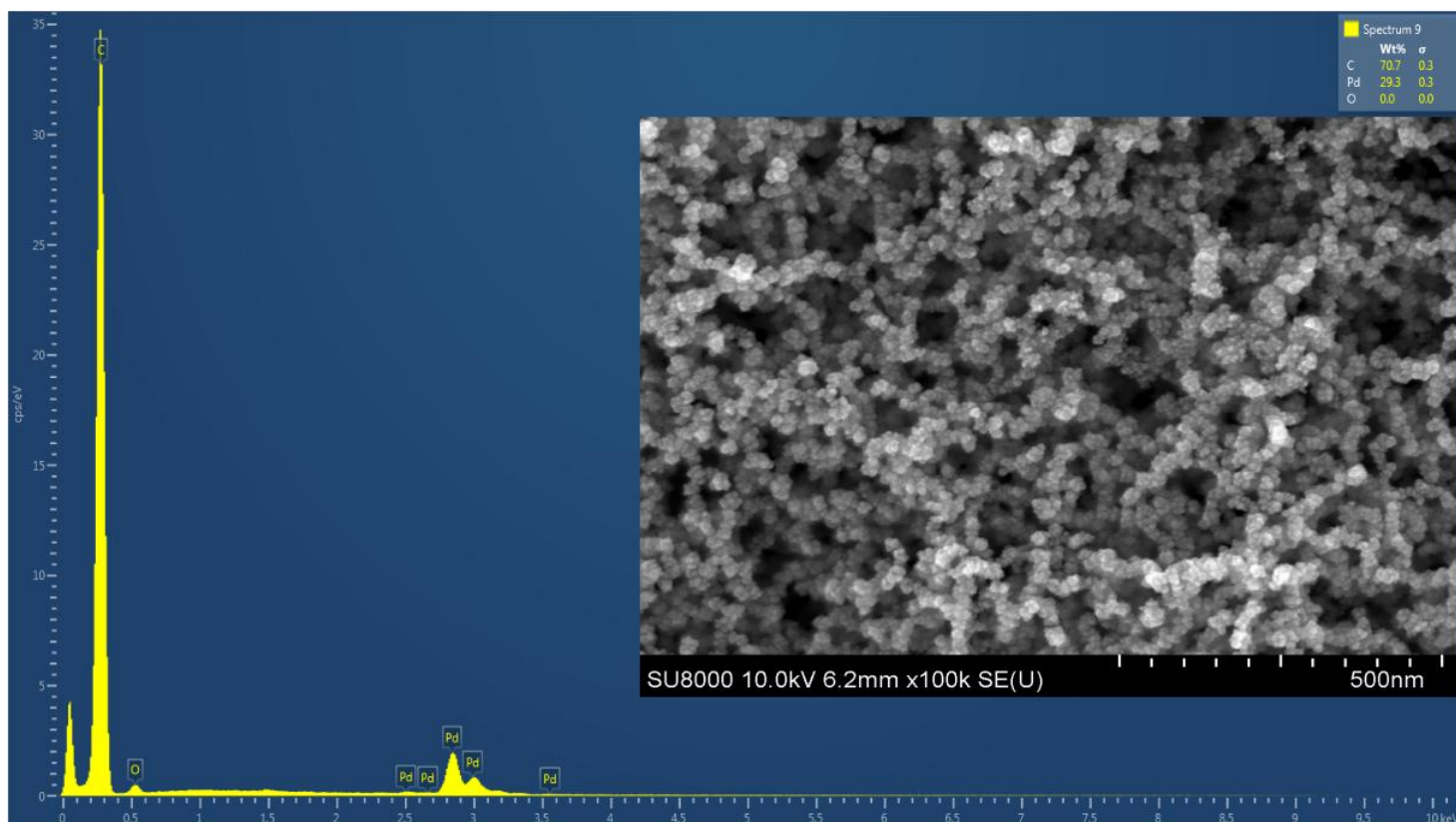


**Figure S98.** FE-SEM image and EDS spectrum of Pd residue isolated from the reaction mixture after heating compound **1a** with  $\text{Et}_3\text{N}$  (10 eq) in DMF at  $100\text{ }^\circ\text{C}$  within 1 h.

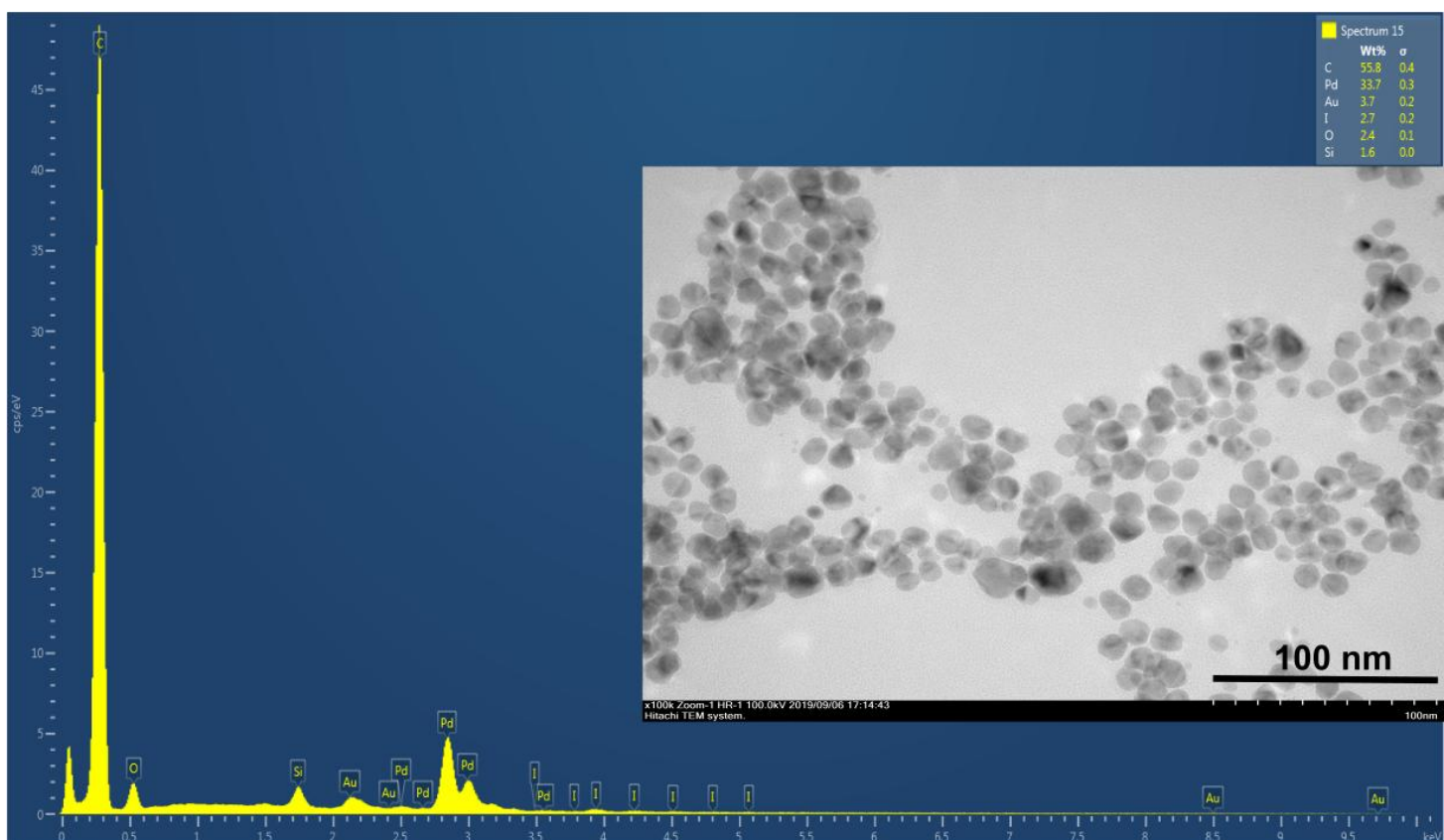


**Figure S99.** TEM image and EDS spectrum of Pd residue isolated from the reaction mixture after heating compound **1a** with  $\text{Et}_3\text{N}$  (10 eq) in  $\text{CDCl}_3$  at  $60\text{ }^\circ\text{C}$  within 20 h.